



universität
wien

DISSERTATION

Titel der Dissertation

„Characterization of an Interaction Partner of Density
Enhanced Phosphatase 1 (DEP-1)“

Verfasserin

Mag. Patricia Heier

angestrebter akademischer Grad

Doktorin der Naturwissenschaften (Dr. rer.nat.)

Wien, 2009	
Studienkennzahl lt. Studienblatt:	A 091 442
Dissertationsgebiet lt. Studienblatt:	Anthropologie
Betreuerin / Betreuer:	Univ. Prof. Dr. Bernd Binder

TABLE OF CONTENTS

List of Abbreviations	4
Abstract	7
Zusammenfassung	9
Introduction	11
1. Cell cycle regulation	11
2. Phosphorylation	14
3. Protein kinases: Regulators of cell growth	15
3.1. The ERK1/2 MAPK Pathway	16
3.1.1 ERK1/2 proteins	18
3.1.2. The specificity of ERK1/2 interactions	19
3.4. The role of MAPKs in cancer development	20
4. Protein phosphatases	22
4.1. The family of PTPs	23
4.1.1. The genomic distribution of PTPs	24
4.1.2 The PTP gene organization	25
4.1.3. PTPs and diseases	26
5. Density Enhanced Phosphatase 1 (DEP-1)	27
6. Hepatitis B core-Antigen binding protein (HBCBP)	36

Aims	37
Methods	38
1. Plasmids and Constructs	38
2. Cell Culture	39
3. Co-Immunoprecipitations (CoIPs)	41
4. Interaction on ELISA-plates	42
5. Western blotting	42
6. Immunostaining	43
7. Flow Cytometry	43
8. Promotor analysis	44
9. Quantitative Real-Time PCR (Q-PCR)	44
10. Reporter Assays	45
11. Recombinant HBCBP	45
12. In silico analysis:	46
Results	48
1. Regulation of ERK1/2 MAP-Kinase pathway	48
2. Interaction of HBCBP with DEP-1	54
3. How does HBCBP affect Elk1 activity?	60
4. HBCBP in MAP-Kinase dependent processes	64
5. HBCBP expression in tissues	68
6. HBCBP Promotor	70

7. In silico structural analysis of HBCBP protein	78
8. Recombinant HBCBP	84
Discussion	85
References	96
Curriculum Vitae	107

LIST OF ABBREVIATIONS

ABTS	2,2-Aazine-di-(3-Ethylbenzothiazoline-6-Sulfonate)
AP-1	Activator Protein 1
APC	Anaphase Promoting Complex
ARB1	Arrestin beta 1
AREB6	see ZEB1
ATP	Adenosine triphosphate
BrdU	Bromodeoxyuridine
Byp	mouse DEP-1
CD-domain	Common docking domain
CDK	Cyclin-Dependent Kinase
c-Fos	FBJ Murine Osteosarcome viral Oncogene homolog
c-Myc	Myelocytomatosis Viral Oncogene homolog
CoIP	Co-Immunoprecipitation
DEP-1	Density Enhanced Phosphatase
DMSO	Dimethyl Sulfoxide
DSP	Dual-Specificity Phosphatase
DUSP	Dual-Specificity Phosphatase
EGF	Epidermal Growth Factor
EGFP	Enhanced Green Fluorescent Protein
Elk1	Ets related proto-oncogene
ELM server	Eukaryotic Linear Motif resource for Functional Sites in Proteins (D)
ERK1/2	Extracellular Signal-Regulated Kinases 1 and 2
FITC	Fluorescein Isothiocyanate
FN	Fibronectin
Gab1	GRB2-Associated Binding Protein 1
GLEPP1	Glomerular Epithelial Protein 1
GRB2	Growth Factor Receptor-Bound Protein 2
GTP	Guanosine triphosphate
HBcAG	Hepatitis B Core-Antigen
HBCBP	Hepatitis B Core-Antigen Binding Protein
HEK293	Human Embryonic Kidney 293 cells
HepG2	Hepatocellular Carcinoma Cells
HGF	Hepatocyte Growth Factor
HPTP	Human PTP
HUVECs	Human Umbilical Vein Endothelial Cells
IFN	Interferon
INSR	Insulin Receptor
IP	Immunoprecipitation
IRF	Interferon regulatory factor
Jak2	Janus Kinase 2
JMML	Juvenile Myelomonocytic Leukemia
JNK	c-Jun N-terminal Kinase
Kip-1	Kinase Inhibitory Protein 1
KSR	Scaffold Kinase Suppressor of Ras
LNCaP	Prostate Epithelial Cancer Cells

LOH	Loss of Heterozygosity
MAPK	Mitogen Activated Protein Kinase
MAP-Kinase	Mitogen Activated Protein Kinase
MEK1/2	ERK Kinases 1 and 2
MEN2	Multiple Endocrine Neoplasia type 2
Met	Hepatocyte Growth Factor/Scatter Factor Receptor
MKP	MAPK phosphatase
MP1	MEK Partner 1
MTC	Sporadic Medullary Thyroid Carcinomas
NES	Nuclear Export Signal
PBGD	Porphobilinogen Deaminase
PDGF	Platelet-Derived Growth Factor
PEI	Polyethylenimin
PI	Propidium Iodide
PMA	Phorbol 12-myristate 13-acetate
PPAR	Peroxisome Proliferator-Activated Receptor
PPM	Mg ²⁺ - or Mn ²⁺ -dependent Protein Phosphatase
PPP	Phosphoprotein Phosphatase
P-Ser	Phospho-serine
P-Thr	Phospho-threonine
PTP	Phosphotyrosine Phosphatase
PTP-BAS	Basophile PTP
PTPRJ	PTP Receptor-Type J (equals DEP-1)
QPCR	Quantitative Real-Time PCR
Raf	v-Raf-1 Murine Leukemia Viral Oncogene Homolog
Ras	Rat Sarcoma Viral Oncogene Homolog
RPTP	Receptor Type PTP
rPTP	Rat PTP
RWPE1	Prostate Epithelial Cells
SAP-1	Serume Response Factor Accessory Protein 1
SDS-PAGE	Sodium-Dodecyl-Sulfate Polyacrylamine Gel Electrophoresis
SHP	SH2 Domain Containing Phosphatase
SMART	Simple Modular Architecture Research Tool (Heidelberg, D)
SNP	Single Nucleotide Polymorphism
Src	Sarcoma Kinase
SST	Somatostatin
SSTR	Somatostatin Receptor
STAT	Signal Transducer and Activator of Transcription
Ste5p	Pheromone-Response Scaffold Protein
TCPTP	T-Cell PTP
TGF	Transforming Growth Factor
TNF	Tumor Necrosis Factor
Tpl2	Tumor Progression Locus 2
TSG101	Tumor Susceptibility Gene 101
VE-Cadherin	Vascular Endothelial Cadherin
VEGFR	Vascular Endothelial Growth Factor Receptor
vSMCs	Vascular Smooth Muscle Cells

WCL	Whole cell lysate
WY14643	PPAR-alpha ligand
Y2H	Yeast-Two-Hybrid
ZEB1	Zinc Finger E-box Binding Homeobox 1 (equals AREB6)

ABSTRACT

Density Enhanced Phosphatase 1 (DEP-1) plays an important role in the regulation of cell growth, differentiation and transformation. DEP-1 was shown to be frequently lost in mammary, lung and colon tumors and in addition, the gene has been described as tumor suppressor gene. The protein is known for its antiproliferative effect due to the inhibition of MAP-Kinases.

A knock-out mouse model demonstrated that DEP-1 is of fundamental importance for the vascular development.

In the present study, we wanted to characterize a potential interaction partner that was identified before in my diploma thesis by a yeast-two-hybrid (Y2H) screen, Hepatitis B Core-Antigen Binding Protein (HBCBP). According to confocal microscopy data, the protein is a cytoplasmic protein.

We could show that overexpression of full-length HBCBP significantly downregulated the activity of the ERK1/2 MAP-Kinase pathway in Elk-1 reporter assays, while truncated HBCBP did not. Furthermore, this inhibition could only be shown in dense cells, while in samples with sparse cells this activity was absent.

Unfortunately we could not confirm the interaction between HBCBP and DEP-1 in the human system by co-immunoprecipitation. In addition, we found that the inhibition of the ERK1/2 MAP-Kinase pathway by HBCBP does not require the presence of DEP-1 and that similarly the inhibition by DEP-1 does not require the presence of HBCBP. In western blots the amount of phosphorylated ERK1/2 was reduced in cells overexpressing HBCBP, though not in a statistically significant way. HBCBP did not interact with ERK1/2 directly and we could not find another interaction partner of HBCBP that mediated the effect.

To see, if HBCBP has a quantifiable effect on ERK1/2 MAP-Kinase dependent processes, we used proliferation and apoptosis studies showing that HBCBP had no influence.

Searching for hints, in which processes HBCBP could be involved, we found the HBCBP expression to not be organ-specific, but detected an upregulation of HBCBP expression upon TGF β 1 and IFN γ treatment in HUVECs, though not significant.

We used different software programs to analyze the protein sequence of HBCBP to get information about conserved domain patterns, evolutionary relationships,

homologous regions and phosphorylation sites, but none of these approaches could give us promising results. Interestingly a ClustalW2 analysis indicated an HBCBP-orthologue in chimpanzee, but there are no related genes in human.

Also our last attempt to express and purify recombinant HBCBP for later antibody production was confronted with severe limiting difficulties.

Taken together, we found that HBCBP does not interact with DEP-1 in a detectable way. Although we found an inhibition of the ERK1/2 pathway in reporter assays by HBCPB that were confirmed by siRNA analyses, this signaling pathway did not involve apoptosis or proliferation, leaving the option that HBCBP influences other ERK1/2 dependent processes.

ZUSAMMENFASSUNG

Density Enhanced Phosphatase 1 (DEP-1) spielt eine wichtige Rolle in der Regulation von Zellwachstum, Differenzierung und Transformation. Es wurde gezeigt, dass DEP-1 in verschiedenen humanen Tumoren mutiert ist. DEP-1 wurde zusätzlich als Tumorsuppressor-Gen beschrieben. Das Protein inhibiert MAP-Kinasen und hat daher einen antiproliferativen Effekt.

In Knock-out-Mäusen konnte gezeigt werden, dass die Anwesenheit von DEP-1 von fundamentaler Wichtigkeit für die Entwicklung des Gefäßsystems ist.

In dieser Studie wollten wir einen potentiellen Interaktionspartner von DEP-1 charakterisieren, der zuvor durch einen Yeast-Two-Hybrid (Y2H) screen identifiziert worden ist, Hepatitis B Core-Antigen Binding Protein (HBCBP). Konfokale Mikroskopie zeigte, dass HBCBP ein cytoplasmatisch lokalisiertes Protein ist.

Wir konnten zeigen, dass Überexpression von HBCBP, aber nicht von gekürzten HBCBP-Konstrukten, die Aktivität des ERK1/2 MAP-Kinase-Signalweges in Elk-1 Reporterassays signifikant gehemmt hat. Dies war auf die Inhibition in konfluenten Zellen beschränkt, während der Signalweg in subkonfluenten Zellen nicht gehemmt wurde.

Im humanen System konnte eine Interaktion zwischen HBCBP und DEP-1 nicht durch Co-Immunoprecipitation bestätigt werden. Zusätzlich fanden wir, dass die Inhibition des ERK1/2 MAP-Kinase-Signalweges durch HBCBP von DEP-1 unabhängig war und dass ebenfalls die Inhibition durch DEP-1 von HBCBP unabhängig war.

In Western-Bots war in HBCBP-überexprimierenden Zellen die Menge von phosphoryliertem ERK1/2 reduziert, jedoch nicht statistisch signifikant. HBCBP interagiert nicht direkt mit ERK1/2 und wir konnten auch keinen Interaktionspartner von HBCBP finden, der diesen Effekt vermittelte. Proliferations- und Apoptosestudien zeigten, dass HBCBP darauf keinen Einfluss hatte.

Die Expression von HBCBP war nicht organspezifisch, aber konnte eine Hochregulierung der HBCBP-Expression in HUVECs durch TGF β 1 und IFN γ festgestellt werden, jedoch nicht in einem signifikanten Ausmaß.

Wir benutzten unterschiedliche Softwareprogramme für die Analyse der Proteinsequenz von HBCBP, um Information über konservierte Domänen,

evolutionäre Verwandtschaft, homologe Regionen und Phosphorylierungsstellen zu bekommen, aber , aber auch diese lieferten keine Hinweise auf die Funktion von HBCBP. Interessanterweise ließ eine ClustalW2-Analyse vermuten, dass HBCBP nur im Chimpanse wiederzufinden ist, es gibt keine eng verwandten Gene im Menschen.

Der Versuch, rekombinantes HBCBP für spätere Antikörperproduktion zu exprimieren und zu reiningen, wurde durch das ausschließliche Vorkommen in Inclusion-Bodies interkariert.

Zusammenfassend haben wir gefunden, dass HBCBP mit DEP-1 nicht in einem detektierbarem Ausmass interagiert. Obwohl wir eine Inhibierung des ERK1/2-Signalweges durch HBCBP in Reporterassays fanden, was durch si-RNA-Analysen bestätigt wurden, konnten wir keine Auswirkungen auf Apoptose oder Proliferation feststellen, was die Möglichkeit offen lässt, dass HBCBP andere ERK1/2-abhängige Prozesse beeinflusst.

INTRODUCTION

1. Cell cycle regulation

Proliferation is the biological process of cell growth, in which two identical daughter cells are generated by cell division of a single progenitor cell. Different types of cells have very different rates of proliferation. For example, cells of the skin are vividly dividing, whereas liver cells only divide in case of injury to recover the damaged tissue. Certain specialized cells are entirely in growth arrest, like neurons or muscle cells. The rate of proliferation is tightly controlled by the cell cycle (Fig.A).

In the cell cycle, the chromosome cycle can be distinguished from the growth cycle. The chromosome cycle includes DNA replication and the physical separation of the two complete genomes to daughter nuclei, while the growth cycle accounts for the replication of other cellular devices, like proteins, membranes, organelles, etc. and for the physical separation of the daughter cells. Accurate replication and partitioning is essential for the daughter cells to preserve the possibility of further cell divisions. The chromosome and growth cycles have to be strictly coordinated. Otherwise the cells would get gradually larger or smaller with each division (Tyson et al, 2002).

The chromosome cycle of eukaryotic cells includes two basic processes. The DNA synthesis phase (S phase) is responsible for the replication of the DNA to produce identical pairs of sister chromatids. The mitosis phase (M phase) can be divided into prophase (chromosome condensation), metaphase (chromosome alignment at midplane of mitotic spindle), anaphase (separation of sister chromatids) and telophase (formation of daughter nuclei). The two phases are separated by two “gaps”, creating the generic cell cycle: G1-S-G2-M. Repeated S phases without M phases in between lead to the formation of large, polyploid cells which are generated in some cases of terminally differentiated cells (Tyson et al, 2002).

To ensure a proper progression of the cell cycle checkpoints are controlling certain transitions. At the G1 checkpoint, the cell has to be large enough for DNA synthesis, any DNA damage has to be repaired and the external conditions have to be sufficient for mitosis before S phase is to be started. Cell division in multicellular organism

additionally underlie influences from growth hormones, cell-cell contacts and different other factors. The G2 checkpoint is responsible for the affirmation that the DNA was fully replicated, that damages were repaired and that the cell is large enough for division (Elledge et al, 1996).

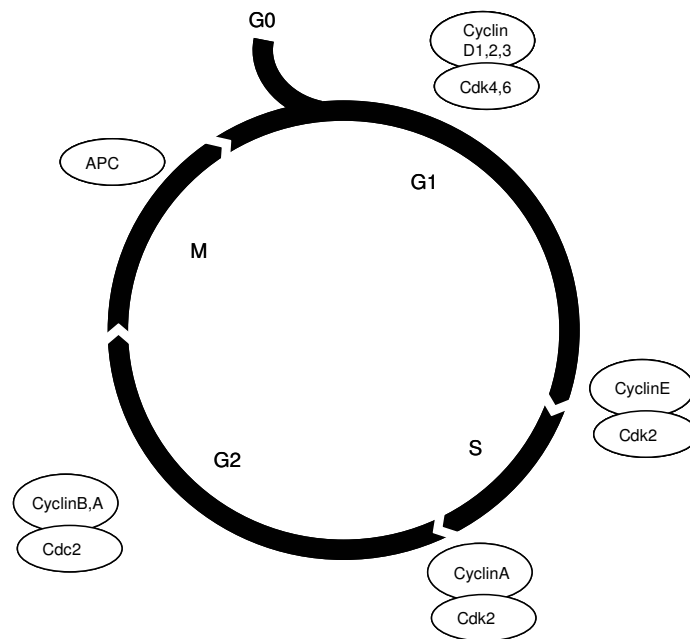


Figure A: Cell cycle. Cyclin-Cdk-complexes formed at the indicated points of the cell cycle.

The main molecules regulating the cell cycle are enzymes called cyclin-dependent protein kinases (CDKs). CDKs are present in the cell throughout the cell cycle in a constant concentration. Their activity depends on the association with appropriate cyclins that vary in concentration during the different phases of cell cycle (Fig. A). The changing concentration of the different cyclins leads to the formation of certain cyclin-CDK-complexes at certain phases, determining the time frame of the different phases of the cell cycle. In that context, CDKs, by phosphorylation of target proteins, trigger major events like DNA replication, chromosome condensation and nuclear envelope breakdown (Tyson et al, 2002).

Another important regulating factor for the cell cycle is the anaphase promoting complex (APC). It initiates degradation of the cyclin component of CDKs and causes

the separation of sister chromatids, and daughter cells are prepared for a new cell cycle. For a new round of cell cycle, the APC activity must then be turned off, so that CDK activity can accelerate (Novak et al, 1998).

That indicates antagonistic interactions between CDK and APC. CDK inactivates APC and APC degrades the cyclin subunit of the CDK complex (Nasmyth, K., 1995).

2. Phosphorylation

Phosphorylation is the key for basic processes in the cell. Complicated procedures, including gene regulation, cell cycle control, metabolic processes, motility, secretion, adhesion, proliferation and differentiation are synchronized by phosphorylation. Therefore the state of phosphorylation has to be under tight control.

When a phosphate group binds to a protein, it causes a conformational change. Because of its two negative charges, the phosphate group could, for example, attract a cluster of positively charged amino acids. After the removal of the phosphate from the protein, it again takes over its former conformation.

When a protein gets phosphorylated, a protein kinase transfers a phosphate group from adenosine triphosphate (ATP) to the hydroxyl group of a serine, threonine or a tyrosine amino acid side chain within the protein. Protein phosphatases can reverse this process (Fig. B).

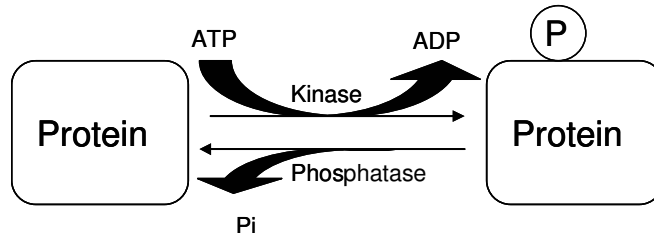


Figure B: Scheme of the reversible phosphorylation of a protein. The kinase adds a phosphate group to the protein by hydrolyzing an ATP-molecule. A phosphatase removes the phosphate group, reconstituting the native conformation of the protein.

The family of protein kinases includes a high number of diverse proteins that are specialized for a single protein or for a certain group of proteins. The same specificity can be found in phosphatases that also dephosphorylate a defined target or a group of targets. In the healthy cell the degree of phosphorylation and dephosphorylation is kept in an accurate balance (Alberts et al, 2002).

3. Protein kinases: Regulators of cell growth

Mitogen Activated Protein Kinases (MAP-Kinases, MAPKs) are involved in the control of many cellular programs, such as embryogenesis, proliferation, differentiation and cell death (Lewis et al, 1998). Nearly 20 MAPKs were found in mammals, which show a high sequence identity (Caffrey et al, 1999). A few examples are the extracellular signal-regulated kinases 1 and 2 (ERK1/2), c-Jun N-terminal kinase (JNK(1-3)) and p38 (α , β , γ and δ) families. ERK3, ERK5 and ERK7 are other MAPKs that are differently regulated and have distinct functions (Raman et al, 2007).

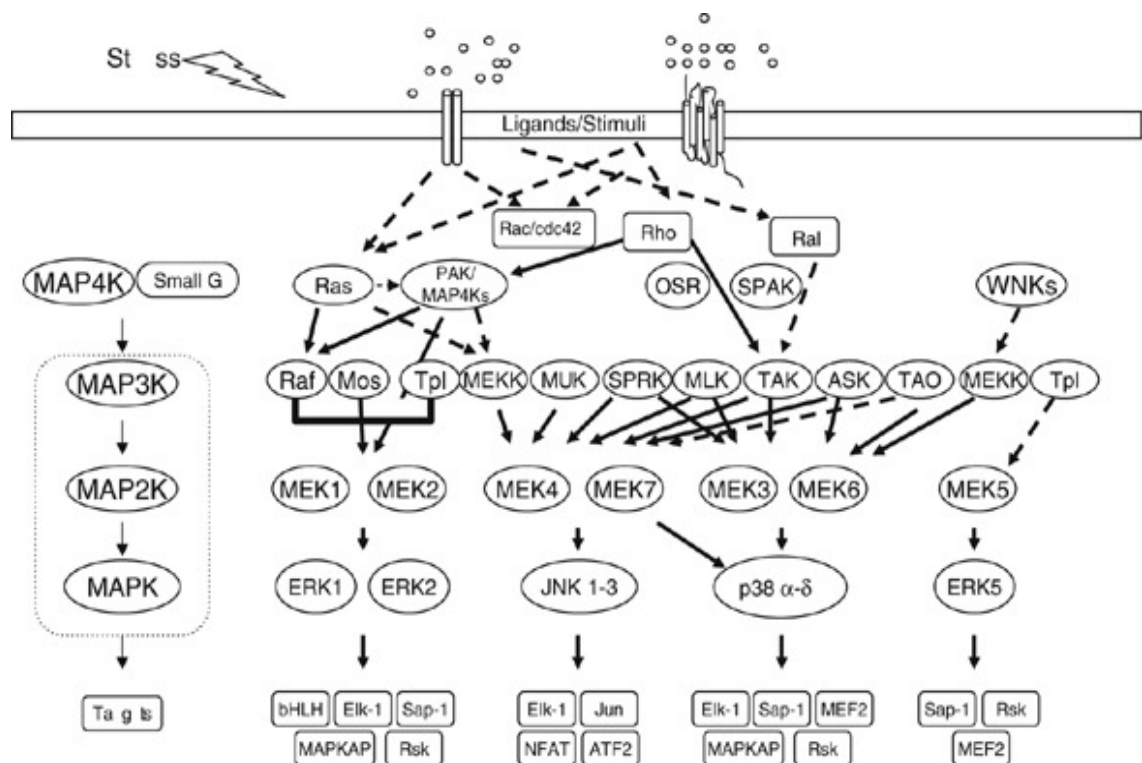


Figure C: MAPK cascades. Illustration of the three steps of the signaling of the MAPK family members ERK, JNK and p38. (Raman et al, 2007)

MAPKs are a part of signaling cascade that consists of a core of three kinases (Fig. C). The MAPKs get phosphorylated by the mitogen-activated protein kinase kinases

(MAP2K), which are activated by phosphorylation by other kinases, the MAP3Ks. Although the pathway seems to be a simple system, the enzymes are able to respond to a large number of stimuli in a remarkably specific way. The specificity is dependent on the kinetics of their activation and inactivation, the cellular localization, the formation of complexes and the availability of substrates. Furthermore scaffolding accessory proteins can influence and modulate the signaling components (Raman et al, 2007).

MAPKs, MAP2Ks and MAP3Ks are all inactivated by the specific removal of phosphate from either the tyrosine or the threonine. This dephosphorylation is catalyzed by three major groups of protein phosphatases based on preference for dephosphorylation of phospho-tyrosine, phospho-serine/threonine, or both types of phosphoresidues (dual-specificity phosphatases (DSP, DUSP) (Cobb et al, 1999). Thus, phosphoprotein phosphatases act on all parts of MAPK cascade, they can function both ways, activating or suppressing.

DUSPs are sharing a similar structure and sequence with protein tyrosine phosphatases (PTPs) and contain the conserved consensus site "HCX₅R", but they have different kinases as a substrate *in vitro* and *in vivo*. A subgroup of the DUSPs is called MAPK phosphatases (MKPs) because they specifically act on MAPK family members (Camps et al, 2000).

3.1. The ERK1/2 MAPK Pathway

ERK1 and ERK2 (Fig. D) are highly identical proteins that are ubiquitously expressed and play an important role in the regulation of a high number of cellular processes like proliferation, differentiation, survival, cell adhesion, angiogenesis and chromatin remodelling (Yoon et al, 2006). Through the activation of p90 ribosomal S6 kinase (RSK), mitogen and stress activated kinase (MSK) and MAPK interacting kinase (MNK) ERK1/2 are involved in cell attachment and migration, and they also phosphorylate the transcription factors Elk-1 (Ets related proto-oncogene), c-Fos (FBJ murine osteosarcoma viral oncogene homolog), c-Myc (myelocytomatosis viral oncogene homolog) and Ets domain factors among many others. ERK1/2 get activated by growth factors, serum, phorbol esters and ligands for heterotrimeric G

protein-coupled receptors, cytokines, transforming growth factors, osmotic and other kinds of cell stress, and microtubule depolymerization. Depending on the stimulus ERK1/2 are involved in different cellular responses like cell motility, proliferation, differentiation and survival (Chen et al, 2001; Johnson et al, 2002).

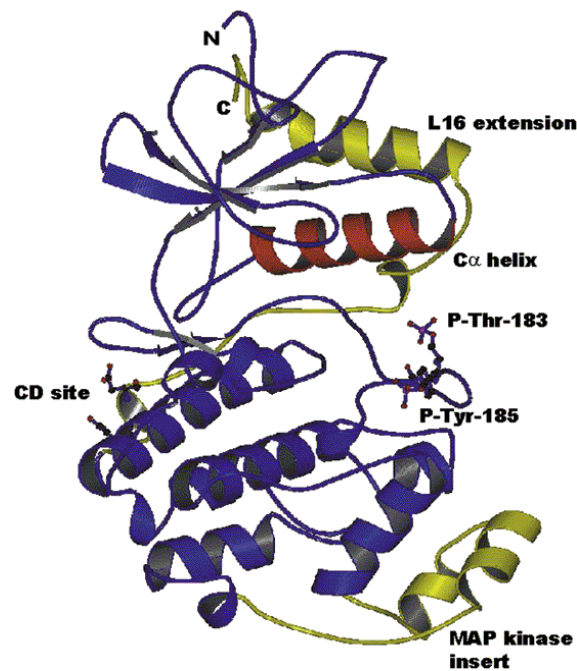


Figure D: Three-dimensional structure of ERK2. The active site of protein kinases are formed at the interface of the two folding domains. ATP is represented in the ERK2 active site. Phosphorylation sites (Y185 and T183) within the activation loop, the MAPK insert, the common docking domain (CD domain), helix C, and the C-terminal extension, L16, are indicated. (Chen et al, 2001)

The MAP2Ks acting upstream of ERK1/2 are the dual specificity ERK Kinases 1 and 2 (MEK1 and MEK2), which phosphorylate tyrosine and threonine in the ERK1/2 activation loops. In this pathway the different v-Raf-1 Murine Leukemia Viral Oncogene Homolog (Raf) isoforms (A-Raf, B-Raf and C-Raf (Raf-1)) are the main MAP3Ks activating MEK1/2. Like other MAP3Ks they phosphorylate two serine residues or a serine and a threonine residue in the activation loop of the MAP2Ks. The Raf family members are activated by a combination of binding to and phosphorylation by small G proteins of the Rat Sarcoma Viral Oncogene Homolog (Ras) family (Rapp et al, 2006).

Another example for a MAP3K is Tumor Progression Locus 2 (Tpl2) which is able to activate ERK1/2, c-Jun N-terminal Kinase (JNK), p38 and ERK5 by the phosphorylation of their upstream MAP2Ks depending on the kind of stimulus (Chiariello et al, 2000).

3.1.1 ERK1/2 proteins

ERK1 and ERK2 are highly similar proteins. Their kinase domain sequences are also related to the sequences of other MAPKs like Raf-1 and MEK1 (Fig. E).

ERK1/2 localize throughout the cell. 50% of ERK1/2 of the cell are bound to cytoplasmic microtubules where they influence the polymerization dynamics to the cytoskeleton (Reszka et al, 1995). ERK1/2 are also associated at adherens junctions and focal adhesions, where they play a role in the regulation of cell-cell and cell-matrix adhesion (Ishibe et al, 2004).

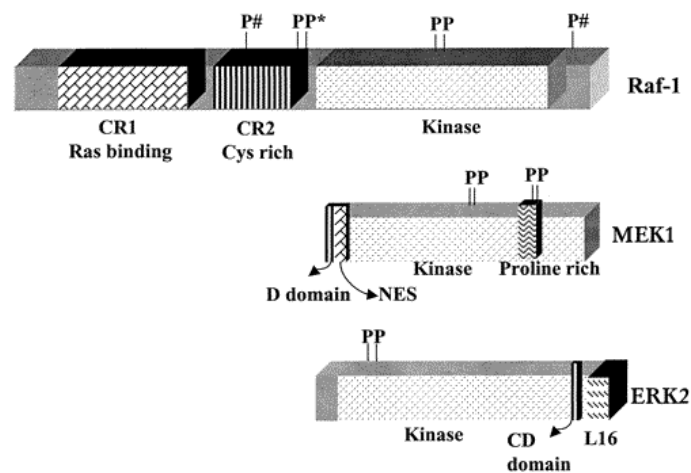


Figure E: Related kinase domain structure of MAPKs. Top: Raf-1. Raf-1 protein consists of a kinase domain and two cystein-rich domain (CR1 and CR2). The phosphorylation sites that are activating Ras are indicated by an asterisk (*). Middle: MEK1. Next to the kinase domain, MEK1 consists of a proline rich sequence and a nuclear export signal (NES). MEK1 gets activated by phosphorylation sites in the activation loop. Bottom: ERK2. ERK2 shows 80% similarity to ERK1. The picture indicates the kinase domain, the common docking domain (CD) and the C-terminal extension (L16) (Chen et al, 2001).

Upon activation by growth factors and other ligands ERK1/2 translocate into the nucleus where they can access nuclear transcription factors and other nuclear proteins to be activated or stabilized. As a consequence the expression of diverse genes is modified. The localization of ERK1/2 in the cell is strictly regulated. MEK1 is known to be an important regulator for the ERK1/2 distribution. MEK1 protein has a nuclear export signal (NES) and serves as a shuttle for ERK1/2 by binding it and being exported in associated form (Adachi et al, 2000). Both, active and inactive ERK1/2 can be transported into the nucleus by a passive process which involved the binding of ERK1/2 to DEF motif (FXF repeats, ERK and FXFP docking motif) of nucleoporins in the nuclear pore complex (Matsubayashi et al, 2001). In addition phosphorylated ERK1/2 can be actively transported into the nucleus (Ranganathan et al, 2006).

3.1.2. The specificity of ERK1/2 interactions

MAPKs contain docking motifs and reciprocal interaction motifs that play a crucial role for the specificity in MAPK signaling. The common docking motif (CD motif) is a cluster of positively charged residues with at least two hydrophobic residues next to it and it is located N-terminal to the characteristic serine/threonine/proline phosphorylation site that is phosphorylated by ERK1/2 (Tanoue et al, 2001). Another motif found in ERK1/2 substrates is the DEF motif. Elk-1, Serum Response Factor Accessory Protein 1 (SAP-1), c-Fos and the Scaffold Kinase Suppressor of Ras (KSR) contain this motif (Jacobs et al, 1999) (Chang et al, 2002).

Another way how the specificity of the interactions of ERK1/2 is determined is the regulation of signalling by scaffold proteins. Scaffolding proteins are assembling certain components of the MAPK cascade to initiate the action of their target proteins to start the signalling cascade (Elion et al, 2001; Kolch et al, 2005; Morrison et al, 2003). Scaffolding proteins were first discovered in the yeast pheromone mating pathway, where Pheromone-Response Scaffold Protein (Ste5p) assembles a MAPK module that gets coupled with cytoskeletal components of the cell. Ste5p does not exist in higher eukaryotes, but there is a number of other binding proteins that fulfil

similar function. Scaffolds for the ERK1/2 pathway are MEK Partner-1 (MP1) and Arrestin- β 1 (ARB1).

The role of the most scaffolds in regulating ERK1/2 is not clearly established. MP1 for example is known to initiate the formation of ERK complexes upon Epidermal Growth Factor (EGF) stimulation (Teis et al, 2002).

Another way how the activity of MAPKs is influenced is the action of MAPK phosphatases (MKPs), which selectively dephosphorylate MAPKs. These phosphatases belong to the family of dual-specificity phosphatases, what means, that they are able to dephosphorylate serine/threonine residues as well as tyrosine residues (Owens et al, 2007).

Partially the specificity of ERK signalling may be also due to temporal variation in the strength and localization of ERK (Murphy et al, 2006). A constitutive but not transient ERK signalling induces genes involved in cell-cycle entry, like Cyclin D1, and represses genes involved in the inhibition of proliferation (Yamamoto et al, 2006). But if ERK signalling is too high elevated, the cell goes into cell-cycle arrest by the stabilization of Cdk-inhibitors like p27 and p21. These mechanisms are important in the development of cancer, where deregulation of the MAPK signalling plays an important role. Obviously the balance between the strength of ERK signalling and appropriate negative feedback loops is fundamental to avoid the induction of cell-cycle arrest, but it also indicates, that some MAPK inhibitors could induce tumorigenesis (Sewing et al, 1997; Woods et al, 1997).

3.4. The role of MAPKs in cancer development

A high percentage of cancers show a deregulation of the MAPK pathways, indicating their important role in tumorigenesis. The development of a tumor requires a number of mutations in the cell in order to acquire certain abilities. These are: high proliferative property also without growth factors, mechanisms to avoid apoptosis, insensitivity of anti-growth signals, telomerase activity for unlimited replication, the ability to metastasize and to induce vascularization for nutrient supply (Hanahan and Weinberg, 2000).

Deregulation of the ERK pathway is involved in 30% of human cancers. In particular the signalling which is activated through growth factors is important in that context.

Most of these mutations are concerning the apex of the pathway, that includes the overexpression of growth factor receptors, a higher supply of activating ligands, and mutations of Ras and Raf. In addition also a high number of transcription factors were found to be over-activated in cancers, like Myc and Activator Protein 1 (AP-1) (Giancotti et al, 1999).

Mutated Ras shows a higher activating property by a decreased ability of hydrolysing the guanosine triphosphate (GTP), leading to a constitutively active state (Hancock et al, 2005; Mor et al, 2006).

In the Raf family, only B-Raf has a high tumorigenic potential. Mutated B-Raf, showing a mutation in the activation loop leading to a elevated catalytic activity, is present in two third of human malignant melanomas (Davies et al, 2002; Wan et al; 2004).

The three Raf family members have different activating ability for MEK1 and MEK2, where B-Raf was shown to have the highest potential for MEK1/2 phosphorylation (Marais et al., 1997; Wu et al., 1996).

4. Protein phosphatases

The family of protein phosphatases consists of three distinct gene families. These families differ in a high degree in structure and function, but catalytic domains are highly conserved within the families (Table A). The members belonging to one phosphatase family have a common conserved catalytic domain, but they are gaining diversity by the addition of different functional domains and regulatory subunits. These domains are influencing different features of the protein, including the specificity, the location or the folding.

Nomenclature of protein phosphatases	
PPP family	
Catalytic subunit PP1c	Regulatory subunits GM, GL, M110 + M21, NIPP-1, RIPP-1, R110, p53BP2, L5, sds22, RB gene product, inhibitor-1, CARPP-32, inhibitor-2, splicing factor, kinesin-like protein, γ 134.5 (Herpes simplex), R5
PP2Ac	A subunit (PR65) B subunit (PR55, PR72, PR61), eRF1, PTPA, SET, polyoma middle and small T antigens, SV40 small T antigen
PP2B	B subunit, calmodulin, AKAP-79
Novel protein phosphatases of the PPP family	
PPP1:	PPY, Ppz1, Ppz2, Ppq1
PP2A:	PP4, PP6, PPV 6A, sit4, Ppc1, Ppg1
PPP5:	PP5, RdgC
PPM family	
RR2C Arabidopsis ABI1 Arabidopsis KAPP-1 Pyruvate dehydrogenase phosphatase Bacillus subtilis SpoII ϕ phosphatase	
PTP family	
Tyrosine-specific phosphatases	
Cytosolic, nonreceptor forms	
PTP1B, SHP-1, SHP-2	
Receptor-like transmembrane forms	
CD45, RPTP μ , RPTP α	
Dual-specificity phosphatases	
CDC25	
Kinase-associated phosphatase	
MAP kinase phosphatase-1	

Table A: Nomenclature of protein phosphatase families: The PPP and PPM families of phosphatases are exclusively dephosphorylating phosphoserine and phosphothreonine residues. The family of PTP proteins is divided into tyrosine-specific phosphatases and dual-specificity phosphatases (DSPs, DUSPs). DSPs are able to dephosphorylate tyrosine, as well as serine and threonine residues (Barford et al, 1998).

The protein phosphatase gene families are the phosphoprotein phosphatases (PPP), Mg^{2+} - or Mn^{2+} -dependent protein phosphatases (PPM) and protein tyrosine phosphatases (PTP). PPPs and PPMs are serine/threonine phosphatases, which are dephosphorylating their substrates by a single reaction using a metal-activated nucleophilic water molecule.

The PTP family includes two subgroups: the first subgroup, the classical PTPs, is exclusively dephosphorylating phosphotyrosine residues, whereas the dual-specificity phosphatase (DSP, DUSP) group of PTPs is able to dephosphorylate all three phospho-amino acid types (Barford et al, 1998).

To be able to understand the complex balance of phosphorylation that is kept by both, protein kinases and protein phosphatases, it is necessary to understand more about the specificity of these proteins, their regulation and their catalytic mechanisms.

4.1. The family of PTPs

PTPs play a fundamental role in cellular processes like cell growth, differentiation, cell cycle, metabolism and cytoskeletal function. Together with PTKs they are determining the phosphorylation state of tyrosine residues (Tonks et al, 2001). The imbalance of these functions was shown to be associated with human diseases like autoimmunity, diabetes and cancer (Blume-Jensen, 2001; Tonks et al, 2001).

PTPs are defined by their signature motif $C(X)_5R$, and consist of two subgroups: the tyrosine-specific, classical PTPs, and second, the dual specificity phosphatases (DUSPs, DSPs) (Andersen et al, 2004).

The cystein residue in the phosphatase-binding loop of classical PTPs is responsible for the nucleophilic action during dephosphorylation by accepting the phosphate group (Guan et al, 1991).

The recognition of the phosphate group takes place in the phosphotyrosine recognition loop, where the the depth of the active site creates the selectivity for phosphotyrosine. Phosphoserine and phosphothreonine amino acid side groups are too short to be dephosphorylated in a PTP catalytic site. (Jia et al, 1995).

The second group, the DSP group, is able to dephosphorylate tyrosine, serine and threonine residues as well as inositol phospholipids (Andersen et al, 2004).

4.1.1. The genomic distribution of PTPs

Until today 38 different human PTP genes have been identified. These genes are nonrandomly distributed in the genome, forming clusters on certain chromosomes. The largest accumulations of PTP genes can be found on chromosome 1 and 12 (Fig. F), but they are absent from chromosomes X and Y and also from chromosomes 16, 17, 21 and 22. On chromosomes 5, 8 and 13 only PTP pseudogenes were found.

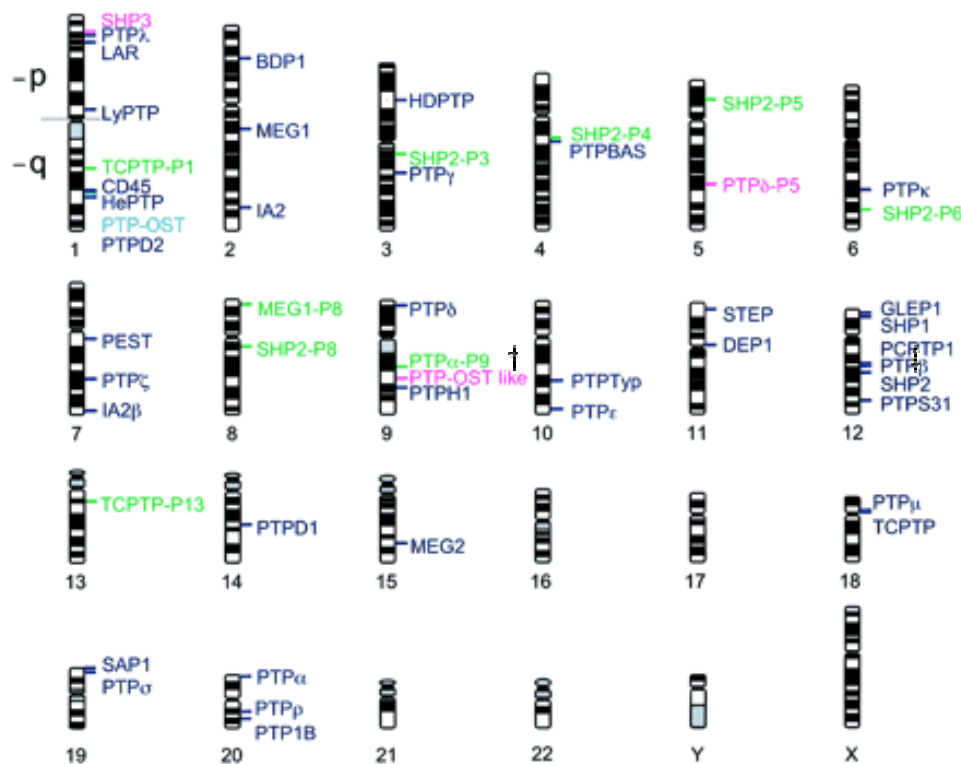


Figure F: PTP related sequences in the human genome: Localization of PTP genes (blue), intronless pseudogenes (green) and pseudogenes containing intron sequences (pink) in the human chromosomes (Andersen et al, 2004).

Highly similar PTPs, like T Cell PTP (TCPTP) and PTP1B, PTPD1 and PTPD2 or PTP α and PTP ϵ rarely share one chromosome, although they highly probably arose from a gene duplication of one ancestral PTP gene. Just chromosome 12 is harboring 2 groups of highly identical PTPs: SH2 Domain Containing Phosphatase 1 (SHP1 and SHP2), the two PTPs sharing the feature carrying a SH2 domain, and three family members of the Receptor Type PTP β (RPTP β) proteins, namely RPTP β , Glomerular Epithelial Protein 1 (GLEPP1) and PTPS31 (Andersen et al, 2004), what possibly could be an indication for a shared regulation or similar functions.

4.1.2 The PTP gene organization

A number of exons of genes encoding PTPs are ranging from 9 (Hematopoietic PTP (HePTP), the smallest PTP, consisting of 339AA) to 47 (Basophile PTP (PTP-BAS), the largest PTP, consisting of 2466AA). In addition, there are remarkable differences in the sizes of the PTP genes. The most compact PTP gene encodes SHP1 in 16 exons spanning only 9960 bp. The largest PTP sequence belongs to RPTP ρ , whose 32 exons are spread over 1117166bp, although the resulting protein is only the ninth largest in the PTP family.

The sequences encoding the catalytic domains (spanning 6-9 exons) of the PTPs are harboring very short introns, compared to the introns found in the sequence of noncatalytic regions or extracellular parts (Andersen et al, 2004; Lim et al, 2001). The conserved sequence motifs, that characterize the PTP family of proteins (Andersen et al, 2004), are not interrupted by introns, except an intron interrupting the phosphatase domains in all transmembrane PTPs and in most nontransmembrane PTPs. The fact that some nontransmembrane PTPs do not show this motif splitting indicates an early evolutionary divergence of these proteins (Besco et al, 2001). The transmembrane segment of receptor-type PTPs, which follows the "positive inside" rule, is encoded by a single exon, supporting the hypothesis of gene assembly by exon shuffling (Fedorov et al, 2001, Koshi et al, 1999).

4.1.3. PTPs and diseases

Diabetes type 2 and obesity were associated with 10 confirmed susceptibility loci in the human genome. 4 PTPs have been suspected to be involved in the development of these diseases, but only PTP1B was proven to be (Ghosh et al, 1999).

Mutated forms of CD45, a transmembrane receptor-like PTP expressed in hematopoietic cells (Trowbridge et al, 1994), was found in patients suffering from severe combined immunodeficiency (SCID), suggesting the important role of CD45 in the activation of T and B cells (Kung et al, 2000 ; Majeti et al, 2000). In addition a silent single nucleotide polymorphism (SNP) in exon 4 of CD45 has been shown to participate in the development of multiple sclerosis (Jacobsen et al, 2000).

Another example for disease related phosphatases is SHP2, whose function is to mediate growth factor and cytokine induced ERK1/2 phosphorylation (Saxton et al, 1997). Mutations in SHP2 sequence causing an inactive SHP2 protein have been reported to be involved in Noonan syndrome, a disease showing symptoms like heart malformation, short stature, learning problems, skeletal malformations, impaired blood clotting and characteristic facial dysmorphia. In addition, SHP2 mutation have been shown to play a role in inherited juvenile myelomonocytic leukemia (JMML), where it causes sustained ERK1/2 activation (Tartaglia et al, 2001).

Initially PTPs were just considered to counteract kinases, leading to an important role as potential tumor suppressors. But the functions of the diverse protein phosphatases appear to be more diverse. For example PTP α is able to activate Src kinase by itself, what can lead to cell transformation (Zheng et al, 1992). An example for a protein tyrosine phosphatase that was shown to function as a tumor suppressor in several kinds of human cancer is Density Enhanced Phosphatase (DEP-1) (Ruivenkamp et al, 2002).

5. Density Enhanced Phosphatase 1 (DEP-1)

Density Enhanced Phosphatase 1 (DEP-1; also known as CD148, Human PTP eta (HPTP η) and PTP Receptor-Type J (PTPRJ)) was first discovered in 1994 by two independent groups. (Honda et al, 1994; Ostman et al, 1994).

Honda et al (1994) isolated DEP-1 mRNA, consisting of 4780 bp, from human placenta. This sequence encoded a protein tyrosine phosphatase composing an extracellular region of 970 amino acids, a transmembrane region of 25 amino acids, and an intracellular region of 342 amino acids.

The intracellular domain of DEP-1 contains only one single catalytic domain, while most of the proteins belonging to the tyrosine phosphatase family contain two catalytic domains, even if one of them is inactive in most of the cases. Another characteristic of DEP-1 is a tandem repeat of multiple fibronectin-typeIII-repeats (FNIII-repeats) in the extracellular domain, which indicate a possible role of DEP-1 in cell-adhesion processes (Fig. G) (Honda et al, 1994).

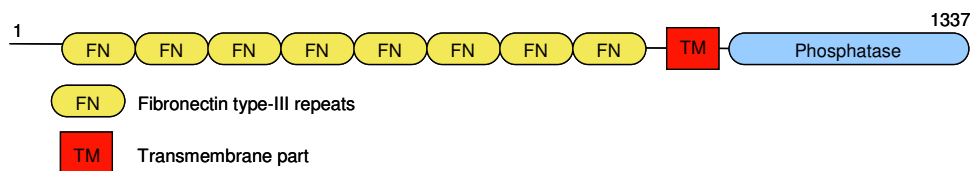


Figure G: Protein structure of DEP-1. Eight FNIII-repeats at the extracellular domain, a short transmembrane domain, and an intracellular phosphatase domain.

This feature classifies DEP-1 as a type III PTP, according to the classification for receptor-type PTPs by Fischer et al (Fischer et al, 1991). In this group of proteins DEP-1 shows a high similarity to SAP-1 and PTP10D.

Depending on the cell type the transfection of full-length DEP-1 leads to protein signals in western blot that are ranging from 180kDa to 250kDa. When these transfected cells are treated with tunicamycin or N-glycosidase F the signal shifts to approximately 140kDa, which fits the predicted molecular weight of DEP-1 calculated according to the amino acid sequence. These findings support the conclusion that

the different molecular weights of DEP-1 that are observed in western blotting are mostly due to N-linked glycosylations at the 34 potential glycosylation sites. (Honda et al, 1994; Ostman et al, 1994).

The DEP-1 gene is located at the short arm of chromosome 11 (11p11.2) (Honda et al, 1994), which is a region that is frequently lost or deleted in diverse human carcinomas like breast or liver carcinoma (Ali et al, 1987; Wang et al, 1988).

Ostman et al (1994) identified DEP-1 in a HeLa cell library. Like Honda et al, they characterized the protein as a RPTP containing several glycosylation sites and FNIII repeats in the extracellular segment. In addition, they hypothesized the function of DEP-1 in contact inhibition of cell growth, because of their observation in experiments with cultured fibroblasts, where DEP-1 expression and activity dramatically increased in dense cultures ($>25,000$ cells/cm²) relative to sparse cultures (<7000 cells/cm²). Because of these findings they proposed the name “high cell density enhanced protein tyrosine phosphatase 1” for the enzyme (Ostman et al, 1994).

FNIII repeats are present in more than 50 different eukaryotic proteins, but most of these domains have no proven function. The FNIII motif number 10 in fibronectin, which is responsible for the adhesion process, contains the conserved motif Arginine-Glycine-Aspartic Acid (RGD). The FNIII repeats of DEP-1 do not show this sequence motif, but five of them contain a XGD motif on the expected loop. This proposes a possible involvement in cell adhesion processes (Ostman et al, 1994).

The amino acid sequences of the cytoplasmic domains in human, mouse and rat DEP-1 exhibit a high homology ($>95\%$), but there are significant differences in the sequences encoding the extracellular regions in which the overall homology between human and mouse or rat in the extracellular domain is 65% or less with exception of the N-terminus and membrane proximal regions. Most obvious is a large insertion in the amino-terminal region of human DEP-1 that is not present in mouse or rat. Mouse and rat DEP-1 show a high similarity of more than 90% in the extracellular domain except in a 24 amino acid insertion in the mouse sequence that is not present in rat and a small region between amino acids 50 to 200 where the homology is 65%. (Zhang et al, 1997).

Although there are remarkable differences in the amino acid sequences of human DEP-1 and the homologous genes in mouse and rat, they show similar structures. All three species show 8 FNIII repeats and 34 potential N-linked glycosylation sites in

the extracellular domain (Zhang et al, 1997; Ostman et al, 1994; Honda et al, 1994; Kuramochi et al, 1996; Osborne et al, 1998; Borges et al, 1996).

DEP-1 is a widely expressed protein. DEP-1 tissue distribution was shown by immunohistochemical analysis, where DEP-1 was found in columnar epithelial cells like those found in small and large intestinal mucosa, appendix, endometrium, oviducts, mammary glands, prostate glands, pancreatic acini and ducts, glandula parotis, sweat glands, and proximal and distal tubules of the kidneys. It is also found in some endocrine cells like thyroid follicular cells, parathyroid gland cells and cells in the islets of Langerhans in the pancreas. Additionally DEP-1 is also expressed in certain endothelial cells, fibrocytes/fibroblasts, Schwann cells and melanocytes. In contrast, neurons and ganglion cells, muscle cells and fat cells do not express DEP-1 (Autschbach et al, 1999).

It is present to different extent in all types of human hematopoietic cell lineages, where it is strongest expressed in granulocytes, followed by monocytes/macrophages. Weaker levels are present in peripheral blood lymphocytes, like CD4- and CD8-positive T-cells, B-cells, platelets, natural killer cells and dendritic cell types. Even less expression is found in transformed lymphoid T- and B-cell lines. The expression of DEP-1 in the thymus was found to be restricted to thymocytes and thymic endothelial cells located in the medulla (De la Fuente-Garcia et al, 1998).

The homologues of DEP-1 in rat (rPTP η) and mouse (Byp) have been reported to be expressed in skin, stomach, pancreas, adrenal gland, placenta, lymphoid tissues, in lung, kidney, liver, brain and many other tissues (Zhang et al, 1997; Kuramochi et al, 1996).

Initial experiments using native and transformed rat thyroid cells demonstrated that DEP-1 was expressed highest in cells that showed features of normal differentiation like thyroglobulin synthesis and thyroid-stimulating hormone dependent growth. However DEP-1 expression could not be detected in cells with highly malignant phenotype that were lacking these differentiation markers and the expression of DEP-1 was shown to inhibit the growth of cancer cells (Zhang et al, 1997).

Trapasso et al performed experiments with rat thyroid cells in which the cells were transfected by retroviruses and cell cycle parameters were analyzed. Malignant cells that were transfected with DEP-1 arrested in G1 phase in a higher extent than control

cells (Trapasso et al, 2000). It was found that the level of Kinase Inhibitory Protein 1 (p27/kip-1) was increased upon transfection with DEP-1 due to a decreased protein degradation mediated by the 26S proteasome, which is activated by the MAPK pathway. Thus, the transfection of cells with DEP-1 inhibited the MAPK pathway, leading to decreased activation of the 26S proteasome, resulting in an increased half-life of p27/kip-1. (Trapasso et al, 2000; Florio et al, 2001). This effect was not seen in control cells transfected with an inactive form of DEP-1 that contains a mutation in the catalytic domain containing a serine instead of the conserved cysteine. In these cells the malignant phenotype could not be reversed (Trapasso et al, 2000).

A loss of heterozygosity (LOH) of DEP-1 was found in 14% of thyroid tumors, including adenomas and carcinomas. Especially the hemizygosity for the DEP-1 polymorphisms Gln276Pro and Arg326Gln was shown to facilitate thyroid carcinogenesis. These data suggest that DEP-1 is a low-penetrance tumor susceptibility gene concerning thyroid carcinogenesis (Iuliano et al, 2004). In addition, it was reported that DEP-1 coimmunoprecipitates with RET receptor tyrosine kinase and that RET gets dephosphorylated by DEP-1. RET gene rearrangements lead to the generation of chimeric RET/Papillary Thyroid Carcinoma (RET/PTC) oncogenes, whereas RET pointmutations occur in familial Multiple Endocrine Neoplasia type 2 (MEN2) and sporadic Medullary Thyroid Carcinomas (MTC). DEP-1 also coimmunoprecipitates with defined MEN2-type mutated RET, but is not able to bind RET/PTC isoforms. Thus RET/PTC mutants are resistant to the dephosphorylating activity of DEP-1 (Iervolino et al, 2006).

DEP-1 is also a candidate tumor suppressor in the colon epithelium. This was shown by the re-introduction of DEP-1 into a DEP-1 deficient colon cancer cell line. These experiments showed that DEP-1 expression caused a remarkable inhibition of cell proliferation and cell migration (Balavenkatraman et al, 2006).

Also other malignant cell types have been tested for the expression of DEP-1. In some high-grade breast carcinoma cell lines the level of DEP-1 expression was markedly decreased. Because DEP-1 upregulation is associated with the differentiation of cells, the decrease of DEP-1 expression could be an indication for the dedifferentiation and autonomous growth of malignant cells (Autschbach et al, 1999).

DEP-1 was identified as a possible candidate for the modulation of the activity of the platelet-derived growth factor β receptor (PDGF β -receptor). In porcine aortic endothelial cells the ligand-dependent tyrosine phosphorylation was decreased after transfection of a construct encoding DEP-1. A direct interaction between DEP-1 and PDGF β -receptor was proven by Co-Immunoprecipitation (CoIP) (Kovalenko et al, 2000).

By using a substrate-trapping mutant form of DEP-1 it was demonstrated, that DEP-1 is interacting with the Hepatocyte Growth Factor/Scatter Factor Receptor (Met). Met was shown to induce mitogenic, motogenic and morphogenic responses upon ligand activation. Disordered signaling through Met has been implicated in certain cancers. When Met was co-expressed with the substrate-trapping form of DEP-1, stable complexes were formed. Additionally, wild-type DEP-1 was found to site-selectively dephosphorylate Met at C-terminal tyrosines, which are involved in the recruitment of signaling and adaptor molecules including GRB2-Associated Binding Protein 1 (Gab1). In contrast, tyrosine residues in the activation loop of Met were only dephosphorylated, when DEP-1 was expressed at high levels. This suggests, that DEP-1 possibly regulates Met-signaling after ligand-induction by Hepatocyte Growth Factor (HGF). In this context it was shown, that Growth Factor Receptor-Bound Protein 2 (Grb2), an interaction partner of Met, was less recruited to Met with increasing expression of DEP-1 (Palka et al, 2003). Interestingly, DEP-1 and Met share some interaction partners, these include Gab1, β -catenin, and p120 catenin (Palka et al, 2003; Holsinger et al, 2002). Holsinger et al. were searching for interaction partners of DEP-1 using a substrate-trapping mutant of DEP-1 and identified p120 catenin, a component of adherens junctions next to β -catenin and γ -catenin. The interaction of DEP-1 and p120 catenin was verified by CoIP experiments. DEP-1 was also found to colocalize with p120 catenin at sites of cell-cell contacts. These findings indicate an important role of DEP-1 in the generation of cell-cell contacts and adherens junctions through the interaction with members of the catenin protein family (Holsinger et al, 2002). With regard to these data, DEP-1 was also reported to inhibit PDGF-stimulated cell migration, by the inhibition of Ras- and Erk1/2-activation by PDGF. Additionally, cell-substrate adhesion was enhanced by DEP-1 and that could have been due to an elevated activity of Sarcoma kinase (Src) after cell attachment (Jandt et al, 2003).

In contact-inhibited endothelial cells the MAPK pathway is inhibited by DEP-1. In contact inhibition Vascular Endothelial Growth Factor Receptor 2 (VEGFR-2) forms a complex with Vascular Endothelial Cadherin (VE-cadherin). DEP-1, by binding β -catenin and p120, could associate with the VEGFR-2-VE-cadherin complex and dephosphorylate the receptor. In addition, it was shown that siRNA against DEP-1 increased VEGFR-2 phosphorylation (Lampugnani et al, 2003).

The role of DEP-1 in somatostatin receptor (SSTR) signaling was demonstrated by experiments done in the rat thyroid cell line PC Cl3 in which a cell cycle arrest in G1 by the PTP-dependent overexpression of the cyclin dependent kinase p27/kip1 was observed in response to somatostatin (SST). These experiments suggested that DEP-1 possibly acts downstream of MEK or directly on ERK1/2 (Florio et al, 2001). These observations have been verified by CoIP experiments in glioma cell lines where SST-activated DEP-1 was directly associated to dephosphorylated ERK1/2. Additionally, the upregulation of p27/kip-1 was seen in this context (Massa et al, 2004).

In PC Cl3 cells this upregulation of p27/kip-1 was found to be due to the inhibition of its phosphorylation by ERK1/2, what is suppressing the ubiquitination of CDKs. As a consequence p27/kip-1 is protected from degradation by the proteasome resulting in an increased half-life of the protein. (Florio et al, 2001).

Interestingly, it was shown that the cytostatic effect of SST-stimulation required the expression and activation of DEP-1. In cell lines lacking DEP-1 expression, SST only induces G1-cell cycle arrest after reintroduction of DEP-1 by transfection, while a dominant-negative form does not show this effect (Massa et al, 2004).

In CHO-K1 cells it was demonstrated that in the resting state of the cells a big multimeric protein cluster is formed that includes the SST-Receptor-1, the G protein, Janus Kinase 2 (Jak2), SHP-2, Src and DEP-1 (Arena et al, 2007). In this complex the G protein activates Jak2 that, in turn, phosphorylates SHP-2. Activated SHP-2 dissociates from the receptor and dephosphorylates Src at its C-terminus. Dephosphorylated Src, in turn, phosphorylates DEP-1 causing the sustained activity of the phosphatase that dephosphorylates and inactivates ERK1/2 (Fig. H) (Arena et al, 2007).

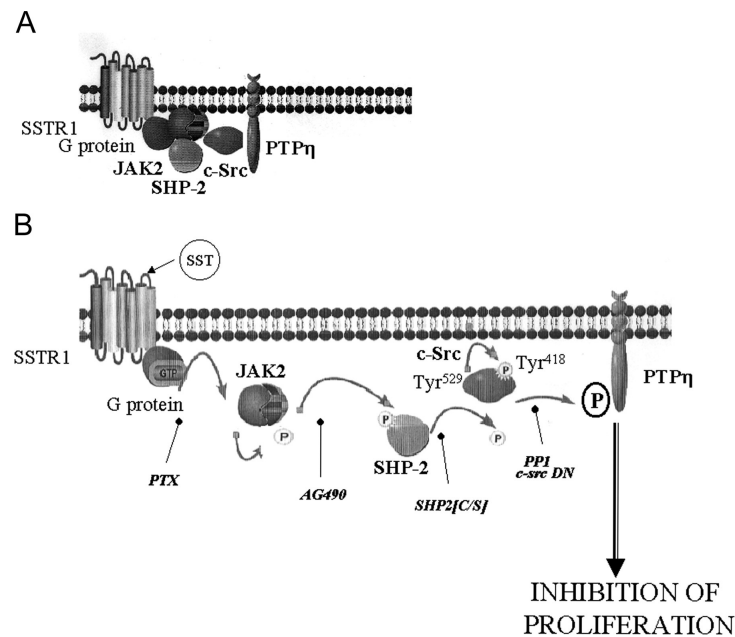


Figure H: DEP-1 activation by somatostatin. A.: The graph shows the multimeric complex that is formed in resting cells. This complex includes SSTR1, G-protein, JAK2, SHP-2, Src and DEP-1 (PTPη). B.: SST inhibits proliferation by activation of DEP-1: SST binding to SSTR1 induces JAK2 phosphorylation via G-protein. JAK2 activates SHP-2, what leads to dephosphorylation of Src at the inhibitory site followed by activation by phosphorylation at T418. Src phosphorylates DEP-1 and activates it (Arenea et al, 2007)

Similar cascades have been identified for both SST receptors (SSTR1 and 2), which involve a similar set of tyrosine kinases and phosphatases, leading to the activation of an effector phosphatase (Fig. I) (Arena et al, 2007; Ferjoux et al, 2003).

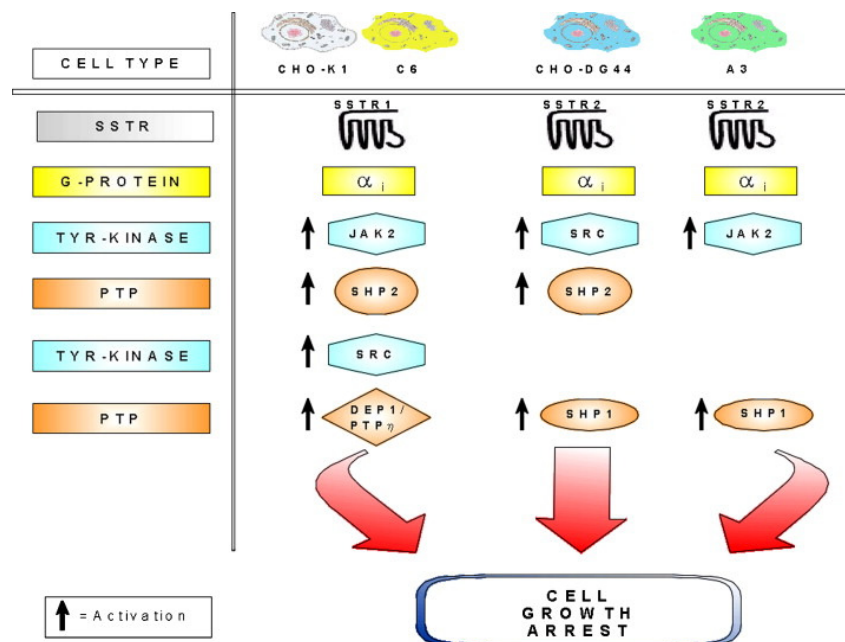


Figure I: Somatostatin receptor pathways. Scheme demonstrating the intracellular cascades for the activation of the effector PTPs DEP-1 and SHP-1. (Florio et al, 2007)

Takahashi et al reported about the generation of homologous recombinant mice expressing mutated DEP-1, in which the intracellular domain was replaced by enhanced green fluorescent protein (EGFP). Homozygous mutant embryos died until E11.5 displaying prominent growth retardation and severe intra- and extraembryonic vascular anomalies (Takahashi et al, 2003).

Until E8.25 homozygous mutant embryos do not display a disturbed phenotype, indicating that DEP-1 is not needed for the specification of angioblasts from the ventral mesoderm, their migration and their formation into major vessels. After E8.25 first defective structures appeared, like enlarged and fused yolk sac vessels and a poorly formed cerebral vascular plexus. Already at E9.5 these embryos show growth retardation, absence of large branching vessels and an accumulation of primitive blood cells in the yolk sac. At E10.5 the homozygous mutant embryos are lacking large branching vessels in the cerebral vasculature, indicating a defective remodeling from the primary vascular plexus to mature vasculature. Peripheral vessels are enlarged and densely interconnected, and yolk sac vessels appear as oversized tubes formed by endothelial cells. The dorsal aorta appeared collapsed and atrophic

and the pericardial cavities were enlarged. Normally, endothelial cell layers attach to mesothelial and endodermal layers. This connection is disturbed in DEP-1 deficient mice (Takahashi et al, 2003).

Homozygous mutant embryos develop a decreased number of vessels but with a notably larger diameter. Additionally, there is a significantly increased number of endothelial cells in the yolk sacs of the homozygous mutant embryos, while the number of endodermal cells is not increased. These observations lead to the hypothesis, that DEP-1 deficiency causes enhanced endothelial proliferation and defective endothelial-mesodermal contact formation. Perivascular structures, including vascular smooth muscle cells (vSMCs) and pericytes, are only sparsely distributed and not properly integrated. Takahashi et al hypothesized, that the endothelial compartment expansion in homozygous mutant embryos is caused by the DEP-1 deficiency resulting in a loss of growth regulation and also by additional growth stimulation by hypoxia-induced VEGF, that was found elevated in the mutant embryos. DEP-1-deficiency possibly impairs initiation or/and maturation of primary cell-cell contacts. Another possibility is that the elevated growth rate of the endothelial cells does not allow the formation of intercellular contacts (Takahashi et al, 2003).

6. Hepatitis B core-Antigen binding protein (HBCBP)

The nucleotide and amino acid sequences of HBCBP were accessible on NCBI (Bethesda, MD) since 2003. The sequence of HBCBP comprises 591 basepairs and has the locus number AF529371. The corresponding protein sequence was published with the locus number AAQ09605 and has a predicted molecular weight of 21531 Dalton. The HBCBP gene is located at chromosome 12q13.3 and does not contain any introns.

Lu et al demonstrated HBCBP as an interaction partner of Hepatitis B Core Antigen (HBcAG) (In the paper they use the name C12, but it resembles the same gene). They identified the protein by an Y2H interaction study using HBcAG as bait. Furthermore, microarray analysis using HBCBP transfected cells indicated that the overexpression of HBCBP was involved in the transcription regulation of several genes, including Insulin Receptor (INSR) and Tumor susceptibility gene 101 (TSG101). A Y2H screen using HBCBP as bait identified a number of potential binding partners that are involved in different cellular processes, like energy metabolism and signal transduction. (Lu et al, 2005).

Since then, no other data dealing with this newly identified gene and protein were published.

AIMS

After we found an interaction between DEP-1 and a newly discovered protein with an utterly unknown function, HBCBP, our primary aim was to find out more about this protein. Our first attempt was to search for a function in which the interaction between HBCBP and DEP-1 could be of importance. Based on the knowledge that DEP-1 affects the cell cycle by the inhibition of MAP-Kinases we considered that HBCBP could also be involved in that process. We were analyzing this aspect by the use of Elk1-Reporter assays.

Furthermore we wanted to proof the interaction between HBCBP and DEP-1 in the human system by CoIPs. In that context we also did immunostaining experiments to see the cellular localization of HBCBP together with DEP-1 and their possible place of interaction.

After dealing with several difficulties with proving an interaction of HBCBP and DEP-1 we used siRNA to knockdown HBCBP and DEP-1 in combination with the Elk1-reporter system to see, if the effect the two proteins have on the MAP-Kinase pathway is dependent on the presence of their suspected interaction partner.

Searching for other potential interaction partners of HBCBP that could mediate the effect that HBCBP has in Elk1-reporters we did CoIPs to see if HBCBP interacts with MEK1, ERK1/2 or DUSPs.

To see the direct effect of HBCBP on MAP-Kinases, we wanted to see its influence of proliferation and apoptosis. We tested these aspects using flow cytometry.

With the aim to find hints for the purpose of HBCBP we analyzed multi-tissue panels for differences in the extent of the expression of the protein. For the same reason we wanted to analyze a hypothetical HBCBP promoter for potential regulatory sites that could indicate in which processes the protein could be involved. In addition we tried to find out more about the protein by the use of different software-programs to make predictions about its evolutionary descent, potential functional domains and phosphorylation sites.

In addition we tried to purify recombinant HBCBP for the purpose of the generation a polyclonal antibody.

METHODS

1. Plasmids and Constructs

pCMV-Myc-HBCBP: Full-length HBCBP was amplified using the (5' GCC CGA ATT CGG ATG ATA AGT GAA GGC GGA TGG GGA TGG CAG GGG 3') containing an EcoRI restriction site and the reverse primer (5' GCT CGT CGA GCC TCG AGC AGC CTA CTT GTT AAC AGA GGA CTT TTT TGT TTC ATC 3') with a XhoI restriction site. The product was cloned between the EcoRI and XhoI site in the pCMV-Myc plasmid (Invitrogen, Carlsbad, CA). This vector was used to overexpress HBCBP in human cell cultures.

Truncated HBCBP constructs: Primers were designed to amplify the N-terminal, the middle, or C-terminal third of the full-length HBCBP sequence. All forward primers contained EcoRI restriction sites and all reverse primers contained Sall sites. For the N-terminal part (Δ 73-196) of HBCBP (pCMV-Myc-HBCBP Δ 73-196) the forward primer (5'CGA ATT CGA ATG ATA AGT GAA GGC GGA TGG GGA TGG CAG G3') and the reverse primer (5'CGG TCG ACC CAG CTA TGA GGA GCT GAC TCT GGG ACA ACT C3') were used. For the middle part (Δ 1-62;140-196) of HBCBP (pCMV-Myc-HBCBP Δ 1-62;140-196) the forward primer (5'CGA ATT CGG GAG TTG TCC CAG AGT CAG CTC CTC ATA GCT G3') and the reverse primer (5'CGG TCG ACC GGT GCC GGG GAC AGA GGG TGA AGG AGA GAG3') were used. For the C-terminal part (Δ 1-139) of HBCBP (pCMV-Myc-HBCBP Δ 1-139) the forward primer (5'CGA ATT CGG CTC TGT CCT TCA CCC TCT GTC CCC GGC ACC3') and the reverse primer (5'GGT CGA CCC TAC TTG TTA ACA GAG GAC TTT TTT GTT TCA TC3') were used. The products were cloned between the EcoRI and Sall restriction site of pCMV-Myc plasmid (Invitrogen, Carlsbad, CA).

pEGFP-C1-HBCBP : The full-length sequence of HBCBP was amplified from pCMV-Myc-HBCBP using the forward primer (5' CGA GCG AAT TCT GCA ATG ATA AGT GAA GGC GGA TGG GGA TGG 3') containing an EcoRI restriction site and the reverse primer (5' CGC GGA TCC CTT CTA CTT GTT AAC AGA GGA CTT TTT TGT TTC 3') with BamHI restriction site. The product was cloned between the EcoRI and BamHI restriction site in the pEGFP-C1 plasmid (Clontech, Paolo Alto, CA). This

vector was used to overexpress HBCBP in human cell cultures for microscopy experiments.

pET24a-HBCBP: Full-length HBCBP was amplified using the forward primer (5' GCC CGA ATT CGG ATG ATA AGT GAA GGC GGA TGG GGA TGG CAG GGG 3') containing an EcoRI restriction site and the reverse primer (5' GCC TCG AGC AGC CTT GTT AAC AGA GGA CTT TTT TG 3') containing an XhoI restriction site. The product was cloned between the EcoRI and XhoI site in the pET24a vector (Novagen, Darmstadt, D) containing a pentameric His-tag at the 3' end of the cloned sequence. The vector was used for expression in bacteria with the purpose of purification. The purified protein aimed to be an antigen for antibody production.

All constructs were confirmed by sequencing with ABI Prism[®] Big Dye[™] Terminator Cycle Sequencing Ready Reaction Kit (Applied Biosystems, Foster City, CA) on 310 Genetic Analyzer (Perkin Elmer, Wellesley, MA)

pSR α -CD148/HA and pSR α -CD148 Δ cyto vectors, to overexpress HA-tagged DEP-1 or non-tagged DEP-1 truncated for its cytoplasmic domain, were previously described. The vector pSR α -CD148/HA was used to overexpress full-length DEP-1 in all following experiments (Takahashi et al, 2006).

Reporter vectors: Vectors from the PathDetect trans-reporting system were purchased from Stratagene (La Jolla, CA). These vectors were pFR-Luc (trans-reporting Luciferase plasmid) and pFA2-Elk1. The PathDetect System was modified for the Dual-Luciferase Reporter-System by the use of the reference vector pRL-CMV (Promega, Madison, WI).

The Nur77 overexpression plasmid pcDNA3.1-Nur77 (1-598 amino acids, full length, wt) were described previously (Gruber et al, 2003).

2. Cell Culture

Human Embryonic Kidney 293 cells (HEK293), Hepatocellular Carcinoma cells (HepG2), LNCaP cells (Prostate epithelial cancer cell line) and RWPE1 cells (Prostate epithelial cell line) were obtained from ATCC (Manassas, VA) and cultured as recommended. Human Umbilical Vein Endothelial Cells (HUVECs) were cultured as previously described (Gruber, F., 2003) and used until the 5th passage. Treatment with different stimuli was done with cells that reached approximately 80% confluency,

if not stated differently. Reagents used for stimuli were: phorbol 12-myristate 13-acetate (PMA, Sigma, St. Louis, MO), transforming growth factor β 1 (TGF β 1, BioSource International, Camarillo, CA), Interferon- α (IFN α , R+D Systems, Inc., Minneapolis, MN), Interferon- γ (IFN γ , R+D Systems, Inc., Minneapolis, MN), tumor necrosis factor α (TNF α , Merck, Darmstadt, D), WY14643 (Biomol, Hamburg, D), Rosiglitazone-maleate (Alexis biochemicals, Lausen, CH) and Prostaglandin E2 (PGE2, Sigma, St. Louis, MO). When stimulating with substances dissolved in dimethyl sulfoxide (DMSO), the control cells were also treated with the corresponding amount of DMSO. HEK293 were transiently transfected for luciferase reporter assays or other experiments using calcium-phosphate-protocol (Perkins et al, 1993) and 1.5 μ g DNA per well in 6-well plates or 1 μ g DNA in 12-well plates and chamber slides. HepG2 cells were transfected using Lipofectamine Plus Reagent (Invitrogen, Carlsbad, CA) according to manufacturer's protocol. In experiments with transfected cells, the cells were used for experiment 48 hours after transfection, in the confluent state, if not indicated differently. Stimulations on transfected cells were done in the subconfluent state. Transfections in combination with siRNA into HEK293 and HepG2 cells were done using polyethylenimin (PEI, Sigma, St Louis, MO). For the transfection of one 12-well 3 μ l of vortexed PEI (35 μ M, pH 7.0) were mixed with 46.5 μ l of 2xHeBS buffer (280mM NaCl, 1.5mM Na₂HPO₄, 50mM Hepes, pH 7.05). In a second tube 5 μ l of siRNA (20 μ M) or scrambled control RNA and expression vectors were mixed with 46.5 μ l of 2xHeBS. The two solutions were mixed together and incubated in the dark at room temperature for 20min. The media on the cells was removed and 400 μ l of serum free media were added. 100 μ l of transfection mix were added per 12-well and incubated for 3 hours and then exchanged to serum containing media. The cells were used for experiment 48 hours after transfection, if not indicated differently. SiRNAs were purchased from Ambion (Foster City, CA). The HBCBP siRNA sense strand was (AGU AUC AAG GGA UGU CAU UdTdT) and the antisense strand was (AAU GAC AUC CCU UGA UAC UdTdT), and the DEP-1 siRNA sense strand was (GCA GUA CAG CAG AAU CCU UdTdT) and the antisense strand was (AAG GAU UCU GCU GUA CUG CdTdT).

3. Co-Immunoprecipitations (CoIPs)

HEK293 cells were seeded in 6-wells. The next day the cells were transiently transfected with pCMV-Myc-HBCBP and/or pSR α -CD148/HA to overexpress Myc-HBCBP and/or HA-DEP-1. 48 hours later, the cells were lysed for 30min in 350 μ l/6-well of CoIP cell lysis buffer (2.7mM KCl, 1.5mM KH₂PO₄, 9.2mM Na₂HPO₄ 2H₂O, 150mM NaCl, 0.7% NP40, 0.3% Triton X-100 and Complete Protease Inhibitor Cocktail (Roche Diagnostics, Basel, Switzerland)). 3 6-wells were used for 1 sample. Lysates were centrifuged to remove cell debris. At this stage whole cell lysate (WCL) aliquots were taken to check protein expression. Where indicated, the NaCl concentration in the cell lysate was increased by the addition of 2M NaCl, otherwise the cell lysate contained 150mM NaCl present in the Lysis Buffer. When Sepharose beads were used, 2 μ g of antibody were added to the cell lysate and rotated at 4 °C for 30min. Then 20 μ l of Sepharose beads were added (for mouse antibodies – protein G-Sepharose, for rabbit antibodies – protein A-Sepharose (Amersham Biosciences, Buckinghamshire, UK), and further incubated at 4 °C for 3.5 hours.

In the case of Dynabeads M-280 Tosylactivated (Invitrogen, Carlsbad, CA), the antibody to be linked was dialyzed in 0.1M borate buffer pH9.5 for 3 hours. Dynabeads were prepared and covalently linked with the antibody according to the manufacturer's protocol. 15 μ l of linked Dynabeads were used for one sample and incubated for 4 hours at 4 °C.

Then the beads were washed 3 times with PBS and then resuspended in Laemmli buffer, vortexed and heated to 95 °C for 10min. The supernatants were collected and subjected to western blot. Antibodies used for CoIP-pull down were mouse anti-CD148 (Invitrogen, Carlsbad, CA), mouse anti-Myc (Oncogene, San Diego, CA), rabbit anti-EGFP (Abcam, Cambridge, UK), rabbit anti-MKP-3 (anti-DUSP6, Santa Cruz Biotechnology, Santa Cruz, CA), rabbit anti-MKP-4 (anti-DUSP9, Santa Cruz Biotechnology, Santa Cruz, CA), rabbit anti-HA (Santa Cruz Biotechnology, Santa Cruz, CA) and the control antibodies normal mouse IgG (Santa Cruz Biotechnology, Santa Cruz, CA), rabbit immunoglobulin fraction (DAKO, Milan, Italy). All CoIP-experiments were repeated at least 3 times.

4. Interaction on ELISA-plates

HEK293 cells were seeded in 6-wells. The next day the cells were transiently transfected with p-CMV-Myc-HBCBP and/or pSR α -CD148/HA. 48 hours after, the cells were lysed for 30min in 350 μ l/6-well of CoIP cell lysis buffer (2.7mM KCl, 1.5mM KH₂PO₄, 9.2mM Na₂HPO₄ 2H₂O, 150mM NaCl, 0.7% NP40, 0.3% Triton X-100 and Complete Protease Inhibitor Cocktail (Roche Diagnostics, Basel, Switzerland)). Lysates were centrifuged to remove cell debris. Microtiter plates (Nunc maxisorp; Nunc, Roskilde, Denmark) were coated with 4 μ g/ml rabbit anti-DEP-1 antibody (Santa Cruz Biotechnology, Santa Cruz, CA) or rabbit immunoglobulin fraction in 100mM NaHCO₃ buffer, pH 9.3 at 4°C overnight. In uncoated wells NaHCO₃ buffer was used without antibodies. The wells were blocked with 1% BSA in PBS for 2 hours at 37°C and then 100 μ l of cell lysate were applied and incubated for 4 hours at 37°C. The wells were incubated with mouse anti-Myc antibody in 0.5% BSA in PBS (1 μ g/ml) for 1 hour at 37°C and then further with second peroxidase-coupled anti-mouse antibody (1 μ g/ml) (Amersham Biosciences, Buckinghamshire, UK). Inbetween all these incubation steps the wells were washed 3 times with 0.5% Tween 20 in PBS. Then 100 μ l ABTS solution containing 1g/l diammonium 2,2-Aazino-di-(3-ethylbenzothiazoline-6-sulfonate) (Roche Diagnostics, Basel, Switzerland), 77 mM Na₂HPO₄, 60 mM C₆H₈O₇, 1 mL/L H₂O₂ was added to the wells. The reaction was stopped with 100 μ l 0.32% NaF and the absorbance at 405 nm was determined using an ELISA reader (EL 808 Ultra Microplate Reader, Bio-TEK Instruments). To determine non-specific binding of Myc-HBCBP uncoated wells were used.

5. Western blotting

Cells were lysed in 1x Laemmli buffer for 10min, and additionally sonicated. The lysates were heated to 95°C for 10min before use. These samples or collected samples from CoIPs were subjected to 10% SDS-polyacrylamide gel electrophoresis (SDS-page) and transferred by western blotting to a polyvinylidene difluoride membrane (Millipore, Bedford, MA). First antibodies that were used are indicated in figure legends. Detection of immunoreactive bands was done by the use of second

HRP-linked antibodies and ECL-Plus reagent (Amersham Biosciences, Buckinghamshire, UK) according to manufacturers protocol. For anti-phospho-Serine (anti-P-Ser) and anti-phospho-Threonine (anti-P-Thr, Sigma, St. Louis, MO), which are biotinylated antibodies, we used Streptavidin-HRP (Becton Dickinson, Franklin Lakes, NJ) as second step to visualize the protein.

6. Immunostaining

HEK293 were grown to 50-80% confluency in chamber slides (Nalge Nunc International, Naperville, IL) and transfected with pEGFP-C1-HBCBP and pSR α -CD148/HA or pSR α -CD148 Δ cyto. The cells were fixed in 4% paraformaldehyde, afterwards permeabilized with Triton X-100 and then stained HA-DEP-1 and Δ cyto-DEP-1 with mouse anti-CD148 (Invitrogen, Carlsbad, CA) at a dilution of 1:300 and Alexa fluor 568 conjugated goat anti-mouse second antibody in 1:300 dilution (Molecular Probes, Eugene, Oregon). Presence of enhanced green fluorescent protein (EGFP) from the transfected vector pEGFP-C1-HBCBP was determined on a LSM510 confocal laser microscope (Zeiss, Germany) at 488nm excitation and 512nm emission wave length and separated from the Alexa Fluor 568 label (excitation wavelength 543nm, emission wavelength 630nm).

7. Flow Cytometry

HepG2 cells were grown in 6-wells to approximately 50% confluency and then transfected with scrambled RNA or siRNA to knock down HBCBP as described above. For BrdU assay, the cells were stained according to the protocol of BrdU Flow Cytometry Assay Kit (BD Biosciences, Franklin Lakes, NJ). For Ki67 analysis the cells were fixed with 4% paraformaldehyde, permeabilized with 0.5% Tween20 in PBS and blocked with 1% BSA in PBS. The cells were stained with FITC-labeled anti-Ki67 (Invitrogen, Carlsbad, CA) in a dilution of 1:300. For AnnexinV analysis the cells were stained according to the protocol of ApoAlert® Annexin V-FITC Apoptosis Kit (Clontech, Palo Alto, CA). For the propidium iodide (PI) analysis the cells were scraped of the dish and resuspended in 1%BSA containing PBS. The cells were

stained with PI (Sigma, St. Louis, MO) in a concentration of 1µg/ml for 10 min. For all the flow cytometry experiments the cells were analyzed using FACSsort machine (Becton Dickinson, Franklin Lakes, NJ). The data sets were analyzed with FCS Express V3 program.

8. Promotor analysis

The genomic sequence that was analyzed was reaching -900 to +300 bp from the transcription start of HBCBP (1200bp). The sequence was analyzed using the MatInspector software (Genomatix, Munich, D), a software tool that utilizes a large library of matrix descriptions for transcription factor binding sites to locate matches in DNA sequences. In this analysis the matrix group of vertebrates was preselected. The list that resulted from this analysis was used to search for active transcription factor binding sites that regulate HBCBP expression.

9. Quantitative Real-Time PCR (Q-PCR)

Human Multi-Tissue RNA Panel and Multi-tissue cDNA Panel were purchased from Clontech (Paolo Alto, CA). The samples from the RNA panel were reverse transcribed. Placenta tissue was kindly provided by Semmelweis Frauenklinik (Vienna, A). HepG2 cells or HUVECs were grown to subconfluency in 6-well plates and treated with different stimuli as indicated. LNCaP cells and RWPE1 cells were seeded in 6-well plates and grown to confluency. RNA from these cells was extracted using TRIzol reagent (Invitrogen, Carlsbad, CA). Total RNA (900ng) was reverse transcribed with MuLV reverse transcriptase using the Gene Amp RNA PCR kit (Applied Biosystems, Foster City, CA) and d(T)₁₆ primers. The mRNA sequences from the genes to be analyzed were obtained from GenBank. The primers were designed using the PRIMER3 software (Whitehead Institute for Biomedical Research, Cambridge, MA). The following forward (“F”) and reverse (“R”) primers were used for human HBCBP: F 5’ CTG GGT CAG CAG GAT GGT AT 3’ and R 5’ CCG AAG CTG GTA AGA GGT CA 3’. Q-PCR was performed by Light Cycler technology using the Fast Start SYBR Green I kit for amplification and detection (Roche Diagnostics,

Basel, Switzerland). In all assays cDNA was amplified using a standardized program (10' denaturing step and 55 cycles of 5'' at 95°C, 15'' at 65°C, and 15'' at 72°C, melting point analysis in 0.1 °C steps, final cooling step. Each LightCycler capillary was loaded with 1.5 µl of DNA Master Mix, 1.8 µl MgCl₂ (25 mM), 10.1 µl H₂O, and 0.4 µl of each primer (10 µM). The final amount of cDNA per reaction corresponded to 2.5 ng total RNA used for reverse transcription. Reverse quantification of target gene expression was performed using a mathematical model by Pfaffl (Pfaffl et al, 2001). The expression of the target molecule was normalized to the expression of human porphobilinogen deaminase (PBGD) using the primers: F' 5'-TCG AGT TCA GTG CCA TCA TC- 3' and PBGD R' 5'-CAG GTA CAG TTG CCC ATC CT-3'.

10. Reporter Assays

The PathDetect Elk1 trans-reporting system (Stratagene, La Jolla, CA) was modified for the Dual-Luciferase Reporter-System (Promega, Madison, WI) to quantify Elk1-activation according to the manufacturer's instructions. For the PathDetect reporter system HEK293 cells were transfected in 12-wells with 200ng/well with plasmids containing the genes of interest (volume adjusted with pCMV-Myc empty plasmid) and 600ng/well reporter plasmid mixture (80% pFR-Luc, 10% pFA2-Elk1, 10% pRL-CMV) using calcium-phosphate method (cell-culture paragraph). 48h after transfection the cells were lysed and used for analysis. In experiments including siRNA, the reporter vectors were combined with 5µl of 20µM siRNA or control siRNA and the mix was transfected using PEI protocol mentioned in cell-culture paragraph. In reporter assays using siRNA 72 hours after transfection the cells were lysed and used for analysis. The cell lysates were subjected to dual luciferase assays according to manufacturer's protocol (Promega, Madison, WI) on a Victor luminometer (Wallac, Turku, FIN). Photinus luciferase activity was normalized to Renilla luciferase activity.

11. Recombinant HBCBP

One colony of the bacteria strain BL2(DE)pLysS (Novagen, Darmstadt, D) transformed with pET24a-HBCBP was inoculated into LB-media containing 50µg/ml

ampicillin and 34µg/ml chloramphenicol and grown overnight at 37°C. In the morning the culture was diluted to an approximate OD₆₀₀ of 0.2 and then further grown to an OD₆₀₀ of 0.6. Expression of the recombinant protein was induced by addition of 1mM isopropyl-beta-D-thiogalactopyranoside (IPTG) at 30°C for 3hours. Aliquots of the culture were also taken at the timepoints 0, 1 and 2 hours. The cells were pelleted and resuspended in PBS containing 1mM phenylmethylsulfonylfluorid (PMSF) as protease inhibitor. After sonication and spinning, the supernatant was collected in fresh tubes and diluted 1:1 with 2x Laemmli buffer and the pellet was resuspended in 1x Laemmli buffer (contains inclusion bodies). The samples were subjected to Western blot.

12. In silico analysis:

ClustalW2 (EMBL-EBI, Sanger Institute, Hixton, UK): The ENSEMBL homepage (Sanger Institute, Hinxton, UK) provided predicted orthologues of human HBCBP in 5 different species (chimpanzee, elephant, armadillo, guinea-pig and lesser hedgehog tenrec). The ClustalW2 software was used to compare the amino acid sequences of these predicted orthologues to human HBCBP. This program is used to analyse similarities of amino acid sequences and therefore serves to find hints for evolutionary descent.

Block Searcher analysis (Fred Hutchinson Cancer Research Center, Seattle Washington, USA): The Block Searcher is an aid to detect and verify a protein sequence homology. It compares a protein or DNA sequence to a database of protein blocks. It is looking for the most highly conserved regions in groups of proteins. We submitted the complete 196 amino acid sequence of human HBCBP to achieve information about possibly related proteins. The resulting sequences are listed showing combined E-values (Expect-values) that indicated the probability of relationship.

SMART: (Simple Modular Architecture Research Tool, Heidelberg, Germany): The program allows the identification and annotation of genetically mobile domains and the analysis of domain architectures. It detects more than 500 domain families found

in signalling, extracellular and chromatin-associated proteins. These domains are exclusively annotated with respect to phyletic distributions, functional class, tertiary structures and functionally important residues. We submitted the full-length amino acid sequence of HBCBP to the program to achieve domain information about the protein. The result is presented in a list.

ELM-EMBL analysis of HBCBP-Amino-Acid sequence: The ELM server (The Eukaryotic Linear Motif resource for Functional Sites in Proteins, Heidelberg, Germany) is a computational biology resource for investigating candidate functional sites in eukaryotic proteins. The current version of the ELM server provides core functionality including filtering by cell compartment, phylogeny, globular domain clash (using the SMART/Pfam databases) and structure. In addition, both the known ELM instances and any positionally conserved matches in sequences similar to ELM instance sequences are identified and displayed. We used this program to analyze the amino acid sequence of HBCBP for conserved domain patterns.

PredPhospho (National Genome Research Institute, Seoul, Korea): PredPhospho is a program that predicts phosphorylation sites in primary protein sequences. We used this program to find possible phosphorylation sites in HBCBP and therefore we submitted the full-length amino acid sequence.

NetPhos 2.0 Server (Technical University of Denmark, Lyngby, Denmark): This program produces predictions for serine, threonine and tyrosine phosphorylation sites in eukaryotic proteins. We used this program to have a second guess on possible phosphorylation sites in HBCBP. Also here we analyzed the entire amino acid sequence of HBCBP.

Statistical analysis: All experiments were done at least twice. Experimental values are expressed as means \pm standard error of the mean (SEM). Statistical significance of differences was analyzed by student's t-test.

RESULTS

1. Regulation of ERK1/2 MAP-Kinase pathway

Since DEP-1 is known to influence the activity of MAP-Kinases, we were interested, if HBCBP could also play a role in the regulation of these pathways. For that purpose we used the PathDetect Elk1 trans-reporting system (Stratagene, La Jolla, CA), and modified the protocol for the Dual-Luciferase Reporter-System (Promega, Madison, WI). The PathDetect Elk1 trans-reporting system includes a transactivator plasmid leading to the expression of a trans-acting transcription activator that consists of the activation domain of Elk-1 fused with the DNA binding domain of yeast GAL4. The pFR-Luc reporter plasmid of the PathDetect system contains a synthetic promoter with five tandem repeats of the yeast GAL4 binding site that control the expression of *Photinus pyralis* (American firefly) luciferase gene. Upon phosphorylation the DNA binding domain of the Elk1 fusion trans-activator protein binds to the reporter plasmid at the GAL4 binding sites and starts transcription of the luciferase gene. Influences on the phosphorylation level of the Elk1 fusion transactivator protein thus influence the expression level of Luciferase and reflect the activation status. Elk1 gets phosphorylated by ERK1/2, thus representing a read out for the activity of the ERK1/2 MAP-Kinase pathway.

The reporter plasmids were transfected into HEK293 cells in combination with HBCBP and/or DEP-1. Cells were confluent when they were harvested.

Overexpression of DEP-1 (pSR α -CD148/HA) reduced significantly the transcriptional activity of Elk-1. Similarly HBCBP overexpression (pCMV-Myc-HBCBP) inhibited the reporter system. Overexpression of both, HBCBP and DEP-1, had an additive effect (Fig. 1.1.1.). As a positive control PMA as a general enhancer of MAP-Kinase activity was used, that highly increased the Elk-1 activity evidencing that the reporter system worked (1.1.2.).

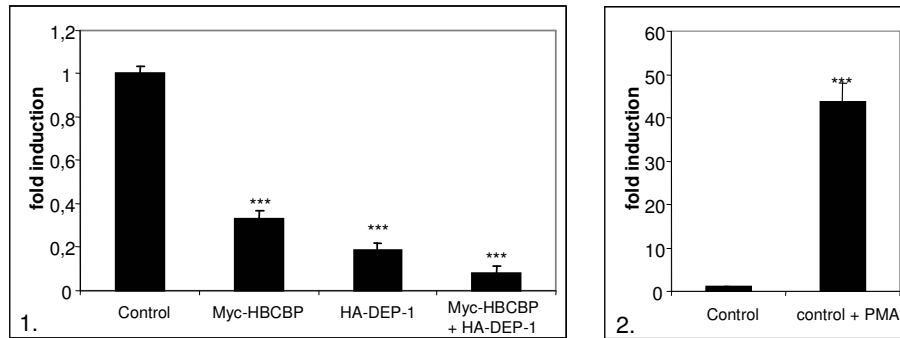


Fig 1.1. Reporter assay on P-elk: Myc-HBCBP and/or HA-DEP-1 were overexpressed in HEK293 cells in combination with Elk-1 Reporter constructs (1). As a positive control cells were stimulated with PMA (50nM) overnight (2). Both, Myc-HBCBP and HA-DEP-1 inhibited the activity of Elk-1 and also acted additive when cotransfected. Pool of 12 values, graph shows means \pm SEM. Statistics calculated using Student's t-test versus control value (***) $P < 0.005$).

To further analyze the HBCBP effect, we did a titration of the pCMV-Myc-HBCBP vector on the Elk1-PathDetect system. As already shown in Fig.1.1.1., DEP-1 and HBCBP reduced Elk1 activity. When half (100ng/12well) or a quarter (50ng/12well) the amount of HBCBP vector was used, the inhibitory activity was lower, a further hint for the specificity of this reporter system (Fig.1.2.).

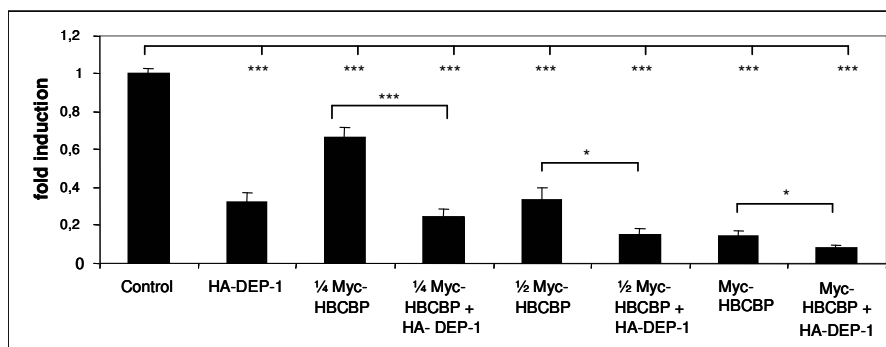


Fig. 1.2. Reporter assay on P-elk: Graph shows a titration of p-CMV-Myc-HBCBP vector in combination with Elk-1 reporter constructs and HA-DEP-1 in HEK293 cells. The down-regulation of Elk-1 activity due to Myc-HBCBP overexpression correlated to the amount of Myc-HBCBP transfected. Pool of 10 values, graph shows means \pm SEM. Statistics calculated using Student's t-test (* t-test $P < 0.05$; *** t-test $P < 0.005$).

To further test the specificity of the Elk1-reporter system, we also analyzed truncated HBCBP constructs. All three truncated HBCBP constructs pCMV-Myc-HBCBP Δ 73-196, pCMV-Myc-HBCBP Δ 1-62;140-196 and pCMV-Myc-HBCBP Δ 1-139 did not show an inhibitory effect on Elk1, further indicating the specificity of the HBCBP effect (Fig.1.3.).

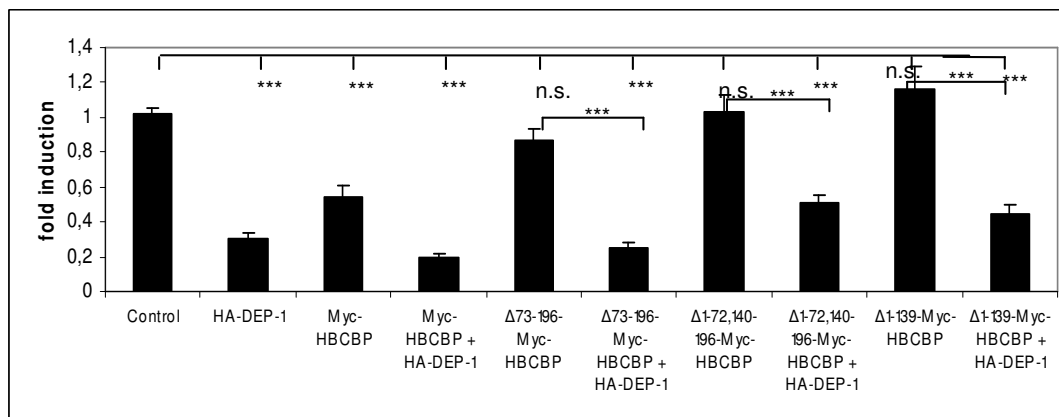


Fig. 1.3. Reporter assay on P-elk: Elk-1 reporter constructs and HA-DEP-1 were cotransfected in combination with p-CMV-Myc-HBCBP or truncated Myc-tagged HBCBP constructs (pCMV-Myc-HBCBP Δ 73-196, pCMV-Myc-HBCBP Δ 1-62;140-196, pCMV-Myc-HBCBP Δ 1-139). Myc-HBCBP and HA-DEP-1 downregulated the activity of Elk-1 and acted additive when coexpressed. In contrast, the truncated Myc-HBCBP constructs did not affect Elk-1 activity, indicating the HBCBP effect to be specific. Pool of 10 values, graph shows means \pm SEM. Statistics calculated using Student's t-test (n.s. (not significant) t-test $P > 0.05$; *** t-test $P < 0.005$).

The activity of DEP-1 is known to depend on the cell density. Thus, we were interested whether the inhibitory effect of HBCBP on Elk1 depended on cell density as well. In the experiments shown previously, only cells that were grown to a dense layer were used. For this set of experiments, cells were seeded in different densities (10000; 25000; 40000 cells/cm²) and then they were transfected with the Elk1-PathDetect vectors in combination with Myc-HBCBP and/or HA-DEP-1. Cells were harvested when the first set of cells was still sparse, the second set subconfluent and the third set fully confluent. Like in the experiments before, Myc-HBCBP showed

inhibitory activity on Elk-1 in the confluent set of cells. In the subconfluent set of cells Myc-HBCBP showed a less inhibiting effect on Elk-1 and that was even more prominent in the set of sparse cells (Fig. 1.4.), indicating that the activity of HBCBP is dependent on the density of the cells. This would correlate to an increasing expression of DEP-1 with an increasing density of the cells, as it was detected previously in fibroblasts (Ostman et al, 1994).

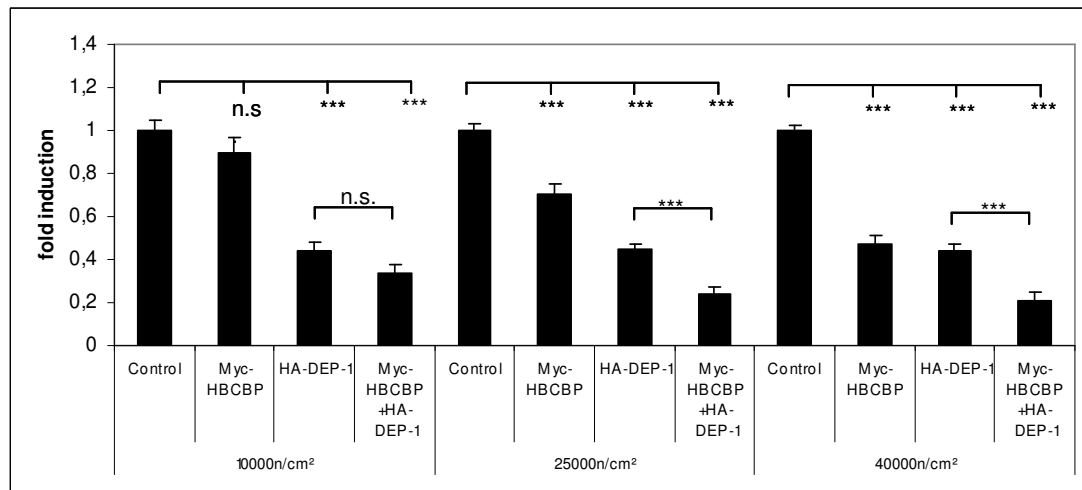


Fig. 1.4. Reporter assay on P-elk: HEK293 cells seeded in different densities as indicated. Overexpression of Myc-HBCBP and/or HA-DEP-1 in HEK293 cells in combination with Elk-1 Reporter constructs. Cells were harvested 2 days after seeding when the 10000n/cm² set of cells was still sparse, the 25000n/cm² set reached medium confluency and the 40000n/cm² set of cells were fully confluent. In the fully confluent set of cells Myc-HBCBP and DEP-1 inhibited the activity of the Elk-1 reporter system. The inhibitory effect on Elk-1 by Myc-HBCBP was less pronounced in the set of subconfluent cells and was absent in the set of sparsely grown cells. Pool of 14 values, graph shows means \pm SEM. Statistics calculated using Student's t-test versus control (n.s. t-test $P > 0.05$, *** t-test $P < 0.005$).

Further, we wanted to test whether the expression of HBCBP could be influenced by the cell density. If that was true, certain experiments could only work when cells are in certain cell densities. For that purpose we used HUVECs, a primary cell line that does not have an altered gene expression or regulation due to malignancy or transformation, and seeded them in different densities (10000 / 25000 / 40000

n/cm²). We analysed HBCBP expression by QPCR when cells reached the desired densities (sparse – subconfluent – confluent). HBCBP expression increased correlating to cell density, although the increase was not significant (Fig.1.5.).

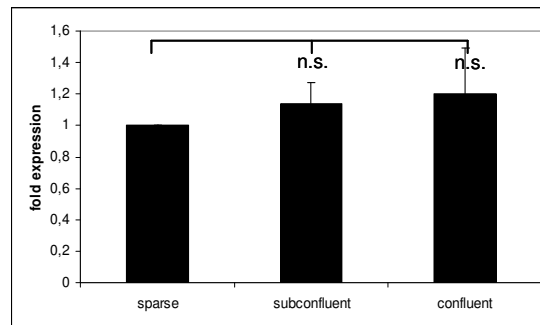


Fig. 1.5. Expression analysis of HBCBP in HUVECs cells at different cell densities: HUVECs cells were seeded in 6-wells in different densities (10000 / 25000 / 40000 n/cm²). When cells reached the desired densities (sparse – subconfluent – confluent) the cells were harvested. The expression of HBCBP was not significantly influenced by different density states of the cells. Values were normalized to PBGD. Pool of values from 2 independent experiments. Graph shows means \pm SEM. Statistics calculated using Student's t-test (n.s. t-test >0.05).

Another idea was that HBCBP expression could be altered upon cell malignancy due to their different proliferation regulation concerning cell-cell contact inhibition. Therefore, we wanted to compare the expression rate of HBCBP in a normal cell line with its corresponding cancer form. For that purpose we used LNCaP cells, deriving from a metastatic prostate epithelial carcinoma, and RWPE1, a normal prostate epithelial cell line (containing a single copy of human papilloma virus 18 (HPV-18) for immortalization), to compare the expression rate by QPCR, but we could not detect significant differences (Fig.1.6.).

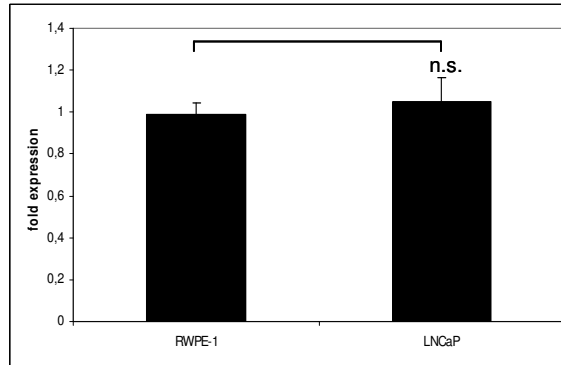


Fig. 1.6. Expression analysis of HBCBP in normal versus cancer cells: LNCaP (prostate epithelial cancer cells) and RWPE1 (prostate epithelial cells, immortalized with HPV-18) were seeded in 6-wells. In the confluent state the cells were harvested. Malignancy of the prostate cell line did not significantly influence the expression rate of HBCBP. Values were normalized to PBGD. Pool of values from 2 independent experiments. Graph shows means \pm SEM. Statistics calculated using Student's t-test (n.s. t-test >0.05).

2. Interaction of HBCBP with DEP-1

The interaction of HBCBP and DEP-1 was shown previously by a yeast-two-hybrid experiment in my diploma thesis. In the present thesis, we were interested, if the interaction of HBCBP and DEP-1 could also be shown in the mammalian system. For this purpose, we used the method of CoIP. Therefore, we overexpressed Myc-tagged HBCBP and HA-tagged DEP-1 alone or in combination in a human cell line (HEK293). Cells were harvested in the confluent state.

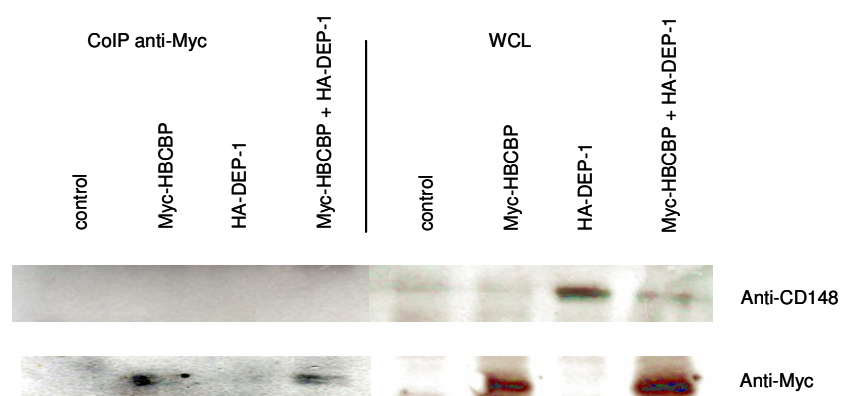


Fig. 2.1. CoIP: HEK293 cells overexpressing Myc-HBCBP and/or HA-DEP-1. CoIP using Protein G Sepharose and anti-Myc antibody (Oncogene, San Diego, CA) in 350mM NaCl-concentration. Samples were applied to WB and developed with anti-DEP-1 antibody (Invitrogen, Carlsbad, CA). Expression of Myc-HBCBP and DEP-1 (overexpressed HA-DEP-1 and endogenously expressed DEP-1) are shown in whole cell lysate (WCL) aliquots. IP of Myc-HBCBP was confirmed by developing with anti-Myc antibody, but DEP-1 was not coprecipitated. Representative of three independent experiments.

At first we tried to co-precipitate DEP-1 with HBCBP by the use of Protein G Sepharose and anti-Myc antibody in a lysate with 350mM NaCl concentration. To demonstrate the expression of Myc-HBCBP and HA-DEP-1, aliquots of the whole cell lysate (WCL) were taken. For the CoIP first the anti-Myc antibody was added to the lysate and preincubated before the Sepharose G was added. After further 3.5 hours of incubation, the beads were washed with PBS and finally dissolved in Laemmli-

buffer, heated and pelleted by centrifugation. The samples were applied to SDS-Page and Western blot and anti-Myc antibody showed that Myc-HBCBP was successfully overexpressed and also precipitated. To see, if DEP-1 (endogenous and ectopic) was co-precipitated with HBCBP the membrane was developed with anti-CD148. HA-DEP-1 was also successfully transfected but did not appear to be co-precipitated (Fig.2.1).

Then, less stringent conditions were used for CoIP (150mM NaCl), because higher salt-concentrations can inhibit weak protein interactions. But also in the less stringent condition DEP-1 was not co-precipitated with HBCBP (Fig.2.2.).

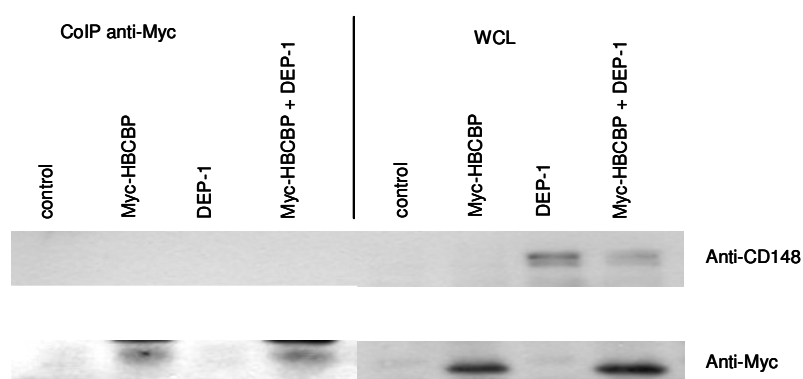


Fig. 2.2. CoIP: HEK293 cells overexpressing Myc-HBCBP and/or HA-DEP-1. CoIP with Protein G Sepharose and anti-Myc antibody in 150mM NaCl-concentration. Samples were applied to WB and developed with anti-DEP-1 antibody. Expression of Myc-HBCBP and DEP-1 (overexpressed and endogenous) are shown in WCL aliquots. IP of Myc-HBCBP was confirmed by developing with anti-Myc antibody, but DEP-1 was not coprecipitated. Representative of three independent experiments.

Reciprocally, anti-CD148 was used to co-precipitate HBCPB. In this set we first used the 350mM NaCl concentration. Similar to the experiments shown before, the expressions of HBCBP and DEP-1 were shown in the WCL aliquots. In the CoIP samples it could be shown that DEP-1 was precipitated by the anti-CD148 antibody,

however Myc-HBCBP did not co-precipitate (Fig.2.3.) and also in the less stringent 150mM NaCl condition anti-CD148 antibody did not co-precipitate Myc-HBCBP (Fig.2.4.).

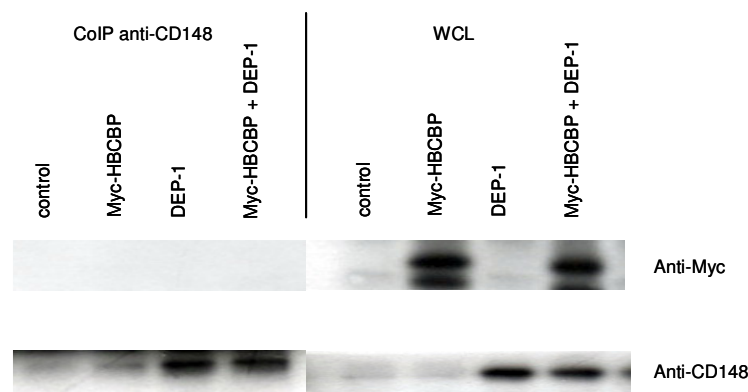


Fig. 2.3. CoIP: HEK293 cells overexpressing Myc-HBCBP and/or HA-DEP-1. CoIP with Protein G Sepharose and anti-CD148 antibody (Invitrogen, Carlsbad, CA) in 350mM NaCl-concentration. Samples were applied to WB and developed with anti-Myc antibody. Expression of Myc-HBCBP and DEP-1 (overexpressed and endogenous) are shown in WCL aliquots. IP of DEP-1 was confirmed by developing with anti-CD148 antibody, but Myc-HBCBP was not coprecipitated. Representative of three independent experiments.

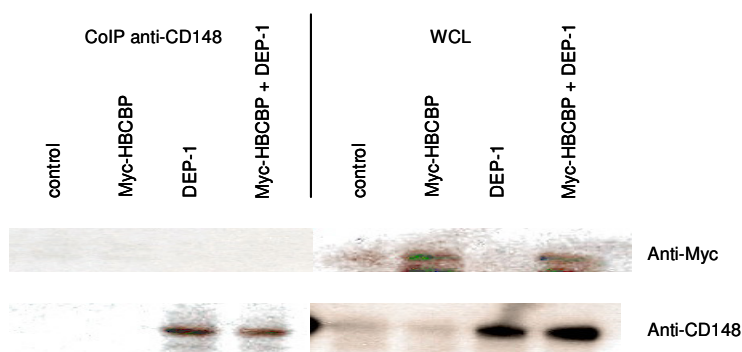


Fig. 2.4. CoIP: HEK293 cells overexpressing Myc-HBCBP and/or HA-DEP-1. CoIP with Protein G Sepharose and anti-CD148 antibody in 150mM NaCl-concentration. Samples were applied to WB and developed with anti-Myc antibody. Expression of Myc-HBCBP and DEP-1 (overexpressed and endogenous) are shown in WCL aliquots. IP of DEP-1 was confirmed by developing with anti-CD148 antibody, but Myc-HBCBP was not coprecipitated. Representative of three independent experiments.

Finally we performed CoIP using Dynabeads. Before the beads were used for the IP they were covalently linked to antibody (mouse anti-CD148 antibody and normal mouse IgG as control). Also in these experiments Myc-HBCBP and DEP-1 expressions were confirmed in the WCL. DEP-1 was precipitated with the CD148 antibody (endogenous DEP-1 and also overexpressed HA-DEP-1) and Myc-HBCBP was co-precipitated with it. But similar bands appeared also in the control IP using normal mouse IgG, while DEP-1 did not co-precipitate. This result indicated that this pull down was not specific (Fig.2.5.)

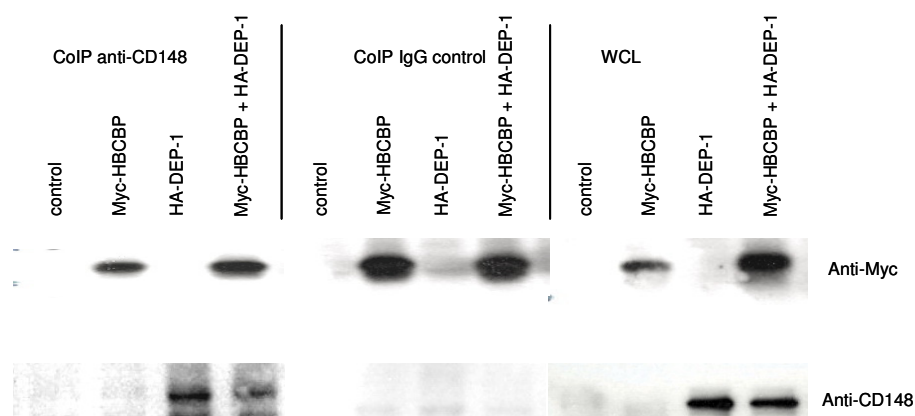


Fig. 2.5. CoIP: HEK293 cells overexpressing Myc-HBCBP and/or HA-DEP-1. CoIP with Dynabeads covalently linked to anti-CD148 antibody with a cell lysate containing 150mM NaCl-concentration. Samples were applied to WB and developed with anti-Myc antibody. Expression levels of Myc-HBCBP and DEP-1 (overexpressed and endogenous) are shown in WCL aliquots. IP of DEP-1 was confirmed by developing with anti-CD148 antibody. HBCBP coprecipitated in samples using anti-CD148 antibody, but similarly it was also detected in samples, where normal mouse IgG were used as a control, indicating that the positive result was unspecific. Representative of three independent experiments.

Next also Sepharose-CoIPs using an anti-EGFP antibody with cells overexpressing EGFP-tagged HBCBP and/or HA-DEP-1 were performed and also with anti-HA antibody for cells overexpressing HA-DEP-1 and/or Myc-tagged HBCBP. In both experimental setups it was not possible to coprecipitate Myc-HBCBP with DEP-1, even in the lowest stringency conditions (data not shown).

After it appeared, that the CoIPs did not work out with Sepharose and Dynabeads, we tried a different approach using ELISA-plates coated with anti-CD148 antibody. Cell lysates containing overexpressed Myc-HBCBP and/or HA-DEP-1 were applied and incubated. Then anti-Myc antibody was added and subsequently second anti-mouse-POX antibody. Similarly to the previous CoIP-experiments, Myc-HBCBP bound to the same extent to the wells containing overexpressed HA-DEP-1 as to the wells containing only endogenously expressed DEP-1. In addition the same pattern appeared in wells in which normal mouse IgGs were coated and also in the non-coated wells, indicating that Myc-HBCBP not only bound unspecifically to the normal IgG but also to the microtiter plate (Fig.2.6.).

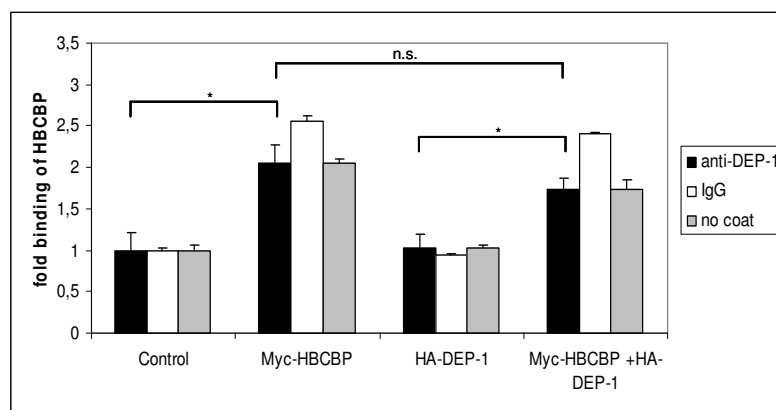


Fig. 2.6. Interaction on ELISA-plates: Microtiter plates were coated with polyclonal anti-DEP-1 antibody (Santa Cruz Biotechnology, Santa Cruz, CA). Then cell lysate containing overexpressed Myc-HBCBP and/or HA-DEP-1 was applied to the wells. Using an anti-Myc antibody we analysed, if Myc-HBCBP bound to the microtiter plates by binding to DEP-1 (overexpressed and endogenous). The results indicated that Myc-HBCBP not only bound in wells coated with anti-DEP-1 antibody, but also in wells coated with rabbit immunoglobulin fraction as a control and even to non-coated wells, indicating that the result was unspecific. Representative of three independent experiments, graph shows means \pm SEM of triplicates. Statistics calculated using Student's t-test (n.s. $P > 0.05$; * $P < 0.05$).

Next, to investigate a potential cellular localization of HBCBP and a possible colocalization of HBCBP and DEP-1, we transfected HEK293 cells in chamber slides to overexpress EGFP-tagged HBCBP in combination with HA-DEP-1 or Δ -cyto-DEP-

1. The slides were stained with anti-CD148 antibody and second Alexa 568 antibody (red). Images were taken using LSM510 microscope (Zeiss, Germany). EGFP-tagged HBCBP (green) was homogenously spread in the cytoplasm. In contrast, EGFP alone was localized in all compartments of the cell (also in the nucleus, data not shown). This indicated that also endogenous HBCBP is excluded from nucleus. DEP-1 is a transmembrane phosphatase and so HA-DEP-1 and Δ -cyto-DEP-1 could be visualized at the cell membrane (red). Concerning colocalization of EGFP-HBCBP and HA-DEP-1, there were slight yellow traces next to the cell membrane in the merge picture. But when comparing, the same picture could be seen in the samples transfected with mutant Δ cyto-DEP-1, indicating that the slight colocalization was not specific and probably only due to overexpression and the proximity of the cellular compartments in which the proteins are located (Fig. 2.7.).

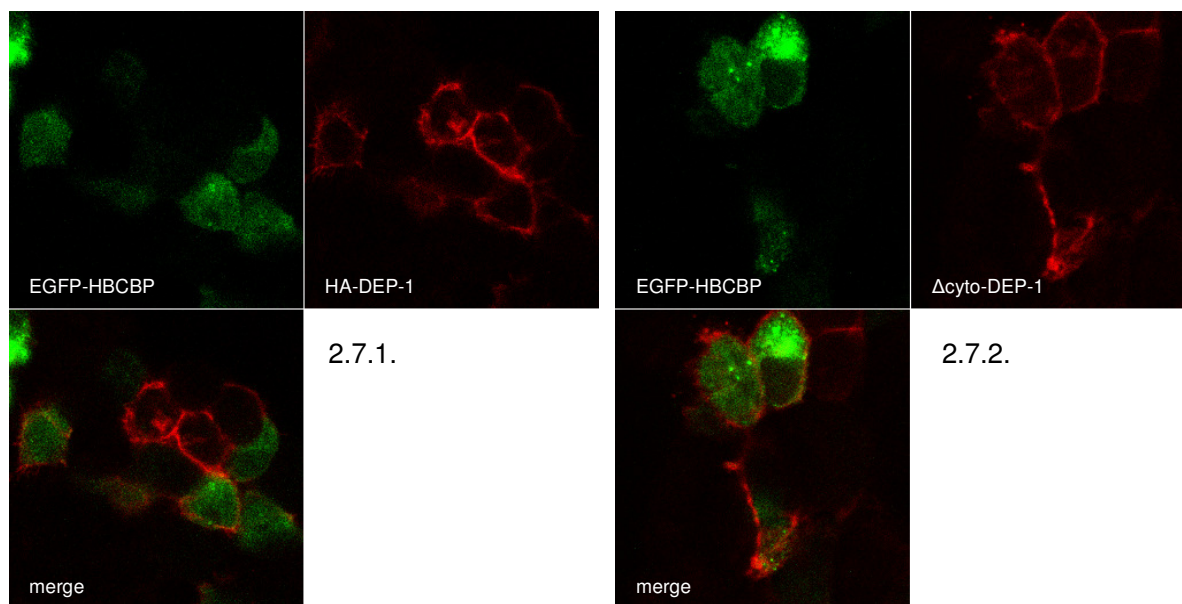


Fig. 2.7. Co-Localization: HEK293 cells in chamber slides transfected with pEGFP-C1-HBCBP and pSR α -CD148/HA (HA-DEP-1) (Fig. 2.7.1) or pSR α -CD148 Δ cyto (Δ cyto-DEP-1) (Fig. 2.7.2). Slides were stained with mouse anti-CD148 antibody (Invitrogen, Carlsbad, CA) and Alexa Fluor 568 conjugated anti-mouse second antibody (Molecular Probes, Eugene, Oregon) (red); green resembles EGFP-HBCBP. Pictures were taken using Confocal microscope. Picture showed a slight colocalization of EGFP-HBCBP with wt-DEP-1 in proximity to the cell membrane, but a similar merge picture could be seen when EGFP-HBCBP was coexpressed with Δ cyto-DEP-1, indicating, that the colocalization was not specific. Representative of three independent experiments.

3. How does HBCBP affect Elk1 activity?

To further investigate the inhibitory effect of HBCBP on Elk-1 we wanted to see if the inhibitory effect of HBCBP was dependent on the presence of DEP-1 and also vice versa. For that purpose we used the Elk-1 reporter system in combination with overexpression of Myc-HBCBP and/or HA-DEP-1 and in addition silencing of HBCBP and DEP-1 by siRNA. In scrambled RNA transfected control cells, Myc-HBCBP, like HA-DEP-1, reduced significantly the transcriptional activity of Elk-1, and overexpression of both had an additive effect. When HBCBP was silenced, the effect of Myc-HBCBP was abolished, but HA-DEP-1 still downregulated the Elk-1 effect. Similarly, when DEP-1 was silenced, the HA-DEP-1 effect was abolished, but Myc-HBCBP still downregulated the Elk-1 effect. These results indicated that both inhibitory effects, of Myc-HBCBP and HA-DEP-1, did not depend on the presence of the other protein (Fig.3.1.). Representative samples were used for the verification of the silencing of HBCBP and DEP-1 by Q-PCR (data not shown).

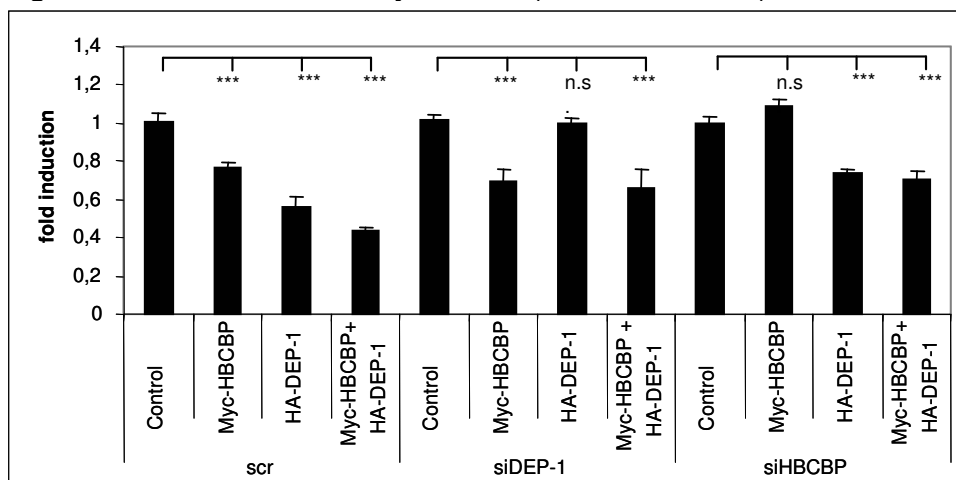


Fig. 3.1. Elk-1 Reporter with HBCBP/DEP-1 knockdown: Reporter assay on P-elk in HEK293 overexpressing Myc-HBCBP and/or HA-DEP-1. Silencing of DEP-1 or HBCBP with siRNA (siDEP-1/siHBCBP). In scrambled RNA control (scr) Myc-HBCBP and HA-DEP-1 downregulated the activity of Elk-1 and when cotransfected, the effect was additive. When DEP-1 was silenced, the inhibitory effect of HA-DEP-1 was abolished, but Myc-HBCBP still decreased Elk-1 activity. Similarly, when HBCBP was silenced, the Myc-HBCBP effect was abolished, but the HA-DEP-1 effect remained. That indicated that the inhibitory effects of both, Myc-HBCBP and HA-DEP-1 did not depend on the presence of the other protein. Pool of 8 values, graph shows means \pm SEM. Statistics calculated using Student's t-test (n.s. t-test >0.05 ; * t-test $P<0.05$; ** t-test $P<0.01$; *** t-test $P<0.005$).

Therefore we tested if HBCBP overexpression has an effect on the phosphorylation state of ERK1/2 at all. We transfected HEK293 cells with Myc-HBCBP. The cells were harvested with Laemmli buffer and applied to SDS-page and Western blots. The membrane was developed with anti-phospho-ERK1/2 antibody and anti-total-ERK1/2 antibody. The intensity of P-ERK1/2 was decreased compared to control upon HBCBP overexpression. Experiments were repeated for several times. Although the difference of ERK1/2 phosphorylation was not significant when analyzing the western blots by densitometry, the trend was always a reduction of ERK1/2 phosphorylation in presence of overexpressed HBCBP (Fig.3.2.).

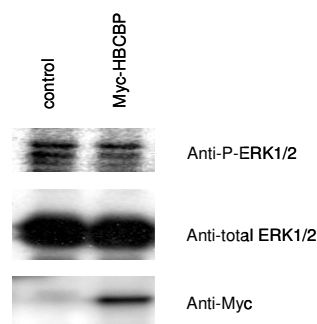


Fig. 3.2. Influence of HBCBP on ERK1/2 phosphorylation: HEK293 cells were transfected with pCMV-Myc-HBCBP vector. Cells were harvested with Laemmli-Buffer. Samples were applied to SDS-Page and Western blot. Membranes were developed with anti-P-ERK1/2 and anti-total-ERK1/2 (Cell Signaling Technology, Inc., Danvers, MA). Anti-Myc-developing confirmed successful pCMV-Myc-HBCBP transfection. Myc-HBCBP expression reduced the phosphorylation state of ERK1/2, although the decrease was not significant. Representative of three independent experiments.

After we knew that the inhibitory effect of Myc-HBCBP on the ERK1/2 MAP-Kinase pathway was not dependent on the presence of DEP-1, we wanted to look for a possible interaction partner of HBCBP that could mediate the effect. First we wanted to see by CoIP, if HBCBP possibly interacts with MEK-1, the upstream kinase of ERK1/2. For that purpose we used Protein G Sepharose and anti-Myc antibody in a lysate containing overexpressed Myc-HBCBP with 150mM NaCl concentration. The whole-cell-lysate aliquots showed the successful transfection of Myc-HBCBP and the

endogenous level of MEK-1. Myc-HBCBP was precipitated in the CoIP, but MEK-1 did not coprecipitate (Fig.3.3.1.).

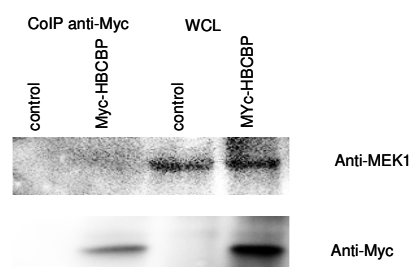


Fig. 3.3.1. Interaction of HBCBP with MEK1: HEK293 were transfected with p-CMV-Myc-HBCBP. CoIP was done with Protein G Sepharose and anti-Myc antibody with lysates containing low-salt concentration. Samples were applied to SDS-Page and Western blot, developed with anti-MEK1 antibody (Cell Signaling Technology, Inc., Danvers, MA). Expression of overexpressed Myc-HBCBP and endogenously expressed MEK1 were shown in WCL aliquots. IP of Myc-HBCBP was confirmed by developing with anti-Myc antibody, but MEK1 was not coprecipitated. Representative of three independent experiments.

In a similar way we checked, if HBCBP interacted with ERK1/2. Again Myc-HBCBP was precipitated in the CoIP, but ERK1/2 did not coprecipitate (Fig.3.3.2.).

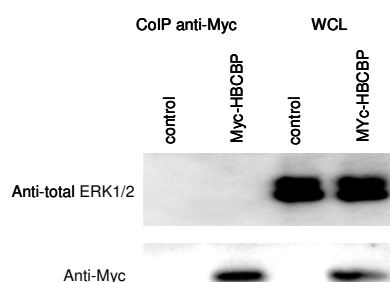


Fig. 3.3.2. Interaction of HBCBP with ERK1/2: HEK293 were transfected with p-CMV-Myc-HBCBP. CoIP was done with Protein G Sepharose and anti-Myc antibody with lysates containing low-salt concentration. Samples were applied to SDS-Page and Western blot, developed with anti-total ERK1/2 antibody (Cell Signaling Technology, Inc., Danvers, MA). Expression of ectopic Myc-HBCBP and endogenously expressed ERK1/2 were shown in WCL aliquots. IP of Myc-HBCBP was confirmed by developing with anti-Myc antibody, but ERK1/2 was not coprecipitated. Representative of three independent experiments.

Another possibility was that HBCBP interacted with certain MAP-Kinase Phosphatases (MKPs) that are known to influence the activity of the ERK1/2 pathway. For that purpose we checked if Myc-HBCBP coprecipitated with two cytoplasmic MKPs, DUSP6 and DUSP9 (Dual-Specificity Phosphatases 6/9). We used Protein A Sepharose and anti-DUSP6 or anti-DUSP9 antibodies. As a control rabbit immunoglobulin fraction was used. The whole-cell-lysate aliquots showed the overexpressed Myc-HBCBP and the endogenously expressed DUSP6 and DUSP9. DUSP6 and DUSP9 were precipitated, but Myc-HBCBP was not coprecipitated (Fig.3.3.3.).

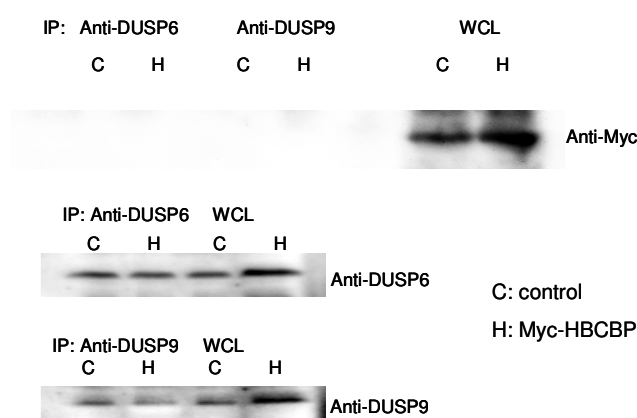


Fig. 3.3.3. Interaction of HBCBP with DUSPs: HEK293 were transfected with p-CMV-Myc-HBCBP (H) or control vector (C). CoIP was done with Protein-A-Sepharose and anti-DUSP6 or anti-DUSP9 antibodies (Cell Signaling Technology, Inc., Danvers, MA) in lysates containing 150mM NaCl concentration. Samples were applied to SDS-Page and Western blot, developed with anti-Myc antibody. Expression of overexpressed Myc-HBCBP and endogenously expressed DUSP6 and DUSP9 were shown in WCL aliquots. IP of DUSP6 and DUSP9 was confirmed by developing with anti-DUSP6/antiDUSP9 antibodies, but Myc-HBCBP was not coprecipitated. Representative of three independent experiments.

4. HBCBP in MAP-Kinase dependent processes

Our previous investigations led us to the hypothesis, that HBCBP could play a role in the regulation of proliferation or apoptosis. To check that we used HepG2 cells because compared to other cell types we analyzed, these had the highest endogenous HBCBP expression (data not shown). In HepG2 cells HBCBP was silenced with siRNA and scrambled RNA was used as control.

In order to analyze the effect on proliferation we used BrdU-assays and Ki67 staining. BrdU assays utilize the nucleotide Bromodeoxyuridine (BrdU), a thymidine-analogue that gets integrated in replicating DNA. The more cells are proliferating, the more BrdU gets integrated and can be detected by an anti-BrdU-antibody (Fig.4.1.).

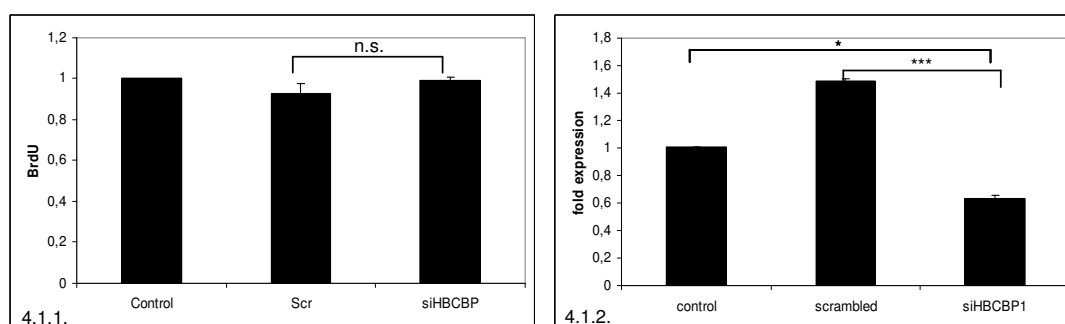


Fig. 4.1.1. HBCBP in proliferation: BrdU assay with HepG2 cells transfected with siRNA to knockdown HBCBP and scrambled RNA as control. 2 days after transfection BrdU was loaded onto the cells for overnight. Then, the cells were stained according to the manufacturers protocol (BD Biosciences, BrdU Flow Cytometry Assay Kit, FITC Detection) and analyzed using flow cytometry. Graph shows cells with positive BrdU staining, background values were obtained from control samples without BrdU loading and were subtracted from experimental values. Control values were set to 1. Knockdown of HBCBP did not have an effect on BrdU uptake to the cells. Pool of 4 values. Graph shows means \pm SEM. Statistics calculated using Student's t-test (n.s. t-test >0.05).

Fig. 4.1.2. Knock-down control: As a control for the each BrdU experiment, a set of HepG2 cells was treated the same way as described above, RNA was isolated and reverse transcribed. Expression of HBCBP was determined by quantitative real-time PCR using specific primers for HBCBP. Values were normalized to the housekeeping gene PBGD. Control values were set to 1. Graph shows means \pm SEM. Statistics calculated using Student's t-test (* t-test <0.05 ; *** t-test <0.005).

The Ki67 antigen is a marker for proliferation because it is only expressed in cells that are actively dividing but is completely absent from resting cells (Fig.4.2.). We used this approach and BrdU to analyze if HBCBP influences cell proliferation, but neither BrdU integration nor Ki67 staining showed a difference after HBCBP knockdown.

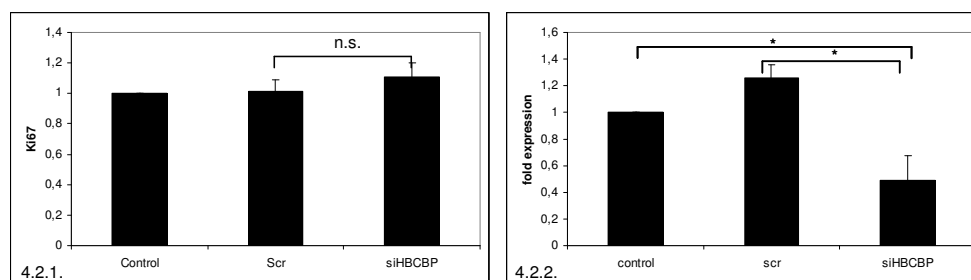


Fig. 4.2.1. HBCBP in proliferation: Ki67 staining with HepG2 cells transfected with siRNA to knockdown HBCBP (siHBCBP) and scrambled RNA (Scr) as control. 3 days after transfection, the cells were fixed and stained with a FITC-labelled Ki67 antibody and analyzed using flow cytometry. Graph shows cells with positive Ki67 staining. Control values were set to 1. HBCBP knockdown did not affect Ki67 expression in the cells. Pool of 6 values. Graph shows means \pm SEM. Statistics calculated using Student's t-test (n.s. t-test >0.05).

Fig. 4.2.2. Knock-down control: As a control for each Ki67 experiment, a set of HepG2 cells was treated the same way as described above, RNA was isolated and reverse transcribed. Expression of HBCBP was determined by quantitative real-time PCR using specific primers for HBCBP. Values were normalized to the housekeeping gene PBGD. Control values were set to 1. Graph shows means \pm SEM. Statistics calculated using Student's t-test (* t-test <0.05).

We used AnnexinV staining and PI staining to analyze the effect of HBCBP on apoptosis. AnnexinV binds to phosphatidylserine (P-Ser) that gets exposed on the cell surface already in early processes of apoptosis. The ApoAlert® Annexin V-FITC Apoptosis Kit uses FITC-labeled AnnexinV to detect these exposed P-Ser molecules (Fig.4.3.). Propidium iodide (PI) is an intercalating agent that is not supposed to enter

intact cells but enters necrotic and apoptotic cells due to their defective cell membrane. When excited by 488nm of laser light, it can be detected with 562-588nm band pass filter (Fig.4.4.). Both methods did not show a difference after HBCBP knockdown. The successful knockdown of HBCBP by siRNA was confirmed by Q-PCR.

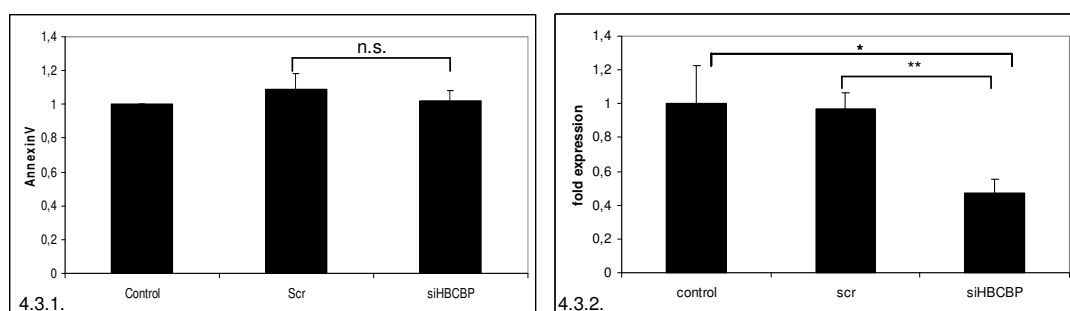


Fig. 4.3.1. HBCBP in apoptosis: AnnexinV staining in HepG2 cells transfected with siRNA to knockdown HBCBP (siHBCBP) or scrambled RNA (Scr) as control. 3 days after transfection, the cells were stained using ApoAlert® Annexin V-FITC Apoptosis Kit according to Manufacturer's protocol and analyzed by flow cytometry. Graph shows cells positive for AnnexinV staining, Control values were set to 1. Cells did not show a difference after HBCBP knockdown. Pool of 4 values. Graph shows means \pm SEM. Statistics calculated using Student's t-test (n.s. t-test >0.05).

Fig. 4.3.2. Knock-down control: As a control for each AnnexinV experiment, a set of HepG2 cells was treated the same way as described above, RNA was isolated and reverse transcribed. Expression of HBCBP was determined by quantitative real-time PCR using specific primers for HBCBP. Values were normalized to the housekeeping gene PBGD. Control values were set to 1. Graph shows means \pm SEM. Statistics calculated using Student's t-test (* t-test <0.05 , ** t-test <0.01).

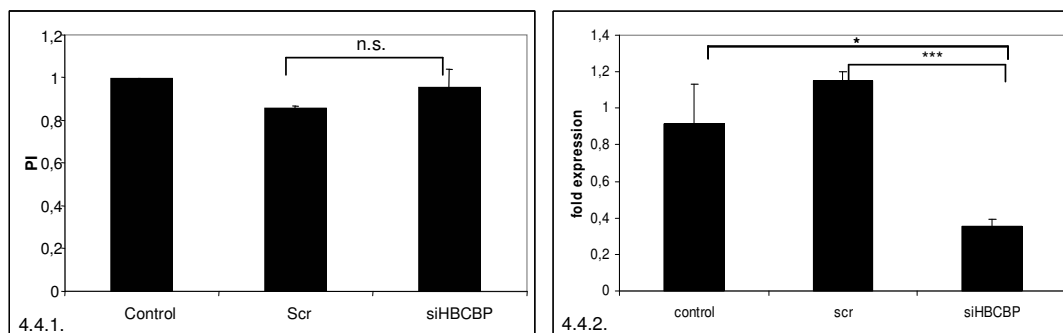


Fig. 4.4.1. HBCBP in apoptosis: PI-staining with HepG2 cells transfected with siRNA to knockdown HBCBP (siHBCBP) or scrambled RNA (Scr) as control. 3 days after transfection, the cells were stained with PI and analyzed by flow cytometry. Graph shows cells positive for PI staining, control values were set to 1. Knockdown of HBCBP does not influence the PI staining of the cells. Pool of 4 values. Graph shows means \pm SEM. Statistics calculated using Student's t-test (n.s. t-test >0.05).

Fig. 4.4.2. Knock-down control: As a control for each PI experiment, a set of HepG2 cells was treated the same way as described above, RNA was isolated and reverse transcribed. Expression of HBCBP was determined by quantitative real-time PCR using specific primers for HBCBP. Values were normalized to the housekeeping gene PBGD. Control values were set to 1. Graph shows means \pm SEM. Statistics calculated using Student's t-test (* t-test <0.05 , *** t-test <0.005).

These results seem to demonstrate, that HBCBP does not influence MAP-Kinase activity that is related to proliferation of apoptosis. So HBCBP is possibly involved in other ERK1/2 related processes like cytoskeleton organization, cell adhesion or differentiation that we did not analyze.

The verification of HBCBP knock down, that was done by Q-PCR, shows an increasing HBCBP expression in scrambled control compared to control in three of the graphs shown above. The absence of this effect in the knock-down control for the AnnexinV-staining indicates a difference in the transfection rate compared to the other experiments and therefore suggests that this result could be less substantial.

5. HBCBP expression in tissues

To analyze whether the expression of HBCBP is tissue type specific and if this could give a hint regarding its function, a Human Multi-Tissue RNA Panel for real-time PCR was screened and normalized to the housekeeping gene PBGD. According to the crossing points of HBCBP in the samples, the gene is generally expressed in only low levels, but showed a major enhancement in placenta tissue (Fig.5.1).

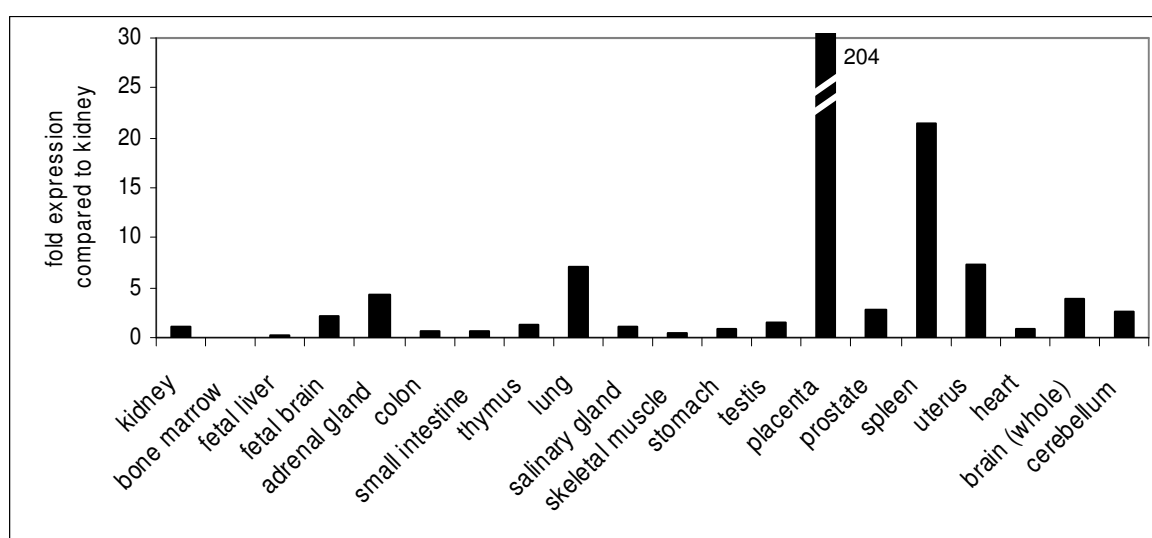


Fig. 5.1. Human Multi-Tissue RNA Panel: RNA samples were reverse transcribed and expression of HBCBP was determined by quantitative real-time PCR using specific primers for HBCBP. Values were normalized to the housekeeping gene PBGD. Graph shows relative expression of HBCBP compared to kidney. RNA panel was composed of one sample per tissue.

In order to confirm the result obtained from the RNA panel (that HBCBP expression levels were significantly higher in placenta tissue compared to other tissues), we analyzed more placenta tissue (obtained from Semmelweis Frauenklinik). The samples were from different weeks of pregnancy reaching from week 36 to week 42, representing samples from late pregnancy. From each placenta the maternal part and fetal part was investigated (data not shown). However, we could not observe expression differences and also the total expression was similar to that in HEK293 cells (Fig.5.2).

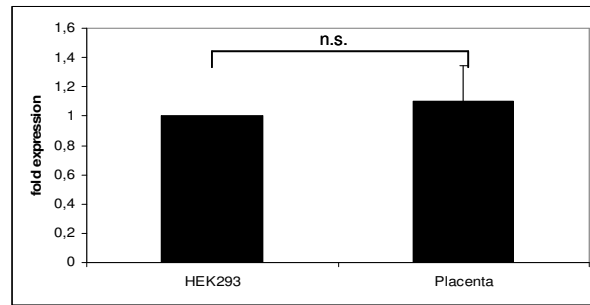


Fig. 5.2. Expression in human placenta: RNA was isolated from placenta tissue, reverse transcribed and expression of HBCBP was determined by quantitative real-time PCR using specific primers for HBCBP. Values were normalized to the housekeeping gene PBGD. HEK293 cells were taken as reference cell line due to comparably low expression value of HBCBP. Pool of 12 values. Graph shows means \pm SEM. Statistics calculated using Student's t-test (n.s. t-test >0.05)

We thought, that the low expression level of HBCBP in the placenta samples could probably refer to the fact that the samples originated from late pregnancies. Another commercially available tissue panel (Multi-Tissue cDNA Panel (Clontech)) was analyzed in which the placenta sample was supposed to contain a pool of placenta cDNA comparable to the RNA-Panel we used before. In this experiment, the expression level in placenta did not stand out of the other tissues, finally hinting, that the higher expression level in the RNA panel was a false positive (Fig.5.3).

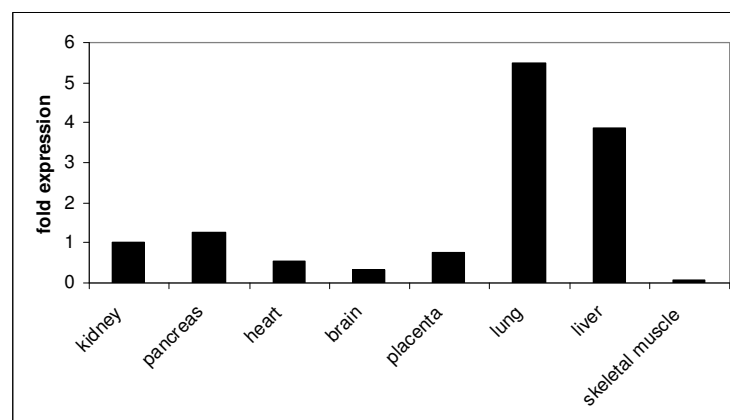


Fig. 5.3. Human Multi-Tissue cDNA Panel: Expression of HBCBP was determined by quantitative real-time PCR using specific primers for HBCBP. Values were normalized to the housekeeping gene PBGD. Graph shows relative expression of HBCBP compared to kidney. The cDNA panel was composed of one sample per tissue.

6. HBCBP Promotor

From the previous experiments we did not yet get a hint about cellular processes HBCBP could be involved in. Therefore, we wanted to analyze a hypothetical HBCBP promoter to see possible transcription factor binding sites that could give a clue in which processes HBCBP expression is modified and needed.

We defined our hypothetical HBCBP promoter reaching -900 to +300 bp from the transcription start of HBCBP and analyzed it using the MatInspector software (Genomatix, Munich, D), that filters out potential binding sites and calculates their probability to be specific by similarities of the core sequence (highest conserved sequence) and their surrounding sequences (Optimized Matrix Similarity Threshold). A value between 0.80 and 1.00 can be considered as a “good match”. The outcome of our analysis was a long list of different possible regulatory sites in this hypothetical HBCBP promoter with variable Optimized Matrix Similarity Thresholds. The list shown in the figures resembles an excerpt of these binding sites (Fig.6.1).

Family/matrix	Further Information	Opt.	From – To	Core sim.	Matrix sim.
V\$CREB/VJUN.01	V-Jun	0.78	48-68	1.000	0.862
V\$CREB/VJUN.01	V-Jun	0.78	49-69	0.750	0.858
V\$SMAD/SMAD3.01	Smad3 transcription factor involved in TGF-beta signaling	0.99	172-180	1.000	0.993
V\$ETSF/ELK1.01	Elk-1	0.82	192-208	0.800	0.824
V\$SMAD/SMAD3.01	Smad3 transcription factor involved in TGF-beta signaling	0.99	370-378	1.000	0.991
V\$PERO/PPARA.01	PPAR/RXR heterodimers	0.70	391-411	0.807	0.702
V\$AREB/AREB6.01	AREB6 (Atp1a1 regulatory element binding factor 6)	0.97	401-413	1.000	0.990
V\$AREB/AREB6.02	AREB6 /Atp1a1 regulatory element binding factor 6)	0.97	591-603	1.000	0.970
V\$AREB/AREB6.03	AREB6 /Atp1a1 regulatory element binding factor 6)	0.98	737-749	1.000	0.991
V\$E2FF/E2F.01	E2F, involved in cell cycle regulation, interacts with Rb p107 protein	0.84	772-786	0.857	0.843

V\$RXRF/VDR RXR.01	VDR/RXR Vitamin D receptor RXR heterodimer site	0.85	824-840	1.000	0.851
V\$PERO/PPARA.01	PPAR/RXR heterodimers	0.70	826-846	0.807	0.745
V\$RORA/TR4.01	Nuclear hormone receptor TR4 homodimer binding site	0.84	834-852	0.750	0.842
V\$ETSF/ELK1.01	Elk-1	0.82	861-877	0.800	0.844
V\$NFKB/CREL.01	C-Rel	0.91	864-878	1.000	0.912
V\$NFKB/NFKAPPAB. 01	NF-kappaB	0.84	864-878	1.000	0.854
V\$IRFF/IRF2.01	Interferon regulatory factor 2	0.80	902-920	0.750	0.804
V\$RORA/NBRE.01	Monomers of the Nur subfamily of nuclear receptors (Nur77, Nurr1, Nor-1)	0.89	942-960	1.000	0.895
V\$RORA/RORA2.01	RAR-related orphan receptor alpha2	0.82	968-986	1.000	0.877
V\$STAT/STAT3.01	Signal transducer and activator of transcription 3	0.74	1021-1019	1.000	0.743
V\$PERO/PPARA.01	PPAR/RXR heterodimers	0.70	1115-1135	0.807	0.794
V\$NFKB/NFKAPPAB. 02	NF-kappaB	0.82	1138-1152	0.750	0.825
V\$SP1F/TIEG.01	TGFbeta-inducible early gene (TIEG)/early growth response gene alpha (EGRAalpha)	0.83	1185-1199	1.000	0.878

Fig. 6.1. Promotor analysis using MatInspector: The genomic sequence that was analyzed was reaching -900 to +300 bp from the transcription start of HBCBP (1200 bp). The table shows an excerpt of the obtained potential binding sites. Family/Matrix: the V\$ indicates vertebrate-group, followed by an acronym for the factor the matrix refers to, and a number discriminating between different matrices for the same factor. Opt.: Optimized matrix similarity threshold: This matrix similarity is the optimized value defined in a way that a minimum number of matches are found in non-regulatory test sequences. Core sim.: Core similarity: The “core sequence” of a matrix is defined as the (usually 4) highest conserved positions of the matrix. The maximum core similarity of 1.0 is only reached when the highest conserved bases of a matrix match exactly in the sequence. Matrix similarity: A perfect match to the matrix hits a score of 1.00 (each sequence position corresponds to the highest conserved nucleotide at that position in the matrix), a “good” match to the matrix usually has a similarity of <0.80. Mismatches in highly conserved positions of the matrix decrease the matrix similarity more than mismatches in less conserved regions.

In order to see, if the predicted TGF β 1 responsible sites in the hypothetical HBCBP promoter are active, we stimulated HepG2 cells for the indicated time periods with TGF β 1 in a concentration of 50ng/ml. We used HepG2 because, after analysis of several cell lines, HepG2 cells showed the highest expression level. The expression level of HBCBP showed an increase after stimulation with TGF β 1. Although that increase was not significant, there was a clear trend (Fig.6.2.1.).

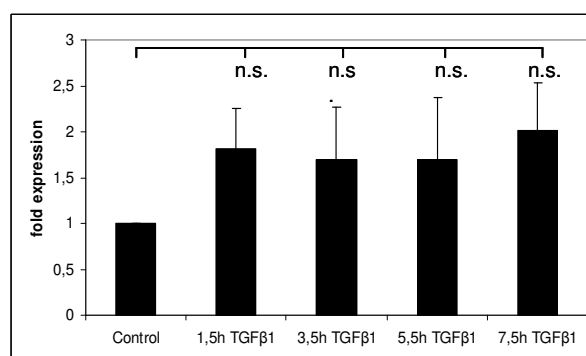


Fig. 6.2.1. Analysis of HBCBP expression regulation: Determination of the expression rate of HBCBP in HepG2-cells treated with TGF β 1. HepG2 cells were seeded in 6-wells. In the subconfluent state, the cells were treated with 50ng/ml TGF β 1 for the indicated time periods, RNA was isolated, reverse transcribed and expression of HBCBP was analyzed by quantitative real-time PCR using specific primers for HBCBP. These values were normalized to the housekeeping gene PBGD. Control values were set to 1. HBCBP expression was not significantly influenced by TGF β 1 treatment. Pool of values from 4 independent experiments. Graph shows means \pm SEM. Statistics calculated using Student's t-test (n.s. t-test >0.05).

We decided that experiments related to expression stimulation should be done in a primary cell line, not influenced by altered gene expression regulation. So for the further experiments we used HUVECs. TGF β 1 stimulation in HUVECs also did not significantly alter the expression of HBCBP but also here the trend was clear (Fig.6.2.2.).

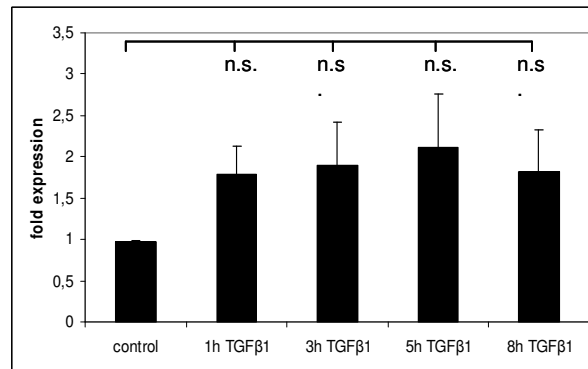


Fig. 6.2.2. Analysis of HBCBP expression regulation: Determination of the expression rate of HBCBP in HUVECs treated with TGFβ1. HUVECs were seeded in 6-wells. In the subconfluent state, the cells were treated with 50ng/ml TGFβ1 for the indicated time periods, RNA was isolated, reverse transcribed and expression of HBCBP was analyzed by quantitative real-time PCR using specific primers for HBCBP. These values were normalized to the housekeeping gene PBGD. Control values were set to 1. HBCBP expression was not significantly influenced by TGFβ1 treatment. Pool of values from 3 independent experiments. Graph shows means \pm SEM. Statistics calculated using Student's t-test (n.s. t-test >0.05)

We found a possible Interferon regulatory factor (IRF) responsive site and a possible Signal Transducer and Activator of Transcription (STAT) responsive site that is known to be regulated by cytokines. Therefore we stimulated HUVECs with the cytokines IFN γ , IFN α or TNF α and analyzed the expression of HBCBP in these cells in comparison to the housekeeping gene PBGD. HBCBP expression was not changed upon stimulation with IFN α or TNF α , but there was a clear trend of upregulation upon IFN γ treatment (though not significant) (Fig.6.2.3.).

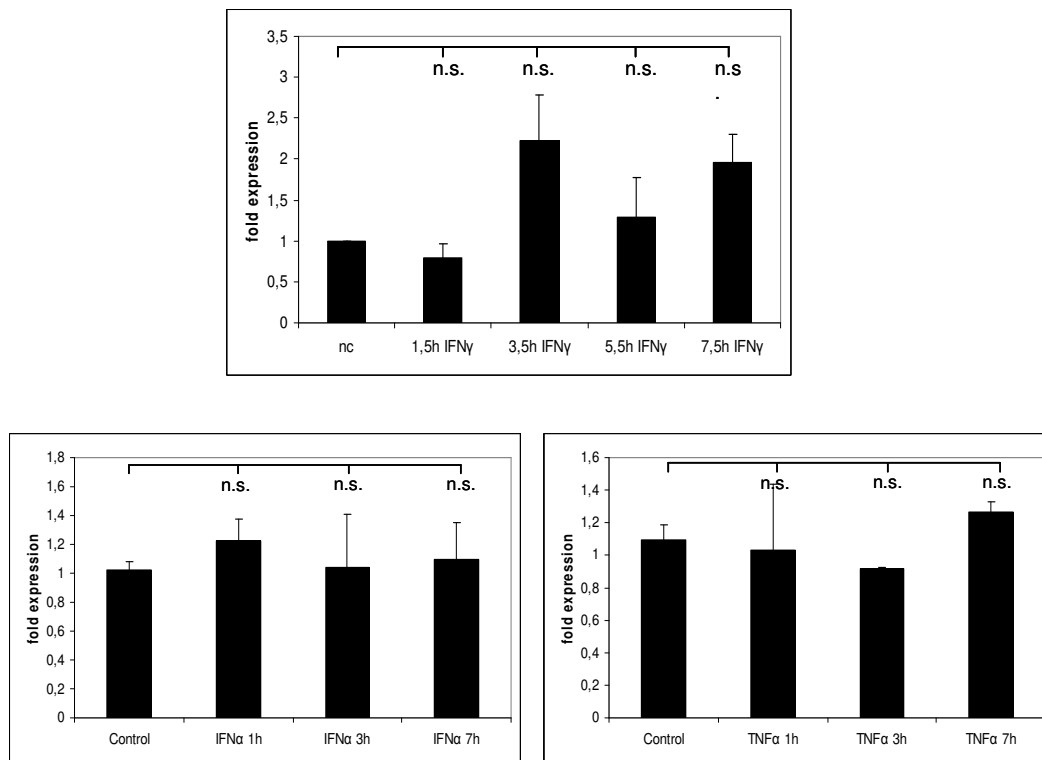


Fig. 6.2.3. Expression analysis of HBCBP in HUVECs treated with different cytokines: HUVECs cells were seeded in 6-wells. In the subconfluent state, the cells were treated with 100ng/ml IFN γ , 100ng/ml IFN α or 100ng/ml TNF α for the indicated time periods. HBCBP expression was not significantly influenced by cytokine treatment. Pool of values from 2 independent experiments. Graph shows means \pm SEM. Statistics calculated using Student's t-test (n.s. t-test >0.05).

Peroxisome proliferator-activated receptors (PPARs) are nuclear receptors that get activated upon binding to their ligands. To check, if the predicted PPAR responsible sites in the analyzed HBCBP promoter are active, we stimulated HUVECs with the PPAR α ligand WY14643 or the PPAR γ ligand Rosiglitazone-Maleate. HBCBP expression was not significantly altered upon PPAR ligand stimulation indicating that these sites are not active (Fig.6.2.4.).

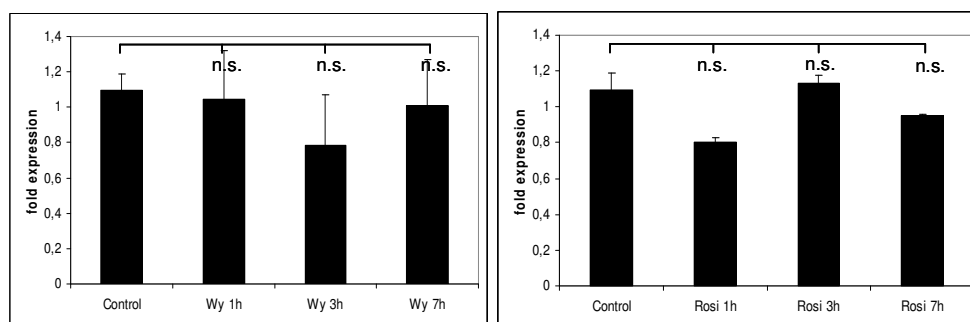


Fig. 6.2.4. Expression analysis of HBCBP in HUVECs treated WY14643 or Rosiglitazone-Maleate: HUVECs cells were seeded in 6-wells. In the subconfluent state, the cells were treated with the PPAR α ligand Wy14643 (100 μ M) or PPAR γ ligand Rosiglitazone-maleate (10 μ M) for the indicated time periods. HBCBP expression was not significantly altered upon PPAR ligand treatment. Pool of values from 2 independent experiments. Control values were set to 1. Graph shows means \pm SEM. Statistics calculated using Student's t-test (n.s. t-test >0.05).

Elk-1, v-Jun and E2F transcription factor responsible sites in the hypothetical HBCBP promoter indicated that the expression of HBCBP could be regulated through MAP-Kinases. Therefore we used the general MAP-Kinase activator PMA to stimulated HUVECs, but the HBCBP expression was not significantly different to that in the control cells (Fig.6.2.5.).

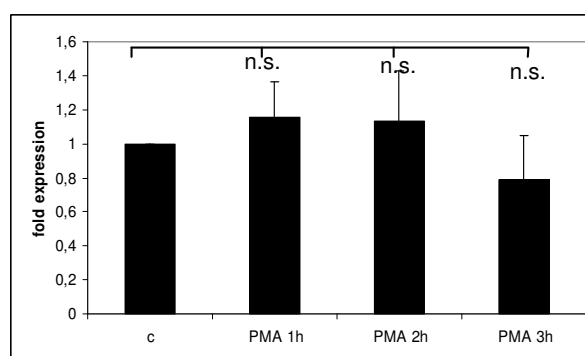


Fig. 6.2.5. Expression analysis of HBCBP in HUVECs-cells treated with PMA: HUVECs cells were seeded in 6-wells. In the subconfluent state, the cells were treated with 50nM PMA for the indicated time periods. HBCBP expression was not significantly influenced by PMA treatment. Pool of values from 2 independent experiments. Graph shows means \pm SEM. Statistics calculated using Student's t-test (n.s. t-test >0.05).

NBRE-sites are binding sites for the nuclear receptors Nur77, Nor1 and Nurr1. In order to find out, if this site is active, we overexpressed Nur77 in HUVECs and analyzed the expression level of HBCBP, but the expression rate was not significantly altered, indicating that this predicted site is not active (Fig.6.2.6.).

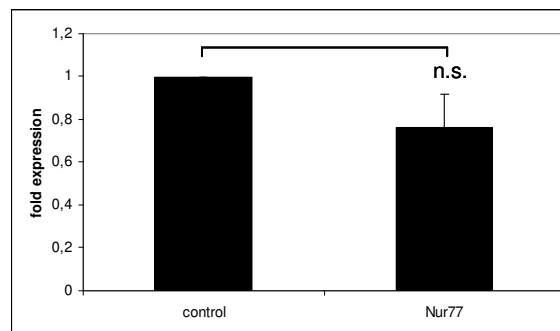


Fig. 6.2.6. Expression analysis of HBCBP in HUVECs overexpressing Nur77: HUVECs were seeded in 6-wells. In the subconfluent state, the cells were transfected using Lipofectamine Plus reagent according to manufacturer's protocol with full length Nur77 overexpression vector pcDNA3.1-Nur77. Nur77 overexpression did not significantly influence the expression rate of HBCBP. Graph shows means \pm SEM. Statistics calculated using Student's t-test (n.s. t-test >0.05).

AREB6 is known to be upregulated upon Prostaglandin E2 (PGE2) stimulation. We analyzed if the predicted AREB6 responsible binding sites are active by treating HUVECs with PGE2 and analyzed the expression rate of HBCBP. There was no significant change upon PGE2 stimulation, indicating that these sites are not active (Fig.6.2.7.).

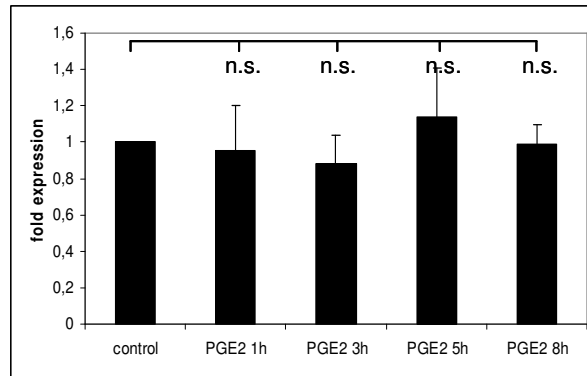


Fig. 6.2.7. Expression analysis of HBCBP in HUVECs treated with Prostaglandin E2: HUVECs cells were seeded in 6-wells. In the subconfluent state, the cells were treated with 10 μ g/ml PGE2 for the indicated time periods. Treatment with PGE2 did not significantly alter the expression rate of HBCBP. Pool of values from 4 independent experiments. Graph shows means \pm SEM. Statistics calculated using Student's t-test (n.s. t-test >0.05).

7. In silico structural analysis of HBCBP protein

Next we analyzed the protein structure to see if that could give a clue about the function of the protein. For that purpose we analyzed the nucleotide or protein sequence of HBCBP in different in-silico programs available.

The ClustalW2 sequence analysis program is a tool to analyze evolutionary relationships between proteins. On the ENSEMBL homepage sequences of predicted orthologues of human HBCBP in different species were found. These sequences were aligned by the ClustalW2 program to get a hint about the evolutionary descent (Fig. 7.1.). The sequences aligned in various extend to human HBCBP. Compared to human HBCBP, chimpanzee HBCBP aligned to 96%, showing the highest similarity. Guinea pig, armadillo and guinea pig HBCBP showed similarities of about 50%. Lesser hedgehog tenrec with only 37 aligning basepairs showed the lowest similarity.

SeqA	Name	Len(aa)	SeqB	Name	Len(aa)	Score
1	Human	196	2	Chimpanzee	197	96
1	Human	196	3	Elephant	183	53
1	Human	196	4	Armadillo	156	54
1	Human	196	5	Guinea	156	54
1	Human	196	6	Tenrec	170	32
2	Chimpanzee	197	3	Elephant	183	50
2	Chimpanzee	197	4	Armadillo	156	52
2	Chimpanzee	197	5	Guinea	156	52
2	Chimpanzee	197	6	Tenrec	170	34
3	Elephant	183	4	Armadillo	156	57
3	Elephant	183	5	Guinea	156	57
3	Elephant	183	6	Tenrec	170	48
4	Armadillo	156	5	Guinea	156	100
4	Armadillo	156	6	Tenrec	170	28
5	Guinea	156	6	Tenrec	170	28

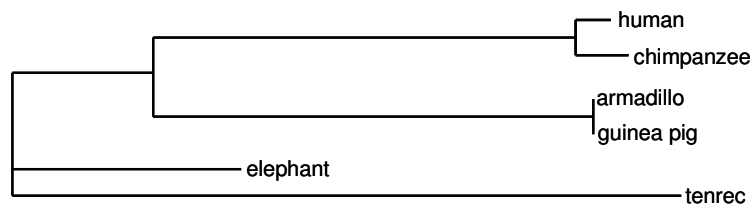


Fig. 7.1. ClustalW2 sequence analysis for potential evolutionary decent of human HBCBP gene: Amino acid sequences of predicted orthologues of HBCBP from ENSEMBL homepage were used for alignment in order to gain information about a possible evolution of human HBCBP gene. The list shows the score calculated from the alignment between the sequences from 2 indicated species. The Len(aa) value resembles the length of the amino acid sequence of the aligned sequence. Among the predicted HBCBP sequences in the different species, only the predicted chimpanzee HBCBP sequence seemed to be an orthologue of human HBCBP. The result of the alignment is shown in a phylogram. Human HBCBP showed a high degree of similarity to chimpanzee HBCBP, indicating a probability of being an orthologue, but it only aligned to a low extend to HBCBP sequences found in the other species.

The Block Searcher program is a software to detect sequence homologies between different proteins in one species, in order to find related sequences. We used this program to find possible related sequences of HBCBP, but only a very short sequence of the Eukaryotic Molybdopterin Domain Signature that aligned partially to human HBCBP in a stretch of 13 amino acids was found. This result indicated that HBCBP has no related sequences in the entire human genome (Fig. 7.2.).

Hits	Aligns to AA	Combined E-value
Eukaryotic Molybdopterin Domain Signature	103-116	0.053

Fig. 7.2. Block Searcher analysis: Block Searcher was used to detect protein sequence homologies of HBCBP to other proteins and to find possible related sequences. The complete 196 amino acid sequence of human HBCBP was analyzed. There was only one possible hit, the Eukaryotic Molybdopterin Domain Signature, that aligned to a very short fragment of human HBCBP (amino acids 103-116), with a resulting E-value (expect value) of 0.053 (optimal value is 0). This result indicated that this alignment was not due to a related descent.

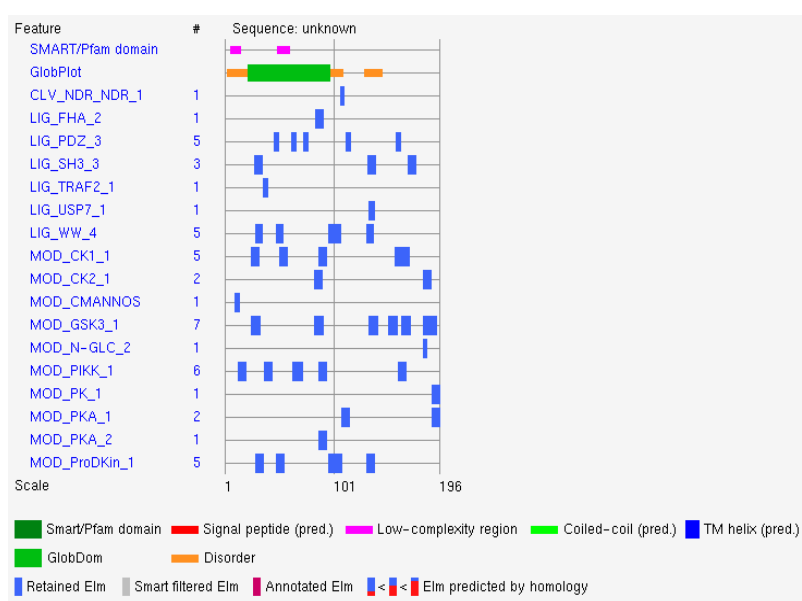
The SMART program is used to identify domain structures in proteins. We submitted the full length HBCBP sequence, but the software could only detect low complexity regions with HBCBP (Fig. 7.3.).

Name	Begin	End	E-value
Low complexity	5	13	-
Low complexity	48	58	-

Fig. 7.3. SMART analysis: The SMART program was used to analyse the HBCBP amino acid sequence to get hints about possible domain structures. The software could only detect low complexity regions in the sequence.

We used the ELM server (Heidelberg, Germany) to analyze the complete 196 amino acid sequence of HBCBP for conserved domains. The majority of the potential conserved domains are predicted to have a function apart from cytosol although we found that HBCBP was exclusively located in the cytoplasm. Among the predicted domains that have a function in the cytosol there were several potential phosphorylation sites, like casein kinase 1 and 2 (CK1, CK2) phosphorylation sites and a potential phosphorylase kinase (PK) phosphorylation site (Fig.7.4.1 and Fig. 7.4.2.).

7.4.1.



7.4.2.

Elm Name	Positions	Elm Description	Cell Compartment
CLV_NDR_NDR_1	106-108	N-Arg dibasic convertase (nordilysine) cleavage site	Extracellular, Golgi apparatus, cell surface
LIG_FHA_2	83-89	Phosphothreonine motif binding a subset of FHA domains that have a preference for an acidic amino acid at the pT+3 position	Nucleus, replication fork
LIG_PDZ_3	45-48; 61-64; 72-75; 111-114; 157-160	Class III PDZ domain binding motif	Cytosol, plasma membrane, membrane
LIG_SH3_3	27-33; 131-137; 168-174	Motif recognized by those SH3 domains with a non-canonical class I recognition specificity	Cytosol, plasma membrane, focal adhesion
LIG_TRAF2_1	35-38	Major TRAF2-binding consensus motif. Members of the tumor necrosis factor receptor (TNFR) superfamily initiate intracellular signaling by recruiting the C-domain of the TNFR-associated factors (TRAFs) through their cytoplasmic tails.	Cytosol
LIG_USP7_1	132-136	The USP7 NTD domain binding motif variant based on the MDM3 and P53 interactions	Nucleus
MOD_CK1_1	24-30; 50-56; 86-92; 156-162; 162-168	CK1 phosphorylation site	Nucleus, cytosol,
MOD_CK2_1	82-88; 182-188	CK2 phosphorylation site	Nucleus, cytosol, protein kinase CK2 complex
MOD_CMANNOS	9-12	Motif for attachment of a mannosyl residue to a tryptophan	Extracellular
MOD_GSK3_1	24-31; 82-89; 132-139; 150-157; 162-169; 182-189; 186-193	GSK3 phosphorylation recognition site	Nucleus, cytosol
MOD_PIKK_1	12-18; 36-42; 62-68; 64-70; 86-92; 159-165	(ST)Q motif which is phosphorylated by PIKK family members	nucleus
MOD_PK_1	190-196	Phosphorylase kinase phosphorylation site	Cytosol
MOD_PKA_1	107-113; 190-196	PKA is a protein kinase involved in cell signaling	Cytosol; cAMP-dependent protein kinase complex
MOD_ProDKin_1	28-34; 47-53; 95-101; 100-106; 130-136	Proline-Directed Kinase (e.g. MAPK) phosphorylation site in higher eukaryotes.	Nucleus, cytosol

Fig. 7.4. ELM-EMBL analysis of HBCBP amino acid sequence: The complete 196 AA sequence of HBCBP was submitted to the ELM server, to analyze the sequence for potential conserved domain patterns. The graph and list shows the obtained result. Considering HBCBP to be a cytoplasmic protein excludes some of the listed matched, leaving mostly potential phosphorylation sites.

The PredPhospho program finds possible phosphorylation sites within sequences by comparing to known phosphorylation site patterns. The program could detect a variety of different possible serine and threonine phosphorylation sites in the full length amino acid sequence of HBCBP (Fig. 7.5.1.).

Query	MISEGGWGWQ	GWGRSQGLRP	APCSWVSRMV	SPPAAIQETQ	LHFLADTLPS	PLSILLPPHK	60
Phospho_site			P	P	P	P P P	60
Query	QEELSQSQLL	IADLLPASDL	GNFQTSRETQ	SYQKAQPTPI	SFSPDHRKVS	RDVIPGAALG	120
Phospho_site			P P			P	120
Query	TASSRCWQML	CPSPSPVPGTR	WGRPQWKLLN	SVTGQSSDTV	ISQFSLAMSF	PNFPVPQLRF	180
Phospho_site	P				P P P P		180
Query	LNTCSTDETK	KSSVNK					196
Phospho_site	P	P PP					196

Fig. 7.5.1.. The PredPhospho software and NetPhos 2.0 server: Analysis of full length amino acid sequence of HBCBP. Using this program a list of potential serine and threonine phosphorylation sites was obtained and their assumed locations.

The NetPhos 2.0 Server is another possibility to analyze a sequence for predicted phosphorylation sites. Using this program to analyze the full length amino acid sequence of HBCBP we also got a list of predicted phosphorylation sites, mostly serine and threonine sites (Fig. 7.5.2). These sites only matched to a low extend the result we got from the PredPhospho program.

7.5.2.a.

196 gi_33328310	
MISEGGWGWQGWGRSQGLRPAPCSWVSRMVSPPAAIQETQLHFLADTLPSPLSILLPPHKQEELSQSQLLIADLLPASDL	80
GNFQTSRETQSYQKAQPTPISFSPDHRKVS RDVIPGAALGTASSRCWQMLCPSPSPVPGTRWGRPQWKLLNSVTGQSSDTV	160
ISQFSLAMSEPNFPVPQLRFLNTCSTDETKKSSVNK	240
.....S.....S.....	80
...TS.....T...S.....S.....	160
.....S...T..S....	240

7.5.2.b.

Phosphorylation sites predicted:				Ser: 7	Thr: 3	Tyr: 0			
Serine predictions				Threonine predictions					
Name	Pos	Context	Score	Pred	Name	Pos	Context	Score	Pred
v					v				
gi_33328310	3	--MISEGGW	0.003	.	gi_33328310	39	AIQETQLHF	0.034	.
gi_33328310	15	GWGRSQGLR	0.005	.	gi_33328310	47	FLADTLPSP	0.106	.
gi_33328310	24	PAPCSWVSR	0.064	.	gi_33328310	85	GNFQTSRET	0.992	*T*
gi_33328310	27	CSWVSRMVS	0.045	.	gi_33328310	89	TSRETQSYQ	0.075	.
gi_33328310	31	SRMVSPPA	0.959	*S*	gi_33328310	98	KAQPTPISF	0.585	*T*
gi_33328310	50	DTLPSPSLI	0.175	.	gi_33328310	121	AALGTASSR	0.041	.
gi_33328310	53	PSPLSILLP	0.021	.	gi_33328310	139	SVPGTRWGR	0.096	.
gi_33328310	65	QEELSQSQL	0.915	*S*	gi_33328310	153	LNSVTGQSS	0.006	.
gi_33328310	67	ELSQSQLLI	0.010	.	gi_33328310	159	QSSDTVISQ	0.030	.
gi_33328310	78	LLPASDLGN	0.157	.	gi_33328310	183	RFLNTCSTD	0.072	.
gi_33328310	86	NFQTSRETQ	0.984	*S*	gi_33328310	186	NTCSTDTEK	0.026	.
gi_33328310	91	RETQSYQKA	0.116	.	gi_33328310	189	STDETKKSS	0.892	*T*
gi_33328310	101	PTPIFSFSPD	0.039	.	^				
gi_33328310	103	PISFSPDHR	0.873	*S*	Tyrosine predictions				
gi_33328310	110	HRKVS RDVI	0.975	*S*	Name	Pos	Context	Score	Pred
gi_33328310	123	LGTASSRCW	0.103	.	v				
gi_33328310	124	GTASSRCWQ	0.104	.	gi_33328310	92	ETQSYQKAQ	0.499	.
gi_33328310	133	MLCPSPSPV	0.049	.	^				
gi_33328310	135	CPSPSPVPGT	0.353	.					
gi_33328310	151	KLLNSVTGQ	0.070	.					
gi_33328310	156	VTGQSSDTV	0.011	.					
gi_33328310	157	TGQSSDTV	0.120	.					
gi_33328310	162	DTVISQFSL	0.085	.					
gi_33328310	165	ISQFSLAMS	0.097	.					
gi_33328310	169	SLAMSF PNF	0.402	.					
gi_33328310	185	LNTCSTDTE	0.612	*S*					
gi_33328310	192	ETKKSSVNK	0.671	*S*					
gi_33328310	193	TKKSSVNK-	0.413	.					
^									

Fig. 7.5.2. NetPhos 2.0 Server (Technical University of Denmark, Lyngby, Denmark): Analysis of full length amino acid sequence of HBCBP. Using this program a list of possible serine and threonine phosphorylation sites and a single tyrosine phosphorylation site was obtained. The result only partially matched the result of the PredPhospho software.

To analyze HBCBP for phosphorylation we used anti-phospho-Ser antibody or anti-phospho-Thr antibody on cell lysates containing overexpressed Myc-HBCBP and truncated Myc-tagged constructs, but we could neither detect a signal for P-Ser nor P-Thr (data not shown).

8. Recombinant HBCBP

For most the previous experiments the overexpression of HBCBP was used as a tool for analyses. To analyze the endogenous protein we expressed and purified the recombinant HBCBP protein in order to use it as an antigen to produce antibodies. For this, the full-length HBCBP sequence was cloned into the bacterial expression vector pET24a creating a fusion construct with His-tag that was expressed in bacteria. After lysis, the cell debris containing the inclusion bodies was separated from the cell lysate by centrifugation and both lysates and inclusion bodies were analyzed using Western blot. An anti-His antibody (Sigma, St. Louis, MO) showed that recombinant HBCBP exclusively was present in the inclusion bodies and was not detectable in the cell lysate. Isolation of recombinant protein from inclusion bodies includes the denaturation of the protein and subsequent renaturation with a high risk of misfolding and so we did not proceed (Fig. 8).

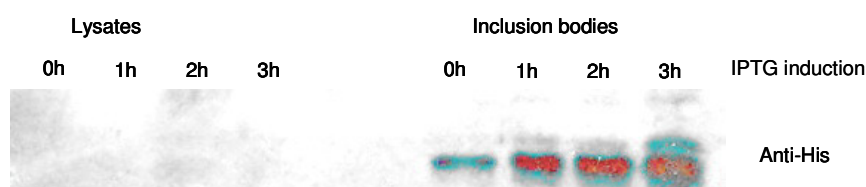


Fig. 8. Expression of recombinant His-tagged HBCBP was induced using IPTG in bacteria. Cell lysates and cell debris containing inclusion bodies were subjected to Western blot. Membranes were developed using an anti-His antibody (Sigma, St. Louis, MO). Recombinant HBCBP was not detectable in the cell lysate, it was exclusively present in the cell debris containing the inclusion bodies. A representative of two independent experiments is shown.

DISCUSSION

DEP-1, by influencing MAP-Kinase pathways, plays an important role in the regulation of cell growth and differentiation. The antiproliferative feature of DEP-1 and the fact, that the gene is often lost in different kinds of human cancers are the reason for its designation as a tumor suppressor gene. In addition, DEP-1 plays a fundamental role in the development of the vascular system during embryogenesis.

In order to find out more about the function of DEP-1, we were searching for new interaction partners, to get a better idea about its place in the diffuse network of signal transduction pathways. A very useful tool for this purpose is the Matchmaker Y2H system as described previously (Maple and Moller, 2007), an in-vivo-system to identify interaction partners of the gene-of interest. My diploma thesis took advantage of the Y2H-system and reported about the confirmed interaction between DEP-1 and a newly identified protein, Hepatitis B core-Antigen Binding Protein (HBCBP).

There was no information available about structure, regulation of function of this new gene and protein. The nucleotide sequence of HBCBP was published in 2003 on NCBI (Bethesda, MD) and was initially identified as an interaction partner of Hepatitis B Core Antigen (HBcAG) in an Y2H screen (Lu et al, 2005). Apart from this publication, there was no scientific data available that described HBCBP. Hence we were interested, how the interaction with DEP-1 influences cellular processes.

A very important function of DEP-1 is the inhibition of MAP-Kinase activity. In this context, we were interested, if HBCBP may also influence these pathways. To study this aspect, we used the PathDetect Elk-1 reporter system as a read-out for ERK1/2 activity which was also previously used by Iwata et al (Iwata et al, 2001), and we found, that overexpression of HBCBP as well as of DEP-1 downregulated the activity of Elk-1 and in case of overexpression of both proteins this inhibition is even more pronounced. The specificity of this effect was proven by the use of PMA, a general MAP-Kinase activator (Harvey et al, 2008; Lang et al, 2004), the titration of pCMV-Myc-HBCBP to see a dose-dependent inhibition and the use of truncated HBCBP constructs that did not affect the activity of Elk-1.

DEP-1 protein is upregulated in cells when they reach confluency (Ostman et al, 1994), and this stops cell growth. To this aspect, we were interested, if HBCBP activity could also be influenced by cell density. Surprisingly we found out, that HBCBP did not inhibit Elk-1 activity in the sparsely grown cells, that it had a limited effect in the subconfluent cells, and that it had the most pronounced effect in the confluent cells indicating that the activity of HBCBP is dependent of the cell density.

In this context we were interested if HBCBP expression is also dependent by cell density, what could have been crucial for further experiments. We used in increasing stages of confluence and analyzed HBCBP expression with Q-PCR according to the analysis model of Pfaffl (Pfaffl et al, 2001), but we could not detect a modified expression regulation of the protein.

Similarly we were interested if the expression could be modified by cell malignancy and compared HBCBP expression of LNCaP cells, a prostate epithelial cancer cell line with that of RWPE1, a normal prostate epithelial cell line, but also here we could not detect significant differences, indicating that HBCBP expression is not depending on cell malignancy.

We reported previously about the interaction of HBCBP and DEP-1 in the yeast system. We also wanted to confirm this interaction in the human system. For this purpose we wanted to do CoIP. When we used an anti-Myc antibody for pull-down, overexpressed Myc-HBCBP was precipitated, but it did not coprecipitate DEP-1 (neither endogenous nor overexpressed HA-DEP-1). For the next step we reduced the stringency by reducing the salt concentration to 150mM (resembles PBS NaCl concentration). But still, DEP-1 did not coprecipitate with HBCBP.

We considered that the Myc-epitope in the folded Myc-HBCBP protein might have been in close proximity to the possible DEP-1 binding domain and that could have prevented their interaction. We tried to do the approach vice versa and used an anti-DEP-1 antibody for the pull down, to precipitate DEP-1 (endogenous and overexpressed) and to coprecipitate Myc-HBCBP. Also in this case, the precipitation of DEP-1 could be detected, but HBCBP was not pulled down with its suspected interaction partner, neither in higher nor less stringent salt concentrations.

For the further CoIPs we used Dynabeads, because their surface can be more efficiently saturated with antibodies, and therefore they should yield a higher amount of pull down. Dynabeads have to be covalently linked to the desired antibody prior to use, promising a better probability of detection of interacting proteins, as described by Froystad (Froystad et al, 1998). As a control, we used Dynabeads linked to normal mouse IgG. As desired DEP-1 was precipitated only with Dynabeads linked to anti-DEP-1 antibody and Myc-HBCBP was found to be coprecipitated in this set of samples (with endogenous as well as overexpressed DEP-1), but unfortunately similar bands were found in the set, in which normal IgG were used for the control IP. This indicated that Myc-HBCBP did not specifically coprecipitate with DEP-1, but bound either to the control IgG or to the Dynabeads themselves.

After we figured out, that Dynabeads are probably not the right approach to do CoIPs, we finally also tried to see the interaction by a “modified ELISA experiment”. Microtiter plates were coated with polyclonal anti-DEP-1 antibody (rabbit) or rabbit immunoglobulin fraction as a control. Also in this approach Myc-HBCBP not only bound to the wells coated with rabbit anti-DEP-1 antibody, but also bound to the wells coated with rabbit immunoglobulin fraction and even to uncoated wells. So Myc-HBCBP could not be detected due to the interaction with DEP-1 but because of unspecific binding.

The results of all trials of CoIPs let us guess, that Myc-HBCBP could possibly bind unspecifically to plastic surfaces as shown with microtiter plates, and probably a similarly unspecific binding resulted in the CoIP result when using Dynabeads. If we hypothesize, that HBCBP possibly is a hydrophobic protein, it would generally bind in an unspecific way to a wide variety of surfaced, not only proteins. But after all, even in the lowest possible stringency, Myc-HBCBP did not interact with DEP-1 in a detectable way. If there was an interaction of Myc-HBCBP and DEP-1 the Myc-HBCBP band should have been stronger in samples with overexpressed HA-DEP-1 and the Myc-HBCBP band should have been literally absent or at least less strong pronounced in the control CoIP using normal IgG or rabbit immunoglobulin fraction compared to the CoIP using anti-DEP-1 antibodies.

When stating the theory, that HBCBP was a hydrophobic protein we also had to consider the possibility of a false positive result in the Y2H-system shown in my diploma thesis demonstrating the interaction between HBCBP and DEP-1. Unspecific binding due to hydrophobic interactions could bring the bait and prey fusion proteins

in close enough proximity to start transcription of the reporter genes and the yeast colonies could grow.

Now we wanted to see, in which compartment of the cell HBCBP was localized. Due to the fact, that we could not prove the interaction of HBCBP and DEP-1 in the mammalian system, we wanted to know, if an interaction is generally possible. For that purpose we studied the co-localization by confocal microscopy (Papac-Milecevic et al, 2009, in revision). EGFP-tagged HBCBP was overexpressed together with HA-tagged wild type DEP-1 or Δ cyto-DEP-1 and the samples were stained with anti-DEP-1 antibody (epitope at extracellular domain of DEP-1) and a second anti mouse Alexa 568 antibody. These experiments showed us, that HBCBP was exclusively localized in the cytoplasm of the cells, meaning that a physical contact with DEP-1 was possible. There were also indications of a colocalization of HBCBP and wild type DEP-1 in proximity of the cell membrane, hinting to a possibility of interaction, but a similar picture could be seen, when HBCBP was coexpressed with Δ cyto-DEP-1. Δ cyto-DEP-1 lacks the entire intracellular domain of the protein, so a direct interaction of HBCBP with this protein was not possible. Although there was now difference visible between the image of HBCBP and full-length or mutant DEP-1, it is possible, that there was an interaction between HBCBP and DEP-1, although too weak to be detectable or that the interaction only occurs under determined circumstances.

After we saw, that there was no interaction between HBCBP and DEP-1 that was strong enough to be detectable, we wanted to see, if the inhibitory effect of HBCBP on the ERK1/2 MAP-Kinase pathway depended on the presence of its previously suspected interaction partner, what would hint toward an active interaction between these two proteins. Elk-1 reporter assay in combination with siRNA to knock down HBCBP or DEP-1 showed that the inhibitory effect of both proteins on this system was independent, because in case of silenced DEP-1 HBCBP still downregulated Elk-1 activity and also vice versa, in case of silenced HBCBP, DEP-1 still downregulated Elk-1 activity. Hence both proteins inhibit the ERK1/2 pathway independently. If HBCBP and DEP-1 did interact, and we were just not able to prove it, then this interaction was not involved in the inhibition of Elk-1.

To confirm the inhibitory effect of HBCBP on the ERK1/2 MAP-Kinase pathway, we chose a more direct approach by analyzing the phosphorylation state of ERK1/2 after HBCBP overexpression. We found phospho-ERK1/2 to be downregulated after HBCBP overexpression, though the decrease was not statistically significant.

The next question was how HBCBP exerts its inhibitory effect, if not by the interaction with DEP-1. Since HBCBP was found to be localized exclusively in the cytoplasm, the inhibiting effect on Elk1 could not be mediated directly. In addition, the finding that the phosphorylation state of ERK1/2 was reduced after HBCBP overexpression suggests an influence that occurs upstream of Elk1. Our first theory was that it could interact with other components of the MAP-Kinase pathway, but neither MEK1 nor ERK1/2 seemed to interact with Myc-HBCBP.

Another possibility we considered was, that HBCBP interacted with MAP-Kinase Phosphatases (MKPs) that are known to inhibit the MAP-Kinase pathway. DUSP6 (MKP-3) (Arkell et al, 2007) and DUSP9 (MKP-4) (Muda et al, 1997) are MAP-Kinase phosphatases that are located in cytoplasm and that are known to inhibit the ERK1/2 pathway (Keyse, 2008). But CoIPs using anti-DUSP6 and anti-DUSP9 showed that there was no interaction between HBCBP and these two proteins.

Eventually we wanted to see, if HBCBP is generally involved in the regulation of proliferation or apoptosis at all, mechanisms in which the ERK1/2 MAP-Kinase pathway is involved. We did proliferation assays using the BrdU Flow Cytometry Assay Kit as previously demonstrated (Schitteck et al, 1991), which uses the thymidine-analogue BrdU that gets integrated in replicating DNA and that can be detected by an antibody. The more cells are proliferating, the more BrdU gets integrated. A second approach for studying proliferation was staining of Ki67, which is a protein that is only expressed in proliferating cells, but not resting cells (Gerdes et al, 1983). After silencing of HBCBP we expected a higher proliferation rate of the cells, but we could not detect differences to control cells. For these experiments we used HepG2 cells, because, compared to other cell lines, this cell type showed the highest expression rate of HBCBP. An additional reason was that we saw in the multi-tissue panel that is shown later, that liver, among the other tissues, showed a comparably high expression of HBCBP.

If HBCBP did not alter proliferation, it could still influence apoptosis. For that purpose we applied AnnexinV staining and PI staining. The ApoAlert® Annexin V-FITC

Apoptosis Kit, previously demonstrated by Gogal (Gogal et al, 2000) uses prelabeled Annexin V that binds to phosphatidyl-serine, a fatty acid that gets exposed to the cell surface in the process of apoptosis. PI is an intercalating agent that is not supposed to pass intact cell membranes. Only in case of membrane damage, as in apoptosis and necrosis processes, the substance enters the cell and intercalates with DNA (Cunningham et al, 2008). We considered that HBCBP could possibly have a suppressing effect on apoptosis, so for this case we expected a higher AnnexinV and PI staining after silencing of HBCBP. But in both setups of experiments, the silencing of HBCBP did not show an effect.

To confirm the silencing of HBCBP we did Q-PCR using specific primers for HBCBP. Scrambled RNA is used as negative control for siRNA experiments and demonstrates that silencing of the gene of interest is due to specificity of siRNA and is not due to unspecific effects. In this context it is a common phenomenon that scrambled RNA itself shows an increasing effect on the expression rate compared to control without transfected RNA. Only in one of the shown graphs, the AnnexinV knock down control (Fig. 4.3.2.), we did not see this effect. This indicates a difference in transfection efficiency in this set of experiments compared to the other graphs related to proliferation and apoptosis, and could therefore be considered as less substantial.

But still, there were no detectable effects of HBCBP on proliferation or apoptosis, although we found HBCBP as an inhibitor of the ERK1/2 MAP-Kinase pathway in Elk-1 reporter assays. These results could be due to the possibility that the effect depends on defined circumstances in the cell or that HBCBP affects ERK1/2 dependent processes other than proliferation or apoptosis like cytoskeleton organization, cell adhesion or differentiation.

Now we were searching for hints, in which topics HBCBP could be involved in and decided, to check the expression level of HBCBP in different human tissues. We hoped that an increased expression level of HBCBP in certain tissues could give us a clue on its function. We screened different tissues by the use of a Human Multi-Tissue RNA Panel that was also used by Zinda (Zinda et al, 2001) and normalized the HBCBP value to the value for the housekeeping gene PBGD. We found out, that HBCBP was generally expressed in low levels, but we found a markedly increased level in placenta tissue. Due to the fact, that the RNA panel was only composed by

one sample per tissue type, we now decided to collect more placenta samples to confirm the high expression rate of HBCBP in this tissue type. We got a number of placenta tissue samples from Semmelweis Frauenklinik, from each placenta one sample from the maternal and the fetal part. The samples derived from placentas ranging from pregnancy week 36 to 42. After analyzing all samples we could see that there was no obvious difference in the expression rate of HBCBP between the maternal and fetal samples and there was also no gradual change from the earlier weeks to the later weeks (data not shown). In addition to that, all the collected samples showed a low expression rate of HBCBP that was not comparable to the high level in the placenta sample of the RNA panel. So we could pool the values from these samples and compared it to a cell type that had a similarly low expression level HBCBP, HEK293. The placenta sample of the RNA panel was supposed to be a pool of samples from different stages of pregnancy. Our collected samples were only from late pregnancy. We purchased another set of samples that included placenta, to exclude the possibility that the divergence was due to the difference in the state of pregnancy. We analyzed the HBCBP expression in the Human Multi-Tissue cDNA panel, which was also used for expression analysis by Yang (Yang, et al 2004) and could see that the placenta sample in this set did not show an increased expression of the protein compared to the other samples. The only conclusion, we could get out of these experiments, was that the result from the RNA panel had to be a false positive. Perhaps this sample was somehow contaminated, or HBCBP expression was somehow upregulated in this sample by an unknown factor, possibly an infection or mutation. Taken together, the tissue screen did not give us a helpful hint, in which tissues or functions HBCBP could play a role in.

The expression rate of HBCBP was generally low in all types of tissues and cells that we examined. The crossing points we got from the Q-PCR experiments did not vary too much between all different tissue types. The differences that can be observed in the graphs partially derive from different levels of the housekeeping gene PBGD in the various tissues and cell types, although we could detect slightly higher expression levels of HBCBP in liver and the liver cell line HepG2 (data not shown).

Next we analyzed a hypothetical HBCBP promoter to find potential transcription factor binding sites. We hoped, that the presence of certain binding sites would give us a hint, how the transcription of the protein is regulated and furthermore, in which

processes it plays a role and used the MatInspector software to search for potential transcription factor binding sites likewise it was previously used to analyze PCAN1 promotor (Liu et al, 2008). The list shown in the figures is an excerpt of the long list of potential active sites we achieved and in the following experiments we tested, if these sites were active.

We started these experiments in HepG2s, but continued stimulation experiments in primary cells, because they had altered cell signalling or gene regulation patterns (human umbilical vein endothelial cells, HUVECs).

Neither the PPAR α ligand WY14643 nor the PPAR γ ligand Rosiglitazone-Maleate that should activate PPAR responsible sites (Papac-Milecevic et al, 2009, in revision) affected the expression rate of HBCBP. Similarly the general MAP-Kinase activator PMA (Harvey et al, 2008, Lang et al, 2004) that was used to check the activity of Elk-1, v-Jun and E2F sites did change the transcription rate. AREB6 (ZEB1) is supposed to be upregulated by PGE2 and thus induce AREB6-responsible sites (Dohadwala et al, 2006), but PGE2 treatment did not alter the expression level of HBCBP. Also overexpression of Nur77, which should upregulate the transcriptional activity of the NBRE-site (Papac-Milecevic et al, 2009, in revision), did not result in significant differences in the HBCBP expression.

Other sites in the list were predicted to be interferon responsive and Signal Transducer and Activator of Transcription (STAT) responsive, which are both regulated by cytokines (He, 2006). To investigate if these sites were active we used the cytokines IFN γ , IFN α and TNF α . IFN α und TNF α did not influence the expression rate of HBCBP, but we found a trend of upregulation of HBCBP expression after 3.5 hrs of treatment with IFN γ , though not to a significant extend.

Likewise, TGF β 1 treatment slightly upregulated the expression of HBCBP, but it was not statistically significant.

TGF β signalling plays an important role in a wide variety of different processes like embryonic development, adult tissue homeostasis, differentiation and cancer progression (Romano, 2009). IFN γ is an important regulator of immunological events (Schroder et al, 2004). After seeing a trend of upregulation of HBCBP expression by TGF β 1 and IFN γ , we could hypothesize a possible role of HBCBP in these processes.

We continued to collect in silico data about HBCBP in order to get information about the protein hoping to get hints to possible functions.

An interesting tool is the ClustalW2 sequence analysis program that is used to examine evolutionary relationships between proteins by comparison of their amino acid sequences (Larkin et al, 2007). We aligned predicted orthologues of human HBCBP from five other species that were available on ENSEMBL homepage. Compared to human HBCBP these sequences aligned to various extend. The predicted HBCBP gene in chimpanzee exhibited 96% similarity to the human version, which very likely seems to be an orthologue. The predicted proteins of guinea pig, armadillo and elephant had an amino acid sequence with an approximate identity of 50% to human HBCBP. In contrast, in the lesser hedgehog tenrec, a mammal living in Madagascar and parts of Africa, only a very short sequence (37 basepairs) aligns to human HBCBP. This small percentage makes it unlikely to be an expressed relative to human HBCBP. Except for the chimpanzee sequence, the low percentage of alignment of the other sequences to the human sequence, rather hinted to a low probability of an evolutionary derivation. We considered it to be more likely to be an incidentally occurred similarity.

Now we were interested, if there were related sequences to HBCBP in the human genome. Therefore we submitted the full length amino acid sequence of HBCBP to the Block Searcher program that aligns sequences to the Blocks Database (Henikoff et al, 2000). The only result we got from this analysis was a very short alignment of a 13 amino acid stretch with the Eukaryotic Molybdopterin Domain Signature. The short stretch of alignment was obviously an incidental similarity because it was too short for a real homology, what is also indicated by the relatively high combined e-value of 0.053, what resembles a low probability of significance.

The SMART program, another program used to identify domain structures in proteins (Letunic et al, 2006), could only detect low complexity regions within the full-length HBCBP amino acid sequence.

But taking a closer look at the published cDNA sequence of HBCBP on NCBI and comparing it to the genomic sequence of chromosome 12, we found, that the gene did not contain introns. Over time genes tend to obtain introns by different mechanisms (Fedorova and Fedorov, 2003), so the HBCBP-gene was probably

introduced to the human genome comparatively recently in evolution and the lack of homologous sequences leaves the question, where the gene originated from.

The ELM server is a tool to analyze amino acid sequences of proteins for conserved domain patterns (Puntervoll et al, 2003). Due to the knowledge that HBCBP is located in cytoplasm, we could exclude the predicted domains which execute functions apart from cytoplasm. The remaining predicted domains were mostly related to phosphorylation, which tempted us to analyze the sequence for phosphorylation sites.

The PredPhospho program (Que et al, 2009) for prediction of possible phosphorylation sites found a variety of different possible serine and threonine phosphorylation sites. In parallel we did a similar analysis using the NetPhos 2.0 Server (Blom et al, 1999), though the results of this analysis matched only to a low extend to that of the PredPhospho program.

But still we were interested if any of these predicted site were really phosphorylated, and whether this phosphorylation could modify the activity of HBCBP. We tried to detect phosphorylated serine (P-Ser) or threonine (P-Thr) in overexpressed Myc-HBCBP or the truncated versions, because the prediction almost exclusively predicted serine and threonine sites to be phosphorylated, but no tyrosines. This analysis indicated that the proteins were not phosphorylated. Nevertheless the possibility remains that it requires some trigger to get phosphorylated, or that the phosphorylation was below detection limits.

In most of the experiments discussed before we had to use the artificial system of transfection of Myc-tagged HBCBP, because there was no antibody available to detect endogenous HBCBP. We thought that the possibility to work with the endogenously expressed protein would probably help in our research and planned to purify recombinant protein to further use it as an antigen for antibody production. Full length HBCBP was cloned into pET24a plasmid that was already previously used for expression and purification of proteins (Gilsdorf et al, 2006).

We started to setup the purification procedure, but we could only see that the entire amount of protein expressed by the bacteria remained bound to the inclusion bodies that were part of the cell debris. There are some attempts that would make it possible to isolate proteins out of inclusion bodies, but these procedures include the

denaturation of proteins that are followed by trials of renaturation. These processes lead to a high probability of missfolding and therefore to exposure of epitopes that should not be on the surface in the wild type protein. We did not try to generate antibodies using peptides, because there is no data available about the 3D-structure of the protein and hence, the amino acid stretches that could be exposed as epitopes.

Although we found HBCBP to be an inhibitor of ERK1/2 related processes by Elk-1 reporter assays and by the trend of downregulation of ERK1/2 in western blot after HBCBP- overexpression, we could not define this function in more detail. Apart of the possible role of HBCBP in some ERK1/2 related process our research did not reveal a defined function of HBCBP. Although all relevant controls were done to show the specificity of the Elk-1 reporter assays that showed the inhibitory activity of HBCBP on the system, we could still hypothesize, that this inhibition was due to some artefact of overexpressing the gene. A possible consideration could be that HBCBP, as a hydrophobic protein, could unspecifically bind to other proteins in the cell, leading to cluster formation, what could be a reason for the demonstrated inhibition.

For some time, we even considered that the gene could be some kind of pseudogene that was actually not actively expressed at all, and that the expression level found in the cells resembled some promoter leakage, that the gene was just in the process to develop to a gene, or that it was on its way to be eliminated from the genome. But it is as well possible, that we just could not find the test conditions needed to study the protein in its most active form.

REFERENCES

- Adachi, M., et al. "Nuclear export of MAP kinase (ERK) involves a MAP kinase kinase (MEK)-dependent active transport mechanism." *J.Cell Biol.* 148.5 (2000): 849-56.
- Alberts B, Bray D, Lewis J (2002 *Molecular Biology of the Cell*. Taylor & Francis Group, London, GB
- Ali, I. U., et al." Reduction of homozygosity of genes on chromosome 11 in human breast neoplasia." *Science* 238.4824 (1987): 185-188.
- Andersen, J. N., et al. "A genomic perspective on protein tyrosine phosphatases: gene structure, pseudogenes, and genetic disease linkage." *FASEB J.* 18.1 (2004): 8-30.
- Arena, S., et al "An Intracellular Multi-Effector Complex Mediates Somatostatin Receptor 1 Activation of Phospho-Tyrosine Phosphatase eta." *Molecular Endocrinology* 21.1 (2007): 229-246.
- Arnell RS, Dickinson RJ, Squires M, Hayat S, Keyse SM, Cook SJ. "DUSP6/MKP-3 inactivates ERK1/2 but fails to bind and inactivate ERK5." *Cell Signal.* 2008 May;20(5):836-43. Epub 2007 Dec 27.
- Autschbach, F., et al "Expression of the membrane protein tyrosine phosphatase CD148 in human tissues." *Tissue Antigens* 54.5 (1999): 485-498.
- Balavenkatraman, K. K., et al. „DEP-1 protein tyrosine phosphatase inhibits proliferation and migration of colon carcinoma cells and is upregulated by protective nutrients." *Oncogene* 25.47 (2006): 6319-6324.
- Barford, D., "The structure and mechanism of protein phosphatases: insights into catalysis and regulation." *Annu.Rev.Biophys.Biomol.Struct.* 27 (1998): 133-64.
- Besco, J. A., et al. "Genomic organization and alternative splicing of the human and mouse RPTPrho genes: Correction." *BMC.Genomics* 2.1 (2001): 5.

- Blom, N., Gammeltoft, S., and Brunak, S. "Sequence- and structure-based prediction of eukaryotic protein phosphorylation sites." *Journal of Molecular Biology*: 294(5): 1351-1362, 1999.
- Blume-Jensen, P., et al., "Oncogenic kinase signalling." *Nature* 411.6835 (2001): 355-65.
- Borges, L. G., et al., „Cloning and characterization of rat density-enhanced phosphatase-1, a protein tyrosine phosphatase expressed by vascular cells." *Circ Res*. 79.3 (1996): 570-580.
- Caffrey, D. R., et al., "The evolution of the MAP kinase pathways: coduplication of interacting proteins leads to new signaling cascades." *J.Mol.Evol.* 49.5 (1999): 567-82.
- Camps, M., A. Nichols, and S. Arkinstall. "Dual specificity phosphatases: a gene family for control of MAP kinase function." *FASEB J.* 14.1 (2000): 6-16.
- Chang, C. I., et al. "Crystal structures of MAP kinase p38 complexed to the docking sites on its nuclear substrate MEF2A and activator MKK3b." *Mol.Cell* 9.6 (2002): 1241-49.
- Chen, Z., et al. "MAP kinases." *Chem.Rev.* 101.8 (2001): 2449-76.
- Chiariello, M., et al. "Multiple mitogen-activated protein kinase signaling pathways connect the cot oncoprotein to the c-jun promoter and to cellular transformation." *Mol.Cell Biol.* 20.5 (2000): 1747-58.
- Cobb, M. H. "MAP kinase pathways." *Prog.Biophys.Mol.Biol.* 71.3-4 (1999): 479-500.
- Cunningham JH, Cunningham C, Van Aken B, Lin LS. "Feasibility of disinfection kinetics and minimum inhibitory concentration determination on bacterial cultures using flow cytometry." *Water Sci Technol.* 2008;58(4):937-44.
- Davies, H., et al. "Mutations of the BRAF gene in human cancer." *Nature* 417.6892 (2002): 949-54.

- De la Fuente-Garcia M. A., et al. "CD148 is a membrane protein tyrosine phosphatase present in all hematopoietic lineages and is involved in signal transduction on lymphocytes" *Blood* 91.8 (1998): 2800-2809.
- Dohadwala M, Yang SC, Luo J, Sharma S, Batra RK, Huang M, Lin Y, Goodglick L, Krysan K, Fishbein MC, Hong L, Lai C, Cameron RB, Gemmill RM, Drabkin HA, Dubinett SM. "Cyclooxygenase-2-dependent regulation of E-cadherin: prostaglandin E(2) induces transcriptional repressors ZEB1 and snail in non-small cell lung cancer." *Cancer Res.* 2006 May 15;66(10):5338-45.
- Elion, E. A. "The Ste5p scaffold." *J.Cell Sci.* 114.Pt 22 (2001): 3967-78.
- Elledge, S. J. "Cell cycle checkpoints: preventing an identity crisis." *Science* 1996;274:1664-1672.
- Fedorov, A., et al. "Intron distribution difference for 276 ancient and 131 modern genes suggests the existence of ancient introns." *Proc.Natl.Acad.Sci.U.S.A* 98.23 (2001): 13177-82.
- Fedorova L, Fedorov A. "Introns in gene evolution." *Genetica.* 2003 Jul; 118(2-3):123-31.Review.
- Ferjoux G., et al. "Critical role of Scr and SHP-2 in sst2 somatostatin receptor-mediated activation of SHP-1 and inhibition of cell proliferation." *Mol.Biol.Cell* 14.9 (2003): 3911-3928.
- Fischer E. H., et al. „ Protein tyrosine phosphatases: A diverse family of intracellular and transmembrane enzymes." *Science* 253.5018 (1991): 401-406.
- Florio T., et al. "The activation of the phosphotyrosine phosphatase eta (r-PTPeta) is responsible for the somatostatin inhibition of PC Cl3 thyroid cell proliferation." *Mol Endocrinol* 26.4 (2001): 1838-1852.
- Frøystad MK, Rode M, Berg T, Gjølén T. "A role for scavenger receptors in phagocytosis of protein-coated particles in rainbow trout head kidney macrophages." *Dev Comp Immunol.* 1998 Sep-Dec;22(5-6):533-49.

- Gerdes J, Schwab U, Lemke H, Stein H. "Production of a mouse monoclonal antibody reactive with a human nuclear antigen associated with cell proliferation" *Int J Cancer*. 1983 Jan 15;31(1):13-20.
- Ghosh, S., et al. "Type 2 diabetes: evidence for linkage on chromosome 20 in 716 Finnish affected sib pairs." *Proc.Natl.Acad.Sci.U.S.A* 96.5 (1999): 2198-203.
- Giancotti, F., et al.,. "Integrin signaling." *Science* 285.5430 (1999): 1028-32.
- Gilsdorf J, Gul N, Smith LA. "Expression, purification, and characterization of Clostridium botulinum type B light chain." *Protein Expr Purif*. 2006 Apr;46(2):256-67. Epub 2005 Oct 26.
- Gogal RM Jr, Smith BJ, Kalnitsky J, Holladay SD. "Analysis of apoptosis of lymphoid cells in fish exposed to immunotoxic compounds." *Cytometry*. 2000 Apr 1;39(4):310-8.
- Gruber, F. et al. "Direct binding of Nur77/NAK-1 to the plasminogen activator inhibitor 1 (PAI-1) promoter regulates TNF alpha -induced PAI-1 expression." *Blood* 101, 3042-3048 (2003).
- Guan, K. L., et al. "Evidence for protein-tyrosine-phosphatase catalysis proceeding via a cysteine-phosphate intermediate." *J.Biol.Chem*. 266.26 (1991): 17026-30.
- Hanahan, D., and Weinberg, RA. "The hallmarks of cancer." *Cell* 100.1 (2000): 57-70.
- Hancock, J. F., et al., "Ras plasma membrane signalling platforms." *Biochem.J*. 389.Pt 1 (2005): 1-11.
- Harvey CD, Ehrhardt AG, Cellurale C, Zhong H, Yasuda R, Davis RJ, Svoboda K. "A genetically encoded fluorescent sensor for ERK activity." *Proc Natl Acad Sci U S A*. 2008 Dec 9;105(49):19264-9. Epub 2008 Nov 25.
- He XS, Ji X, Hale MB, Cheung R, Ahmed A, Guo Y, Nolan GP, Pfeffer LM, Wright TL, Risch N, Tibshirani R, Greenberg HB. „Global transcriptional response to interferon is a determinant of HCV treatment outcome and is modified by race.“ *Hepatology* (2006)

- Henikoff J.G., Greene E.A., Pietrokovski S. & Henikoff S., "Increased coverage of protein families with the blocks database servers", *Nucl. Acids Res.* 28:228-230 (2000).
- Holsinger, L.J., et al. "The transmembrane receptor protein tyrosine phosphatase DEP1 interacts with p120ctn." *Oncogene* 21.46 (2002): 7067-7076.
- Honda, H., et al., "Molecular cloning, characterization and chromosomal localization of a novel protein tyrosine phosphatase, HPTPeta." *Blood* 84.12 (1994): 4186-4194.
- Iervolino, A., et al., "The receptor-type protein tyrosine phosphatase J antagonizes the biochemical and biological effects of RET-derived oncoproteins." *Cancer Res.* 66.12 (2006): 4186-4194
- Ishibe, S., et al. "Paxillin serves as an ERK-regulated scaffold for coordinating FAK and Rac activation in epithelial morphogenesis." *Mol.Cell* 16.2 (2004): 257-67.
- Iuliano, R., et al., "The tyrosine phosphatase PTPRJ/DEP-1 genotype affects thyroid carcinogenesis." *Oncogene* 23.52 (2004): 8432-8438.
- Iwata A, Miura S, Kanazawa I, Sawada M, Nukina N., "alpha-Synuclein forms a complex with transcription factor Elk-1." *J Neurochem.* 2001 Apr;77(1):239-52.
- Jacobs, D., et al. "Multiple docking sites on substrate proteins form a modular system that mediates recognition by ERK MAP kinase." *Genes Dev.* 13.2 (1999): 163-75.
- Jacobsen, M., et al. "A point mutation in PTPRC is associated with the development of multiple sclerosis." *Nat.Genet.* 26.4 (2000): 495-99.
- Jandt. E., et al. "The protein-tyrosine phosphatase DEP-1 modulates growth factor-stimulated cell migration and cell-matrix adhesion" *Oncogene* 22.27 (2003): 4175-4185.
- Jia, Z., et al. "Structural basis for phosphotyrosine peptide recognition by protein tyrosine phosphatase 1B." *Science* 268.5218 (1995): 1754-58.
- Johnson, G. L., et al., "Mitogen-activated protein kinase pathways mediated by ERK, JNK, and p38 protein kinases." *Science* 298.5600 (2002): 1911-12.

- Keyse SM. "Dual-specificity MAP kinase phosphatases (MKPs) and cancer." *Cancer Metastasis Rev.* 2008 Jun;27(2):253-61. Review.
- Kolch, W. "Coordinating ERK/MAPK signalling through scaffolds and inhibitors." *Nat.Rev.Mol.Cell Biol.* 6.11 (2005): 827-37.
- Koshi, J. M., et al., "Major structural determinants of transmembrane proteins identified by principal component analysis." *Proteins* 34.3 (1999): 333-40.
- Kovalenko M., et al., "Site-selective dephosphorylation of the platelet-derived growth factor b-receptor by the receptor like protein-tyrosine phosphatase DEP-1." *J Biol Chem.* 275.21 (2000): 16219-16226.
- Kung, C., et al. "Mutations in the tyrosine phosphatase CD45 gene in a child with severe combined immunodeficiency disease." *Nat.Med.* 6.3 (2000): 343-45.
- Kuramochi S., et al., "Molecular cloning and characterization of Byp, a murine receptor-type tyrosine phosphatase similar to human DEP-1." *FEBS* 1.7 (1996): 7-14.
- Lampugnani M., et al. "Contact inhibition of VEGF-induced proliferation requires vascular endothelial cadherin, beta-catenin and the phosphatase DEP-1/CD148." *J. Cell Biol.* 161.4 (2003): 793-804
- Lang W, Wang H, Ding L, Xiao L. „Cooperation between PKC-alpha and PKC-epsilon in the regulation of JNK-activation in human lung cancer cells." *Cell Signal.* 2004 Apr;16(4):457-67
- Larkin MA, Blackshields G, Brown NP, Chenna R, McGettigan PA, McWilliam H, Valentin F, Wallace IM, Wilm A, Lopez R, Thompson JD, Gibson TJ, Higgins DG. "Clustal W and Clustal X version 2.0" [Bioinformatics.](#) 2007 Nov 1;23(21):2947-8. Epub 2007 Sep 10
- Letunic I, Copley RR, Pils B, Pinkert S, Schultz J, Bork P. "SMART 5: domains in the context of genomes and networks." *Nucleic Acids Res.* 2006 Jan 1;34(Database issue):D257-60.
- Lewis, T. S., et al., "Signal transduction through MAP kinase cascades." *Adv.Cancer Res.* 74 (1998): 49-139.

- Lim, L. P., et al., "A computational analysis of sequence features involved in recognition of short introns." *Proc.Natl.Acad.Sci.U.S.A* 98.20 (2001): 11193-98.
- Liu W, Zhang P, Chen W, Yu C, Cui F, Kong F, Zhang J, Jiang A. "Characterization of two functional NKX3.1 binding sites upstream of the PCAN1 gene that are involved in the positive regulation of PCAN1 gene transcription." *BMC Mol Biol.* 2008 May 4;9:45.
- Lu. Y. Y., et al., "Screening and identification of a novel gene coding for Hepatitis B virus core antigen interacting protein C-12 in hepatocytes." *World J Gastroenterol.* 11.8 (2005): 1122-1125
- Majeti, R., et al. "An inactivating point mutation in the inhibitory wedge of CD45 causes lymphoproliferation and autoimmunity." *Cell* 103.7 (2000): 1059-70.
- Maple J, Møller SG., "Yeast two-hybrid screening." *Methods Mol Biol.* 2007;362:207-23.
- Marais, R., et al. "Differential regulation of Raf-1, A-Raf, and B-Raf by oncogenic ras and tyrosine kinases." *J.Biol.Chem.* 272.7 (1997): 4378-83.
- Massa, A., et al. "The expression of the phosphotyrosine phosphatase DEP-1/PTPeta dictates the responsibility of glioma cells to somatostatin inhibition of cell proliferation" *J Biol Chem.* 279.28 (2004): 29004-29012.
- Matsubayashi, Y., et al., "Evidence for existence of a nuclear pore complex-mediated, cytosol-independent pathway of nuclear translocation of ERK MAP kinase in permeabilized cells." *J.Biol.Chem.* 276.45 (2001): 41755-60.
- Mor, A., et al., "Compartmentalized Ras/MAPK signaling." *Annu.Rev.Immunol.* 24 (2006): 771-800.
- Morrison, D. K. and R. J. Davis. "Regulation of MAP kinase signaling modules by scaffold proteins in mammals." *Annu.Rev.Cell Dev.Biol.* 19 (2003): 91-118.
- Muda M, Boschert U, Smith A, Antonsson B, Gillieron C, Chabert C, Camps M, Martinou I, Ashworth A, Arkinstall S. "Molecular cloning and functional characterization of a novel mitogen-activated protein kinase phosphatase, MKP-4." *J Biol Chem.* 1997 Feb 21;272(8):5141-51.

- Murphy, L. O. and J. Blenis. "MAPK signal specificity: the right place at the right time." *Trends Biochem.Sci.* 31.5 (2006): 268-75.
- Nasmyth, K. "Evolution of the cell cycle." *Phil. Trans. R. Soc. Lond. B* 349, 271-281, 1995.
- Novak B., et al. "Model scenarios for evolution of the eukaryotic cell cycle. *Phil. Trans. R. Soc. Lond. B* (1998) 353, 2063-2076.
- Osborne, J. M., et al., „ Murine DEP-1, a receptor protein tyrosine phosphatase, is expressed in macrophages and is regulated by CSF-1 and LPS." *J Leukoc Biol.* 64.5 (1998): 692-701.
- Ostman, A., et al., "Expression of DEP-1 a receptor-like protein-tyrosine-phosphatase, is enhanced with increasing cell density." *PNAS* 91.21 (1994): 9680-9684
- Owens, D. M., et al., "Differential regulation of MAP kinase signalling by dual-specificity protein phosphatases." *Oncogene* 26.22 (2007): 3203-13.
- Palka, H. L., et al., „Hepatocyte Growth Factor Receptor Tyrosine Kinase Met Is a Substrate of the Receptor Protein-Tyrosine Phosphatase DEP-1." *J Biol Chem.* 278.8 (2003): 5728-5735.
- Papac-Milicevic N, Breuss JM, Zaujec J, Ryban L, Plyushch T, Olcaydu D, Wagner GA, Binder CJ, Uhrin P, Binder BR. "The interferon inducible gene 12, a novel factor modulating transcriptional activities of selected nuclear receptors." *Cell* 2009, Paper in revision.
- Perkins, N. D., et al., " A cooperative interaction between NF-kappa B and Sp1 is required for HIV-1 enhancer activation" *EMBO* 12 (1993): 3551-3558.
- Pfaffl, M. W., "A new mathematical model for relative quantification in real-time RT-PCR." *Nucleic Acids Res.* 29 (2001).
- Puntervoll P, Linding R, Gemünd C, Chabanis-Davidson S, Matningsdal M, Cameron S, Martin DM, Ausiello G, Brannetti B, Costantini A, Ferrè F, Maselli V, Via A, Cesareni G, Diella F, Superti-Furga G, Wyrwicz L, Ramu C, McGuigan C, Gudavalli R, Letunic I, Bork P, Rychlewski L, Küster B, Helmer-Citterich M, Hunter

- WN, Aasland R, Gibson TJ. "ELM server: A new resource for investigating short functional sites in modular eukaryotic proteins." *Nucleic Acids Res.* 2003 Jul 1;31(13):3625-30.
- Que S, Wang Y, Chen P, Tang Y, Zhang Z, He H. "Evaluation of Protein Phosphorylation Site Predictors." *Protein Pept Lett.* 2009 Nov 10.
- Raman, M., et al., "Differential regulation and properties of MAPKs." *Oncogene* 26.22 (2007): 3100-12.
- Ranganathan, A., et al., "The nuclear localization of ERK2 occurs by mechanisms both independent of and dependent on energy." *J.Biol.Chem.* 281.23 (2006): 15645-52.
- Rapp, U. R., et al., "BuCy RAFs drive cells into MEK addiction." *Cancer Cell* 9.1 (2006): 9-12.
- Reszka, A. A., et al. "Association of mitogen-activated protein kinase with the microtubule cytoskeleton." *Proc.Natl.Acad.Sci.U.S.A* 92.19 (1995): 8881-85.
- Romano MF. "Targeting TGFbeta-mediated processes in cancer." *Curr Opin Drug Discov Devel.* 2009 Mar;12(2):253-63.
- Ruivenkamp, C. A., et al. "Ptprij is a candidate for the mouse colon-cancer susceptibility locus Scc1 and is frequently deleted in human cancers." *Nat.Genet.* 31.3 (2002): 295-300.
- Saxton, T. M., et al. "Abnormal mesoderm patterning in mouse embryos mutant for the SH2 tyrosine phosphatase Shp-2." *EMBO J.* 16.9 (1997): 2352-64.
- Schitteck B, Rajewsky K, Förster I. „Dividing cells in bone marrow and spleen incorporate bromodeoxyuridine with high efficiency.“ *Eur J Immunol.* 1991 Jan;21(1):235-8.
- Schroder K, Hertzog PJ, Ravasi T, Hume DA. „Interferon-gamma: an overview of signals, mechanisms and functions.“ *J Leukoc Biol.* 2004 Feb;75(2):163-89. Epub 2003 Oct 2.

- Sewing, A., et al. "High-intensity Raf signal causes cell cycle arrest mediated by p21Cip1." *Mol.Cell Biol.* 17.9 (1997): 5588-97.
- Takahashi, T., et al., "A Mutant Receptor Tyrosine Phosphatase, CD148, Causes Defects in Vascular Development ." *Mol Cell Biol.* 23.5 (2003): 1817-1831.
- Takahashi, T. et al., "A monoclonal antibody against CD148, a receptor-like tyrosine phosphatase, inhibits endothelial-cell growth and angiogenesis. *Blood.* 2006 August 15; 108(4): 1234-1242.
- Tanoue, T., et al. "Identification of a docking groove on ERK and p38 MAP kinases that regulates the specificity of docking interactions." *EMBO J.* 20.3 (2001): 466-79.
- Tartaglia, M., et al. "Mutations in PTPN11, encoding the protein tyrosine phosphatase SHP-2, cause Noonan syndrome." *Nat.Genet.* 29.4 (2001): 465-68.
- Teis, D., W. Wunderlich, and L. A. Huber. "Localization of the MP1-MAPK scaffold complex to endosomes is mediated by p14 and required for signal transduction." *Dev.Cell* 3.6 (2002): 803-14.
- Trapasso, F., et al., "Rat protein tyrosine phosphatase eta suppresses the neoplastic phenotype of retrovirally transformed thyroid cells through the stabilization of p27/kip-1." *Mol Cell Biol.* 20.24 (2000): 9236-9246.
- Trowbridge, I. S. and M. L. Thomas. "CD45: an emerging role as a protein tyrosine phosphatase required for lymphocyte activation and development." *Annu.Rev.Immunol.* 12 (1994): 85-116.
- Tyson, J J, et al., "The dynamics of cell cycle regulation." *BioEssays* 24:1095-1109,2002.
- Wan, P. T., et al. "Mechanism of activation of the RAF-ERK signaling pathway by oncogenic mutations of B-RAF." *Cell* 116.6 (2004): 855-67.
- Wang, H. P., et al., „ Deletion in human chromosome arms 11p and 13q in primary hepatocellular carcinomas." *Cytogenet Cell Genet.* 48.2 (1988): 72-78.

Wera, S., et al., "Serine/threonine protein phosphatases." *Biochem.J.* 311 (Pt 1) (1995): 17-29.

Woods, D., et al. "Raf-induced proliferation or cell cycle arrest is determined by the level of Raf activity with arrest mediated by p21Cip1." *Mol.Cell Biol.* 17.9 (1997): 5598-611.

Wu, X., et al. "Selective activation of MEK1 but not MEK2 by A-Raf from epidermal growth factor-stimulated Hela cells." *J.Biol.Chem.* 271.6 (1996): 3265-71.

Yamamoto, T., et al. "Continuous ERK activation downregulates antiproliferative genes throughout G1 phase to allow cell-cycle progression." *Curr.Biol.* 16.12 (2006): 1171-82.

Yang L, Li N, Wang C, Yu Y, Yuan L, Zhang M, Cao X. "Cyclin L2, a novel RNA polymerase II-associated cyclin, is involved in pre-mRNA splicing and induces apoptosis of human hepatocellular carcinoma cells." *J Biol Chem.* 2004 Mar 19;279(12):11639-48. Epub 2003 Dec 17

Yoon, S. and R. Seger. "The extracellular signal-regulated kinase: multiple substrates regulate diverse cellular functions." *Growth Factors* 24.1 (2006): 21-44.

Zhang, L., et al., "Thyroid cell transformation inhibits the expression of a novel rat protein tyrosine phosphatase." *Exp Cell Res.* 235.1 (1997): 62-70.

Zheng, X. M., et al., "Cell transformation and activation of pp60c-src by overexpression of a protein tyrosine phosphatase." *Nature* 359.6393 (1992): 336-39.

Zinda MJ, Johnson MA, Paul JD, Horn C, Konicek BW, Lu ZH, Sandusky G, Thomas JE, Neubauer BL, Lai MT, Graff JR. "AKT-1, -2, and -3 are expressed in both normal and tumor tissues of the lung, breast, prostate, and colon." *Clin Cancer Res.* 2001 Aug;7(8):2475-9

I tried to find out all owners of digital copyrights and to get their agreement to use their images in this work. Though, if there still should appear an infringement of copyright, I kindly ask to announce it to me.

CURRICULUM VITAE

Patricia Caroline Heier

Date of birth:	16 th September, 1980
Status:	Single, no children
Nationality:	Austrian
e-mail adress:	patriciaheier@hotmail.com

EDUCATION

1986 - 1990	Primary School Hackerberg Austria (excellent success)
1990 - 1994	Secondary School Neudau Austria (excellent success)
1994 - 1998	Gymnasium (BORG) Güssing Austria „A“ levels average 1.8
1998 - 2004	University of Vienna Faculty of Natural Sciences Degree: Magistra der Naturwissenschaften (average University degree 1.57 and diploma degree 1)

Since 2005	PhD student at University of Vienna Faculty of Natural Sciences
2007	European Vascular Genomics Network (EVGN) Summer School, Smygehuk, Sweden,

EXPERIENCE

2001	Traineeship at the Department of Vascular Biology and Thrombosis Research, under the supervision of Prof. Margarethe Geiger. The group deals with the characterization of Protein C Inhibitor (PCI).
2003 - 2004	Diploma thesis at the Department of Vascular Biology and Thrombosis Research, Medical University of Vienna, Austria. The group carried out research on Density Enhanced Phosphatase 1 (DEP-1) interaction partners.
2004 - 2008	Member of the director's group at the Department of Vascular Biology and Thrombosis Research, Medical University of Vienna, Austria. Involved in the determination of properties of Hepatitis B Core-Antigen Binding Protein (HBCBP), an interaction partner of DEP-1.

SUMMARY OF RELEVANT SKILLS AND ACTIVITIES

Experimental skills in standard cell culture techniques, transfections, cloning, sequencing, yeast-two-hybrid screening, western blotting, PCR techniques (standard PCR, Q-PCR, RT-PCR) immunofluorescence microscopy, immunoprecipitation, reporter assays, DNA and RNA isolations, siRNA techniques, flow cytometry.

5 years of laboratory experience

Languages:	German English French (intermediate)
-------------------	--

POSTERS:

“Crosstalk Between the MAP-Kinase Pathways and the Urokinase Receptor, Urokinase, Plasminogen Activator Inhibitor 1 System.” Heier PC, Brunner PM, Ehart M, Mihaly J, Prager GW, Breuss J, Binder BR. CCHD Meeting, Vienna, Austria, 2006

“DEP-1 Synergistic Inhibitor (DEPSI, HBCBP) is an Interaction Partner of Density Enhanced Phosphatase 1 (DEP-1).” Heier PC, Binder BR, YSA PhD Symposium, Vienna, Austria, 2006

“Hepatitis B Core-Antigen Binding Protein (HBCBP) is an Interaction Partner of Density Enhanced Phosphatase 1 (DEP-1).” Heier PC, Binder BR. European Vascular Genomics Network (EVGN) Summer School, Smygehuk, Sweden, 2007.

ABSTRACTS

“The Density Enhanced Phosphatase 1 (DEP-1) Down-Modulates Urokinase Receptor (uPAR) Surface Expression in Confluent Endothelial Cells.” Brunner PM, Heier PC, Prager GW, Mihaly J, Priglinger U, Binder BR. XIth International Workshop on Molecular & Cellular Biology of Plasminogen Activation, Saltsjöbaden, Sweden, 2007.

“A recently identified protein is an Interaction Partner of Density Enhanced Phosphatase 1 (DEP-1).” Heier PC, Binder BR. Cancerdegradome Final Annual Meeting, Kranjska Gora, Slovenia, 2008.